AFML-TR-76-90

THE INFLUENCE OF STRAIN-RATE HISTORY AND TEMPERATURE ON THE SHEAR STRENGTH OF COPPER, TITANIUM AND MILD STEEL

DEPARTMENT OF ENGINEERING SCIENCE
UNIVERSITY OF OXFORD

MARCH 1976

TECHNICAL REPORT AFML-TR-76-90
FINAL REPORT FOR PERIOD 1 FEBRUARY - 31 JULY 1975

AIR FORCE MATERIALS LABORATORY
AIR FORCE WRIGHT AERONAUTICAL LABORATORIES
AIR FORCE SYSTEMS COMMAND
WRIGHT-PATTERSON AIR FORCE BASE, OHIO 45433

DISCLAIMER NOTICE

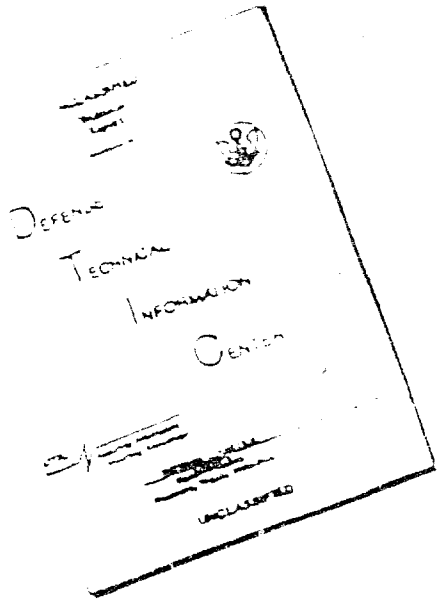

THIS DOCUMENT IS BEST QUALITY AVAILABLE. THE COPY FURNISHED TO DTIC CONTAINED A SIGNIFICANT NUMBER OF PAGES WHICH DO NOT REPRODUCE LEGIBLY.

NOTICE

When Government drawings, specifications, or other data are used for any purpose other than in connection with a definitely related Government procurement operation, the United States Government thereby incurs no responsibility nor any obligation whatsoever; and the fact that the government may have formulated, furnished, or in any way supplied the said drawings, specifications, or other data, is not to be regarded by implication or otherwise as in any manner licensing the holder or any other person or corporation, or conveying any rights or permission to manufacture, use, or sell any patented invention that may in any way be related thereto.

This report has been reviewed by the Information Office (IO) and is releasable to the National Technical Information Service (NTIS). At NTIS, it will be available to the general public, including foreign nations.

This technical report has been reviewed and is approved for publication.

T. NICHOLAS
Project Scientist

FOR THE DIRECTOR

V. J. RUSSO
Chief, Metals Behavior Branch
Metals and Ceramics Division
Air Force Materials Laboratory

Copies of this report should not be returned unless return is required by security considerations, contractual obligations, or notice on a specific document.

UNCLASSIFIED

SECURITY CLASSIFICATION OF THIS PAGE (When Data Entered)

REPORT DOCUMENTATION PAGE

READ INSTRUCTIONS BEFORE COMPLETING FORM

1. REPORT NUMBER: AFML-TR-76-90	2. GOVT ACCESSION NO.
3. RECIPIENT'S CATALOG NUMBER	
4. TITLE (and Subtitle): THE INFLUENCE OF STRAIN-RATE HISTORY AND TEMPERATURE ON THE SHEAR STRENGTH OF COPPER, TITANIUM AND MILD STEEL.	5. TYPE OF REPORT & PERIOD COVERED: Final report for period 1 Feb 71 - 31 July 75
	6. PERFORMING ORG. REPORT NUMBER
7. AUTHOR(s): A.M. Eleiche and J.D. Campbell	8. CONTRACT OR GRANT NUMBER(s): AFOSR 71-2056
9. PERFORMING ORGANIZATION NAME AND ADDRESS: Department of Engineering Science, University of Oxford, Oxford, England	10. PROGRAM ELEMENT, PROJECT, TASK AREA & WORK UNIT NUMBERS: 61102 F, 7353-03
11. CONTROLLING OFFICE NAME AND ADDRESS: Air Force Materials Laboratory (LLN) Wright-Patterson AFB, Ohio 45433	12. REPORT DATE: March 1976
	13. NUMBER OF PAGES: 101
14. MONITORING AGENCY NAME & ADDRESS (if different from Controlling Office): European Office of Aero-Space Research & Development, FPO New York 09510	15. SECURITY CLASS. (of this report): Unclassified
	15a. DECLASSIFICATION/DOWNGRADING SCHEDULE

16. DISTRIBUTION STATEMENT (of this Report)
Approved for public release; distribution unlimited.

17. DISTRIBUTION STATEMENT (of the abstract entered in Block 20, if different from Report)

18. SUPPLEMENTARY NOTES

19. KEY WORDS (Continue on reverse side if necessary and identify by block number)
Strain-rate history, temperature, shear strength, copper, titanium, mild steel, Hopkinson bar.

20. ABSTRACT (Continue on reverse side if necessary and identify by block number)

Experiments have been carried out to determine the strain-rate sensitivity of the shear flow stress of OFHC copper, commercially-pure titanium and mild steel over the temperature range -150 to 400°C. All the tests were performed on thin-walled tubular specimens of short gauge length, mounted in a torsional split Hopkinson-bar apparatus adapted to permit quasi-static straining as well as dynamic straining. For each material, the constant-rate behaviour was first measured at nominal strain rates of 10^{-3} and $10^{3}s^{-1}$, for six different temperatures. Tests were then carried out in which the strain rate was suddenly

DD FORM 1 JAN 73 1473 EDITION OF 1 NOV 65 IS OBSOLETE

UNCLASSIFIED

SECURITY CLASSIFICATION OF THIS PAGE (When Data Entered)

increased from 10^{-3} to $10^{3}\ s^{-1}$ at various values of plastic strain.

Comparison of the results obtained in the two series of tests shows that the response of all three materials depends on the strain-rate history, so that a 'mechanical equation of state', relating stress to strain, strain rate and temperature is not valid; however, the influence of strain-rate history is less marked for titanium than for copper or mild steel. The results are discussed in terms of plastic flow mechanisms involved, thermal activation, changes in microstructure, strain ageing and dynamic recovery. Possible forms of macroscopic constitutive relation are also discussed.

FOREWORD

This technical report was prepared by the Department of Engineering Science, University of Oxford, England. The work reported herein was supported, in part, under AFOSR Grant No. AFOSR 71-2056. The grant was initiated under Project No. 7353, Task No. 735303. The program was monitored by the Metals Behavior Branch, Metals and Ceramics Division, Air Force Materials Laboratory, with Dr. T. Nicholas (AFML/LLN) acting as project scientist.

This report covers work conducted from February 1, 1971 to July 31, 1975. The report was submitted by the authors in March 1976.

The authors are grateful to the members of the staff of Oxford University Engineering Laboratory who assisted in the construction of apparatus, in the experimental work and in the preparation of this report. In particular, Mr. R.C. Stone undertook the detailed design of the cryostat and was responsible for obtaining the photomicrographs.

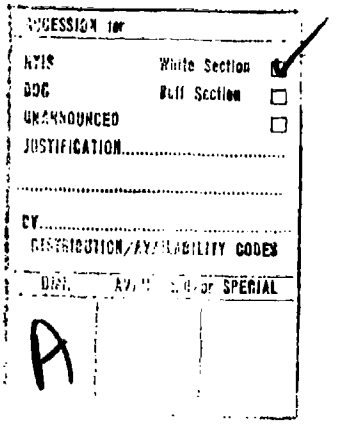

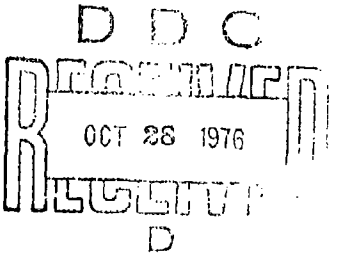

TABLE OF CONTENTS

LIST OF ILLUSTRATIONS

LIST OF ABBREVIATIONS AND SYMBOLS

A_i	frequency factor in rate equation
b	magnitude of Burgers vector
f, f_1, f_2	functions involved in macroscopic flow equations
F	function defining mechanical equation of state
k	Boltzmann's constant
s_i	structure factor in rate equation
t	time
T	absolute temperature
$\bar{v}$	average dislocation velocity
V	activation volume
V^*	apparent activation volume
x	distance measured along axis of Hopkinson bars
Z	Zener-Hollomon parameter
α	pre-strain
γ, $\dot{\gamma}$	shear strain, shear strain rate
γ^p, $\dot{\gamma}^p$	plastic shear strain, plastic shear strain rate
$\dot{\gamma}_1$, $\dot{\gamma}_2$	quasi-static and dynamic shear strain rates
ΔG, ΔG_i	free activation energies in rate equation
$\Delta\tau$	'instantaneous' increment in shear flow stress
η	function defining variation of strain rate with strain
η_o	initial value of strain rate
μ_{12}	apparent strain-rate sensitivity parameter
$\tilde{\mu}_{12}$	intrinsic strain-rate sensitivity parameter
ρ_m	density of mobile dislocations
τ	applied shear stress
τ_A	athermal component of shear stress
τ^*	thermal component of shear stress
τ_1, τ_2	applied shear stresses at strain rates $\dot{\gamma}_1, \dot{\gamma}_2$.

SECTION 1

INTRODUCTION

A previous report (Eleiche and Campbell 1974, subsequently referred to as I) dealt with the influence of strain-rate history on the shear strength of OFHC copper at room temperature ($\sim$24°C), 200 and 400°C, and of commercially pure (alpha) titanium at room temperature. Shear stress-strain curves were first obtained at a quasi-static rate ($\sim 10^{-3} s^{-1}$) and at constant high rates ($\sim 10^{3} s^{-1}$); tests were then performed in which the rate was suddenly increased from the low to the high rate after a certain amount of plastic deformation.

It was found that at a given temperature the high-rate flow stress always exceeded that required at the same strain in the low-rate test. The high-rate flow stress was also found to depend on the previous deformation: immediately after the rate was increased, the flow stress was less than that obtained at the same strain in a high-rate test. This difference was small for titanium, but relatively large for copper; in each case, the difference decreased with further straining, i.e. the 'memory' of the previous deformation decayed. The strain required for effective elimination of the difference was much larger for copper than for titanium, and it increased with increasing pre-strain.

The results for copper showed that the incremental stress, i.e. the difference between the high-rate value and the low-rate value, varied relatively little with temperature, over the range covered. Thus it did not appear to be described by a simple rate equation with a constant activation volume. The purpose of the present work was to obtain further results for the same two metals over a wide temperature range including values below ambient; to obtain comparable data for a third contrasting material, namely mild steel; and to interpret the results for all three

materials in terms of proposed microscopic and macroscopic theories of rate-dependent plastic flow in metals.

Particular questions of dynamic plasticity to which the investigation is relevant include the following:-

(1) The extent to which the structure of metals and alloys is a function of the previous strain-rate history, rather than the current value of plastic strain.

(2) The extent to which the rate dependence can be explained in terms of thermal-activation rate analysis.

(3) The applicability of proposed forms of macroscopic constitutive relation to deformation of metals and alloys at varying strain rates.

If it is assumed that the observed plastic strain-rate $\dot{\gamma}^p$ is the sum of rates caused by a number of different thermally-activated micro-mechanisms of deformation, each dependent on the stress τ and the current structure of the material, we may write

$$\dot{\gamma}^p = \sum_i A_i(\tau, T, s_i) \exp\left[-\frac{\Delta G_i(\tau, T, s_i)}{kT}\right], \qquad (1)$$

where A_i is the frequency factor and ΔG_i is the free activation energy for the ith deformation mechanism, k is Boltzmann's constant, T is the absolute temperature and the parameters s_i represent the current structure of the material. The parameters s_i must evidently be determined by the number and distribution of all the lattice imperfections, solute atoms, second-phase particles, grain or twin boundaries and other features of the microstructure. For a given material, some of these parameters are governed by the initial state of the material, while others depend on the plastic deformation itself. The simplest assumption that can be made is that for a given initial state the structure is uniquely defined by the plastic strain. Making this assumption

(1) reduces to what has become known as the 'mechanical equation of state', which may be written

$$F\ (\tau,\ \gamma^p,\ \dot{\gamma}^p,\ T) = 0. \qquad (2)$$

Equations of this type were proposed by Ludwik (1909), Zener and Hollomon (1944, 1946); MacGregor and Fisher (1946); and Hollomon (1947). Such equations imply that the material behaviour is independent of the deformation history, being governed only by the current stress, strain and temperature. If the deformation is controlled by a single thermally-activated process, it may be possible to simplify (2) further by employing a single variable to characterize both the strain rate and the temperature. One such quantity is the Zener-Hollomon parameter defined by

$$Z = \dot{\gamma}^p \exp \left[\Delta G/kT\right], \qquad (3)$$

where ΔG is the activation energy for the rate-controlling mechanism. Then (2) becomes

$$F\ (\tau,\ \gamma^p,\ Z) = 0. \qquad (4)$$

Alternatively, we may use the 'velocity-modified temperature' introduced by MacGregor and Fisher (1946). Fig. 1 illustrates diagrammatically the behaviour predicted by (2) or (4): a sudden change of temperature or strain rate, represented by AB or CD, gives a reversible change of stress but no identifiable change of structure.

An equation such as (4), if applicable, is obviously of great value in predicting the behaviour of materials, and such equations have been used successfully for high-temperature deformation at constant strain rates and temperatures (Jonas et al. 1969). However, deviations from an equation of state have been reported by many workers; for example, Barraclough and Sellars (1974) showed from hot torsion tests on stainless steel that the equation does not hold if Z changes by more than about two orders of

magnitude during a change of unity in the true tensile strain. Similar effects in f.c.c. metals have been discussed by Klepackzo (1975), and the b.c.c. metals molybdenum and niobium have also been shown to be sensitive to strain-rate history (Campbell and Briggs 1975). It seems clear therefore that in general the parameters s_i in (1) must be related to the previous mechanical and thermal treatment rather than simply to the current values of strain and temperature. One suggestion which satisfiesthis condition is that the structure is determined by the mean amplitude of the long-range internal stresses present in the material. In principle this may be measured by the applied stress needed to cause flow at a temperature high enough to render short-range obstacles ineffective (the 'athermal' component of stress); this stress should be essentially rate-independent. A general treatment of this kind has recently been given by Boček (1975).

Hart (1970) has proposed a similar theory in which the structure is characterized by a single parameter y which depends on the previous deformation history, the rate of change of y with strain being a known function of the state variables. Kocks et al. (1975) have reviewed this and other similar constitutive laws.

Most of the available data relating to history effects in the deformation of metals were obtained at low strain rates, using rate changes of one or two orders of magnitude. In the present experiments, however, rate changes of up to 6 orders of magnitude could be imposed during a shear strain increment of order 10^{-2}. Very large changes in deformation history were therefore possible, so that deviations from a mechanical equation of state were to be expected. The inclusion of temperature as a variable permitted an approximate correction to be made to take account of the effects of adiabatic heating. The use of pure shear rather than

tensile or compressive straining eliminated the need for conversion to true stress and true strain, and also enabled deformation to be continued to large strains. Thus in addition to providing data for analysis and comparison with proposed forms of constitutive relation, the results may have direct relevance to machining or other metal-forming processes involving deformation at high strains and varying strain rates over a range of temperatures.

SECTION 2

EXPERIMENTAL DETAILS

2.1 Apparatus

All tests were conducted on a horizontal torsional split Hopkinson-bar apparatus(Fig.2) the details of which, together with the associated instrumentation, were described before in I. Quasi-static loading was achieved by means of a slow rotational-drive unit at one end of the system, while the release of a pre-stored torque in a clamped portion of the input bar at the other end imposed the dynamic loading. A theoretical analysis of the wave propagation in the bars as well as the actual observed wave structure as affected by the performance of the clamp, are discussed in detail in Appendix A. An axial pulse is found to be initiated at the clamp and this arrives at the specimen before the main torsional pulse; however, the amplitude of the axial pulse is small and its effects are not significant.

As described in I, a furnace was also used for testing at elevated temperatures. This was continuously kept filled with dry argon when testing titanium or mild steel specimens, to prevent oxidation. For testing at sub-ambient temperatures, cooling of the specimens was achieved by controlling the flow of liquid nitrogen into a tufnol container surrounding the specimen. Details of this arrangement are presented in Appendix B.

2.2 Specimens and Bonding

Three materials were chosen for studying the effects of strain-rate history on shear strength. Various considerations led to the choice of metals of different crystallographic structure, of varying purity and practical importance: OFHC copper, commercially-pure (alpha) titanium and low-carbon steel. Compositions of the three materials are given in Table 1. After machining to the nominal configuration shown in Fig. 3, and measurement of the critical dimensions, the specimens were annealed in a vacuum, resulting in the grain densities given in Table 2. Photomicrographs of annealed (as well as tested) specimens were taken; some of these are presented in section 3.

Before testing, each annealed specimen was firmly attached to the inner ends of the two torsion bars, thus reducing the system (at any testing temperature) to a continuous bar of constant mechanical impedance, except for the short tubular gauge length of the specimen. A difficulty always exists in torsional split-bar experiments concerning the method of bonding, which should ensure continuity as well as strength at any testing temperature. Various methods are discussed in some detail in Appendix C. In all tests conducted at room and low temperatures, Araldite epoxy cement was used to bond the specimen directly to the torsion bars. At elevated temperatures, copper and mild steel specimens were each brazed to a pair of stainless-steel tubes, and the assembly then attached with Araldite to the torsion bars. With titanium, each specimen was first mechanically attached to two short stainless-steel grips of proper dimensions (Figs. C1 and C2), and this assembly was then connected to the bars as described for copper and mild steel specimens.

2.3 Test Procedure and Data Reduction

An account of the test preparation, procedure and calibration as well as the data reduction has been presented in I. One exception occurred for elevated-temperature testing of titanium at the quasi-static strain rate: because of design considerations, the specimen I.D. was chosen to be smaller than the standard one, as can be seen from Figs. 3 and C1. Relatively small torques were therefore sufficient to deform these specimens plastically, and recording of these torques could not be achieved on the Sanborn recorder without excessive vibration of the recorder pen. Quasi-static test results were therefore recorded partly on the Sanborn chart (twist versus time), and partly on the oscilloscope (applied torque versus time). Most of the quasi-static pre-straining in rate-jump tests was also recorded in the same way; in such a test, the oscilloscope settings were readjusted just before releasing the clamp, to record the dynamic portion of the test on the same photograph.

2.4 Typical Test Records

A representative collection of records is presented in Figs. 4, 5 and 6 for copper, titanium and mild steel respectively, tested for a variety of temperatures and strain-rate histories. In all oscillograms, the upper trace shows the output-bar gauge signal (i.e. output torque), and the lower trace shows the input-bar gauge signal (i.e. input and reflected torque). In certain tests, the timebase for the upper traces was delayed relative to that of the lower; this delay is specified in the list of illustrations. The amount of quasi-static pre-strain in each rate-jump test is given on the figures.

2.4.1 Copper

Constant-rate and rate-jump test results at -150, -100 and -50° C are recorded in Fig. 4; these results complement those given in Figs. 7-9 of

t. A definite yield point is observable in each of the constant-rate records (Figs. 4(a), (c), (e)). The rate-jump test records (Figs. 4 (b), (d), (f)) have a general appearance similar to that observed for copper at room and elevated temperatures. Each output trace shows two dips, one preceding the torsional pulse, the other about 900 μs later; these are apparently caused by the axial pulse initiated during the clamp release (see Appendix A). Figs. 4 (b), (d) and (f) show distinct, though small, elastic stress increments immediately following the change in strain rate; such increments were not discernible in the higher temperature results (see Figs. 8 and 9 in I).

2.4.2 Titanium

Constant-rate and rate-jump test records obtained for titanium at room temperature were presented in I (Figs. 11 and 12). These may be compared with those obtained at lower and higher temperatures, which are shown in Fig. 5.

The elevated-temperature titanium specimen design appears to be satisfactory, as can be seen from Figs. 5 (h)-(k). Quasi-static results were recorded on an oscilloscope for torque (see Fig. 5 (g) as an example) and on a Sanborn chart for twist. Constant-rate dynamic test results (Figs. 5 (h) and (j)) did not exhibit any peculiarities which could be related to the mechanical grips. The small oscillations on the upper trace at the start of yield were also observed in some of the lower temperature tests (see for example Figs. 5 (c) and (e)); the small ripples superimposed on this trace are a consequence of the high gain used.

For rate-jump tests, the quasi-static pre-straining was sometimes also recorded on the oscilloscope (Fig. 5 (k)) or interpreted from the twist-time Sanborn chart record; proper checking of the pre-strain level could be

achieved by comparing the original baseline for the output trace on the oscillogram and the level reached after triggering during the dynamic strain-rate jump. At all temperatures, the rate-jump test records show an elastic rise in stress; the subsequent flow occurred at nearly constant stress at the two high temperatures, while considerable work-hardening is observed at room temperature and below.

2.4.3 Mild Steel

Fig. 6 presents a selection of constant-rate and rate-jump test results for mild steel obtained at various temperatures ranging from -150 to 400°C. At the quasi-static rate, dynamic strain-ageing was very well exhibited on the chart or oscilloscope torque record when testing at 200°C, as shown in Figs. 6 (d) and (e). At higher or lower temperatures, such effects were not observed (see Figs. 6 (a), (b) and (c)).

At the constant dynamic rate, strain-ageing does not occur, because of the short time available. Also, the upper yield points are much more pronounced, at all temperatures (Figs. 6 (f), (i), (l) and (o). At large strains, the strain-hardening is reduced by thermal softening, especially at room and lower temperatures (Figs. 6 (f) and (i).

Perhaps the results of the rate-jump tests on mild steel are the most interesting, as seen in Figs. 6 (g), (h), (j),(k), (m), (n), (p) and (q). At all temperatures, a well defined elastic stress increase can be observed on the traces following the strain-rate jump; at high temperatures this is followed by a sharp drop of stress to a lower yield point (Figs. 6 (m), (n), (p) and (q)). Flow continues at an increasing or decreasing stress, the strain-hardening rate depending on the test temperature and the amount of pre-strain.

SECTION 3

RESULTS AND DISCUSSIONS

3.1 Copper

3.1.1 Constant-strain-rate response

The quasi-static flow characteristics of OFHC copper at the strain rate of 0.003 s^{-1} and various temperatures are presented in Fig. 7, while those for a dynamic rate of about 900 s^{-1} are shown in Fig. 8. Each curve in these figures represents the average of at least two tests; variation of strain rate and flow stress values for an individual test did not exceed 5% at most from the values used in plotting the curves.

Yield and flow stresses as well as strain-hardening rates are seen to be sensitive to temperature. At any constant temperature, these quantities are also influenced by strain rate, as shown in Fig. 9 (a)-(f). No evidence of the discontinuous yielding or serrated flow, characteristic of impure metals, is observed at any temperature. Similarly, the flow curves at the higher rate do not show any drops in stress at yield, such as those found by Dowling et al. (1970) and Harding (1971) during impact punch loading on copper of commercial purity.

The temperature dependence of the flow stress at various values of strain is illustrated in Figs. 10 (a) and (b) for the two strain rates, 0.003 and 900 s^{-1} respectively. At the higher rate, flow stress values are expected to be reduced because of temperature rise which accompanies rapid plastic deformation; calculated curves showing the adiabatic temperature rise ΔT are plotted in Fig. 9. The measured flow stress value at any strain thus represents the specimen strength at a temperature slightly higher than that existing at the start of the deformation. Assuming that all the mechanical work is converted into heat, and that the effect of temperature history can be neglected, a correction can be made as shown in Fig. 10 (b); it is seen that the resulting change in flow stress is negligible at low strains or high temperatures, and amounts

to a maximum of about 10% at a strain of 0.5 and at the lowest temperatures covered. The actual corrections will be somewhat lower because of heat loss during deformation and the storage of some energy in the deformed lattice.

From the curves of Fig. 10 (a) and the corrected curves of Fig. 10 (b), the rate dependence of the flow stress may be determined as a function of specimen temperature. The mean strain-rate sensitivity may be defined as

$$\mu_{12} = (\tau_2 - \tau_1)/\ln (\dot{\gamma}_2 / \dot{\gamma}_1), \qquad (5)$$

where τ_1 and τ_2 are the flow stresses measured at an arbitrary strain γ and temperature T in the quasi-static and dynamic tests at rates $\dot{\gamma}_1$ and $\dot{\gamma}_2$ respectively. Values of μ_{12} are plotted against temperature in Fig. 11 and against strain in Fig. 12.

3.1.2 Strain-rate-change response

At each test temperature, the response of copper to quasi-static deformation followed by a sudden increase in strain rate was determined. The average result of at least two specimens subjected to nominally the same pre-strain and strain-rate history was calculated and plotted, together with the flow curves obtained in the constant-rate tests discussed above. These plots are also shown in Fig. 9; an estimate of the experimental accuracy involved has been made in I and is therefore not given here. Also shown in Fig. 9 are the variation of strain rate and the adiabatic temperature rise with strain during the high-rate deformation.

A significant first observation relates to the shape of the flow curves following the strain-rate change. At all testing temperatures, the curves are continuous and no stress drops are observed (see also the corresponding oscillograms in Fig. 4). Yield points have been observed by Zeyfang et al. (1974) when strain-rate changes in the range 10^{-4} to 10^{-6} s^{-1} were imposed during the deformation of high-purity copper single

crystals using an Instron tensile-testing machine at various temperatures, but these were explained in part by the overshoot of the Instron control system. Yield drops are frequently obtained in single and polycrystals of some f.c.c., b.c.c. and h.c.p. metals when subjected to a low-temperature pre-strain followed by additional deformation at a higher temperature; such a yield-point phenomenon at the beginning of re-straining is usually called 'work-softening' (Cottrell and Stokes, 1955; Kelly, 1956; Hammad and Nix, 1966; Sakui et al., 1968; Hammad et al., 1970; Longo and Reed-Hill, 1970; Güleç and Baldwin, 1973; Longo and Reed-Hill, 1974). The effect appears to occur only when unloading takes place between pre-straining and re-straining (Haasen and Kelly, 1957; Güleç and Baldwin, 1973). It can also be observed by pre-straining metals at a high strain rate followed by reloading at a lower strain rate (Langenecker, 1961; Sakui et al., 1968; Longo and Reed-Hill, 1970). However, in f.c.c. metals work-softening seems to occur only if the stacking-fault energy is moderate to high; it is not observed in copper, nor in α brass, which have low stacking-fault energies (Sakui et al., 1968), but is always encountered in aluminium and nickel. In this respect, it seems appropriate to recall the results of Frantz and Duffy (1972) for aluminium, in which small yield drops were always observed after a rapid increase in shear strain rate.

The curves of Fig. 9 indicate that the initial response to the strain-rate jump is approximately elastic at all temperatures; however, as already noted, a well-defined yield point is only found at low temperatures. The results clearly show that a mechanical equation of state relating stress, strain, strain-rate and temperature is not applicable under any of the test conditions. The observed rate dependence of the yield and flow stresses thus reflects two facts: (a) the yield stress at a given internal structural state depends on strain rate (and temperature); and (b) the structural state

and the corresponding strain-hardening after a given amount of plastic straining also depend on the strain rate at which the pre-straining took place. (In this context, the term internal structure covers features such as small-angle boundaries, subgrains and cells, the density and configuration of dislocations, dislocation tangles, etc.)

At any given pre-strain, the increment in flow stress $\Delta\tau$ following the change in strain rate can be taken as representative of the true or intrinsic rate sensitivity of the material. At all temperatures, the intrinsic rate sensitivity for copper is much lower than the apparent sensitivity based on flow curves obtained at constant strain rates. The intrinsic rate sensitivity at a given strain, $\bar{\mu}_{12}$, is defined as before for μ_{12} in Eq. (5), but here τ_2 is the yield stress exhibited at the end of the elastic increment prior to work-hardening. From the results shown in Figs. 9 (d), (e) and (f), corresponding to room temperature and above, it is not possible to determine τ_2 unambiguously, because of the absence of a well-defined yield point; $\Delta\tau$ is clearly very small, if not zero. Curves showing $\bar{\mu}_{12}$ at the lowest temperatures, for three values of strains, are plotted in Fig. 12.

According to the theory of thermally-activated plastic flow in metals (summarized by Li, 1967), the intrinsic rate sensitivity $\bar{\mu}_{12}$ is related to the activation volume V by the equation

$$\bar{\mu}_{12} = kT/V. \qquad (6)$$

In deriving this equation, it is assumed that the density of thermal activation sites remains constant during the change of strain rate, and that the activation volume is independent of temperature. It is clear that the results of Fig. 11 do not accord with this equation, since the curves for $\bar{\mu}_{12}$ do not pass through the origin.

Assuming that the rate-controlling process is that of dislocation intersection, V is expected to vary inversely as the square root of the forest - dislocation density; hence an increase in $\bar{\mu}_{12}$ with increasing plastic strain is predicted. Fig. 12 shows that the increase is quite small for a five-fold increase in strain.

It seems clear from the present results that (a) at all temperatures the major part of the observed strain-rate dependence in constant-rate tests must be attributed to change in dislocation structure with strain-rate history rather than to the instantaneous strain rate itself; (b) at low temperatures there is a significant dependence of the flow stress on the current strain rate; and (c) the temperature dependence of the rate sensitivity is not well described by the simple thermal-activation rate theory based upon a temperature-independent activation volume.

3.1.3. Micrographic examination

A dummy specimen was sectioned, polished and etched after annealing and the microstructure was found to be uniform, with no apparent directionality in the grain structure; about one-third of the grains showed annealing twins. Specimens were also sectioned, polished and etched after test, and some of the resulting micrographs are presented in Fig 13*. The microstructure was found to be little different from that of the unstrained material. Fig. 13 (b) shows that no significant grain growth occured at 400°C. In Fig. 13 (d) a few very narrow twin bands are visible which could be caused by mechanical twinning; the strain contributed by such twins would however be very small compared with the large strains imposed during the test. The mean grain density (.960 mm^{-2}) corresponds to about 7 grains across the wall thickness.

---

*It should be noted that the section is not necessarily through the axis of the specimen, so that the wall thickness may appear greater than its true value; this also applies in Figs. 20 and 26.

3.2 Titanium

3.2.1 Constant strain-rate response

Quasi-static and dynamic stress-strain curves for each of the six testing temperatures are plotted in Figs. 14 and 15 respectively; each curve was obtained from two or more tests, the results of which varied by not more than 5%. It should be noted that the dynamic test results at the two highest temperatures were obtained at slightly lower strain rates than those at lower temperatures.

Commercially pure titanium can be seen to exhibit a well-defined yield point at all temperatures and at both quasi-static and dynamic strain rates. Also, the flow stress continuously increases with strain up to fracture (designated in Figs. 14 and 15 by the letter F) except in some of the dynamic tests where the strain-hardening rate becomes zero at large strains. The considerable temperature sensitivity of the mechanical properties is evident from Figs. 14 and 15.

From the extensive research on titanium by Reed-Hill and his associates (Monteiro et al. 1970, Santhanam and Reed-Hill 1971, Garde et al. 1972) and by Doner and Conrad (1973), it is evident that dynamic strain-ageing is a very significant factor in the plastic deformation of this metal (when impure). This seems to occur in the temperature range of 700 to 800°K (Conrad et al. 1973); the exact temperature apparently tends to rise with increasing purity. For a titanium alloy of commercial purity, Garde et al. (1972) located this 'blue-brittle' temperature at 750°K. The dynamic strain-ageing phenomenon was found by Doner and Conrad (1973) to manifest itself in the occurrence of yield points, serrations in the stress-strain curves, a rise in the flow stress with increasing temperature, minima in the total elongation versus temperature curves and maxima in the strain-hardening rate versus temperature curves. In all these investigations, tensile specimens were used and low strain rates ranging from 10^{-2} to 10^{-5} s^{-1} were applied. The same phenomenon

is also indicated by the enhancement of creep strength (Kissel and Sinnott 1953, Luster et al. 1953) and high-cycle, long-life fatigue properties (Turner and Roberts 1968) in commercial-purity titanium in the temperature range 600 to 850°K.

The present tests on titanium were limited to a maximum of 673°K, and as far as could be discerned from the test records at the high temperatures none of the above manifestations of dynamic strain-ageing occurred(see Fig.14).

Stress-strain curves for each temperature are shown in Fig. 16 (a) - (f); in each figure, the variation of strain rate and the computed adiabatic temperature rise is shown for the dynamic test. Fig. 17 (a) shows the variation of yield and flow stress with temperature at the low strain rate. The yield stress and work-hardening rate increase steadily as the temperature decreases from 673 to 297°K, and the yield stress continues to increase as the temperature is reduced to 123°K; the work-hardening rate, however, decreases with fall of temperature below 297°K, increasing again at the lowest temperatures. This behaviour may be associated with the onset of twinning as an important mode of deformation (see Section 3.2.3).

Fig. 17 (b) shows the yield and flow stresses for the high strain-rate tests, the correction for adiabatic heating being indicated; as for copper, this correction is negligible at small strains or high temperatures.

Using the definitions already introduced the apparent rate sensitivity μ_{12} has been determined from the curves of Fig. 17 (a) and the corrected curves of Fig. 17 (b). The results are plotted in Fig. 18 (full lines) and, as for copper, μ_{12} shows a moderate increase with increasing strain; it also increases with temperature up to 200°C, falling somewhat at 400°C.

3.2.2 Strain-rate-change response

The response of the titanium specimens subjected to dynamic loading after various amounts of deformation at the low rate (0.006 s^{-1}) is shown in Fig. 16 (a) to (f) for the various starting testing temperatures. Each plotted curve is the average of at least two curves differing slightly (about 3%) in flow stress and strain-rate values and by a maximum of 0.015 in the amount of pre-strain. Also included in Fig. 16 are the average strain rate and adiabatic temperature rise as functions of strain, corresponding to the high-rate part of each test.

At no testing temperature does the rate increase produce transient stress maxima similar to the yield points observed by Santhanam et al. (1970) after a one-decade change in strain rate during quasi-static tension of commercially pure titanium. The flow stress increases rather smoothly and continuously. This increase is characterized by a well-defined elastic increment which is followed by gradual transition of the flow stress to a value similar to that obtained in a test entirely at the dynamic strain rate. Both the elastic stress increment and the rate of the subsequent transition depend on the testing temperature.

As discussed before for copper in section 3.1.2, the initial elastic rise in flow stress following a strain-rate increase can be used to calculate the intrinsic strain-rate sensitivity $\bar{\mu}_{12}$. The variation of $\bar{\mu}_{12}$ with strain at various temperatures is shown in Fig. 18 (broken curves). From the results given in Fig. 18, values of μ_{12} and $\bar{\mu}_{12}$ for a strain of 0.1 have been estimated, and these are plotted against temperature in Fig. 19. It is seen from this figure that at temperatures up to 473°K, $\bar{\mu}_{12}$ is proportional to T, as required for a constant activation volume V. The slope of the plotted line corresponds to a value V = 0.54 nm^3 or 22.4 b^3 where b is the magnitude of the Burgers vector. The value of $\bar{\mu}_{12}$ /T drops considerably at T = 673°K, and corresponds to V = 37.3 b^3. Assuming that V is governed

by the dislocation density, it appears that a significant degree of dislocation rearrangement and mutual annihilation must take place during the prestraining period (about 17 sec) at temperatures above 473°K. At strains larger than 0.1, the behaviour is more complex, since $\bar{\mu}_{12}$ decreases with increasing strain even at room temperature.

Fig. 19 also shows values of μ_{12} at a strain of 0.1, and it is seen that it is not proportional to T; thus the apparent activation volume $V^*_{12} = kT/\mu_{12}$ varies with temperature. The values at T = 123, 297 and 473°K are $11.1b^3$, $18.0b^3$ and $22.9b^3$ respectively. A comparison may be made with results obtained by Harding (1974) in constant-rate tensile tests on a similar material at temperatures in the range 77 to 288°K. These results give values of V^*_{12} varying from 11 b^3 at 77°K to 19.2 b^3 at 288°K, for a tensile strain of 0.05; in converting from the measured tensile stresses to equivalent shear stresses, von Mises' yield criterion has been used. The close similarity between the two sets of values is striking.

3.2.3 Micrographic examination

As discussed by Kocks and Westlake (1967), h.c.p. crystals do not have the five independent slip systems required for generalized polycrystalline deformation. As a result, twinning or other deformation processes must in general occur in these metals. Garde et al. (1973) show that in high-purity titanium deformed at 77°K about thirty percent of the total plastic strain is produced by twinning, while Madhav and Armstrong (1974) estimate that the proportion is fifty to eighty percent at 4.2°K. According to data of Santhanam et al. (Reed-Hill 1973) for commercial-purity titanium, the volume fraction twinned increases linearly with true strain, reaching 50% at a tensile strain of about 0.35, i.e. a shear strain of about 0.6; at a shear strain of 0.1, the fraction is about 13%. Observations by Harding (1974) showed that at a given temperature the density of twinning in titanium increases with rate of strain.

Fig. 20 shows a number of micrographs of specimens tested at low temperatures. Fig 20 (a) gives a general view of the unstrained flange and the heavily deformed gauge length, including the fracture region. Fig. 20 (b) shows the detail of the microstructure in the gauge length adjacent to the flange; twinning is evident in nearly all the grains, and in some grains two families of twins have been developed. Figs. 20 (c) and (d) show part of the gauge length of specimens subjected to two different amounts of pre-strain. Comparing Figs. 20 (b), (c) and (d), it appears that the density of twinning decreases with increasing pre-strain, while the width of the individual twin lamellae increases. This effect is also seen in Figs. 20 (e) and (f), which relate to tests at -150°C without and with pre-straining. Comparison of Figs. 20 (b) and (e) shows the increasing intensity of twinning as the temperature is reduced.

It is clear that, as expected, deformation twinning is an important mechanism of plastic straining in the present tests on titanium, and that some changes take place in the amount and nature of twinning within the range of test conditions used. A quantitative analysis of these changes has not been attempted, but they may account for some of the secondary features of the observed flow behaviour, e.g. the reduction in the 'jump' stress level with increasing pre-strain.

The initial grain density (75 mm^{-2}) corresponds to only about 3 grains across the wall thickness of the specimen; even with this low value, however, there are about 1400 grains on the cross-section.

3.3 Mild Steel

3.3.1 Constant strain-rate response

Experimental data for mild steel were found to be of similar consistency and accuracy to those for titanium. Figs. 21 and 22 show the stress-strain curves obtained at various temperatures for the quasi-static and dynamic strain rates respectively. These are also included in Figs. 23 (a) to (f), in which the effect of strain rate on the flow curves at each temperature can be more easily seen. The low-rate results show the occurrence of dynamic strain-ageing (Baird 1971, 1973; Reed-Hill 1974), the work-hardening rate at low strains being greatest at 200°C, when the stress-strain curve is serrated. Similar 'jerky flow' was observed at 100 and 300°C ('blue brittleness').

At all temperatures, a significant drop of stress occurred at yield in the dynamic tests. In the low-rate tests, on the other hand, no yield drops were obtained, though at room temperature the curve shows a small plateau at yield.

Figs. 24 (a) and (b) show the flow stresses at four strains plotted against temperature, for low and high rates respectively. In Fig. 24 (b) the temperatures are instantaneous values calculated on the assumption that the deformation is adiabatic. The influence of strain-ageing is clearly seen in the curves of Fig. 24 (a). From the curves of Fig. 24 (b), it appears that the flow stress reaches a minimum at a temperature of about 700°K; this agrees with results obtained in an earlier investigation covering initial temperatures up to 773°K (Stevenson and Campbell 1974).

An increase in the blue-brittleness temperature with strain rate is expected from the theory of Cottrell and Bilby (1949); such an increase was observed in tensile and Charpy tests of annealed 4340 steel by Clough et al. (1968), who showed that their results indicated the operation of a thermally-activated process with an activation energy of 37.4 k cal/gm mole

(1.62 eV). Such a process would imply, for a strain rate of 10^3 s^{-1}, a peak in the flow stress at about 750°K. From the present results and those of Stevenson and Campbell (1974), it seems clear that for mild steel the peak occurs at a considerably higher temperature than this, the activation energy being correspondingly lower. Assuming that the activation energy is that for diffusion of carbon (∿ 20 k cal/gm mole), the peak dynamic strength would be expected at a temperature of about 1240°K (967°C), i.e. above the austenite transition temperature.

It is clear that for mild steel the flow stress is governed not only by the instantaneous strain rate per se, but by the time available for strain-ageing to occur and also possibly by structure changes brought about through variation of the strain rate. The apparent rate sensitivity μ_{12} exhibits negative values in the temperature range where strain-ageing can occur in the quasi-static test but has little effect in the dynamic test. Such negative values are of importance in metal-forming or other high-temperature, high-rate processes but they give no indication of the intrinsic rate sensitivity of the material, which can only be measured by the strain-rate-change technique.

3.3.2. Strain-rate-change response

At each testing temperature, rate-jump tests were carried out at several different values of pre-strain, and the results of these tests are plotted in Figs. 23 (a) - (f), together with the corresponding curves for strain rate and adiabatic temperature rise.

The following observations can be made concerning features common to all these results.

(1) There is a very rapid rise in stress level following the rate change.

(2) The jump yield stress is always higher than the flow stress attained at the same strain in the exclusively dynamic test. This behaviour is in contrast to that exhibited by copper and

titanium as shown in Figs. 9 and 16; it has, however, been observed at medium rates in the b.c.c. metals molybdenum and niobium (Campbell and Briggs 1974), and also in low-rate tests involving various rate-change ratios, with and without intermediate unloading, on mild steel (Smith 1961, Tanaka et al. 1972), as well as in HF-1 steel (Chou and Ting 1974). Moreover, it also occurs in temperature-change tests involving pre-straining at RT followed by further straining at a much lower temperature (Nakamura et al. 1968).

It is also worth remarking that the behaviour of mild steel has also been found to differ considerably from that of f.c.c. metals, when the deformation is continued at a strain rate lower than that of pre-straining (Klepaczko 1968, Campbell and Duby 1956, Tanaka et al. 1972).

The initial jump of stress is followed by a yield drop at 200 and 400°C, but not at lower temperatures; this behaviour is evidently linked to the occurrence of dynamic strain-ageing during the low-rate pre-straining, the effect being greatest at 200°C. At each temperature, the initial stress jump is approximately the same at all pre-strains; the subsequent work-hardening rate, however, tends to decrease with increasing pre-strain, becoming negative for large pre-strains. It seems unlikely that thermal softening is entirely responsible for these negative work-hardening rates.

The value of the initial stress increment varies considerably with temperature, as shown in Fig. 25, where the intrinsic rate sensitivity $\bar{\mu}_{12}$ is plotted for a pre-strain of $\gamma = 0.2$, interpolating from the results obtained at other pre-strains. For the two highest temperatures, points are plotted corresponding to both upper and lower yield points. Also shown in this figure are radial lines corresponding to constant values of V/b^3, where $V = kT/\bar{\mu}_{12}$, the activation volume calculated on the assumption of a constant pre-exponential factor during the stress increment. From these

it follows that if this assumption is correct V increases rapidly with T.

It is clear from the curves of Fig. 23 that even a relatively small amount of quasi-static pre-strain affects the dynamic flow stress at large strains; it seems therefore that the dislocation structure of the material is strongly dependent on the strain-rate history, and that the 'memory' of previous straining persists for very large changes in strain.

3.3.3 Micrographic examination

It is well known that deformation twins (Neumann bands) are formed in iron under impact or low-temperature conditions. The present mild steel specimens were therefore sectioned, polished and etched after testing; Fig. 26 shows a selection of the microstructures observed in the gauge length of specimens fractured in dynamic and rate-jump tests at various temperatures. Figs. 26 (b) and (c) show that twinning occurs at -100 and -150°C in dynamically strained specimens, the density of twinning increasing as the fracture surface is approached; at higher temperatures twinning is not found. Figs. 26 (d), (e) and (f) show that very few twins are formed in specimens deformed dynamically after pre-straining, even at low temperatures. In general it seems that the contribution of twinning to the total plastic strain is small.

The micrographs show that there is a region of heavily deformed material in the immediate vicinity of the fracture surface, as is to be expected; apart from this region, however, the structure remains fairly uniform along the gauge length. Micrographs obtained from transverse specimens showed no significant difference in microstructure, apart from the lack of banding of the pearlite. The mean grain density was found to be 690 mm^{-2}, corresponding to about 10 grains across the wall thickness of the specimen.

3.4 General Flow Behaviour

3.4.1 Micro-mechanical aspects

Assuming that the major contribution to the observed plastic strain rate is by the motion of dislocations, the general rate equation (1) may by replaced by Orowan's kinematic relation

$$\dot{\gamma}^p = b\rho_m \bar{v} \quad , \tag{8}$$

where b is the magnitude of the Burgers vector, ρ_m is the density of mobile dislocations and $\bar{v}$ is their average velocity. Various forms of constitutive equation have been derived from (8) by assuming functional relations for the quantities ρ_m and $\bar{v}$ in terms of γ^p and the applied stress τ (Johnston and Gilman 1959, Hahn 1962). However, it appears from the present results that in general $\dot{\gamma}$ depends not only on the current values of γ^p and τ but on the strain-rate history. Since there is no experimental method of measuring ρ_m or $\bar{v}$ during a test on a polycrystalline material, it is not possible to determine which of these is history-dependent; in fact there is a basic difficulty in making such a distinction if the local dislocation velocities are distributed continuously over a wide range of values.

It may be noted however that, in order to account for the present results, especially those for copper and mild steel, the variation in either ρ_m or $\bar{v}$ with strain-rate history would have to be several orders of magnitude. Assuming a constant value for the rate-sensitivity parameter μ_{12} over the strain-rate range involved, it follows that

$$\frac{(\rho_m \bar{v})_j}{(\rho_m \bar{v})_d} = \left(\frac{\dot{\gamma}_2}{\dot{\gamma}_1} \right)^{1-\bar{\mu}_{12}/\mu_{12}} \tag{9}$$

where the subscript j indicates the value immediately after the strain-rate jump and the subscript d the value which would correspond to the same stress

and strain under constant-rate conditions. Thus for copper at low temperatures where $\bar{\mu}_{12}/\mu_{12}$ is about 0.5 (see Fig. 11), $\rho_m \bar{v}$ must vary by a factor of order 10^3; at room temperature and above, the factor is larger still. Studies of dislocation mobility in copper (Greenman, Vreeland and Wood 1967) have shown that the velocity of individual dislocations increases approximately linearly with the applied stress, reaching high velocities at quite low stresses. It seems unlikely therefore that in the present experiments the velocities of individual mobile dislocations can increase greatly during the small stress increment in a jump test.

From these considerations, it seems likely that a large increase in the number of mobile dislocations occurs when the strain rate is suddenly increased. Such a dependence of ρ_m on stress and strain-rate history is implicit in the theory of Alden (1972, 1973, 1975), in which the variation in dislocation structure is taken into account. It is supposed that at low rates or high temperatures a cellular dislocation structure is formed so that considerable regions of the slip plane are relatively free of dislocations. When the rate is suddenly increased, dislocations break free from the cell walls and move into these regions. The theory predicts that the stress increases gradually towards the value characteristic of the high strain rate, as is found experimentally for copper in the present tests.

The effect of strain-rate history on plastic flow has also been discussed by Klepaczko (1975). He has pointed out that in general part of the flow stress is governed by evolutionary changes in dislocation structure, which may be diffusion controlled. Such evolutionary changes are explicit functions of time, rather than of strain rate. Thus the flow stress at a given strain and temperature may be considered to be the sum of an 'athermal' component τ_A which is time dependent, and a thermal component τ^* which is

dependent on the instantaneous strain rate and is governed by the rate-controlling dislocation mechanism. For pure f.c.c. metals τ_A decreases with time because of mutual annihilation of dislocations (dynamic recovery); for impure b.c.c. metals, it may increase with time because of diffusion-controlled dislocation locking (dynamic strain ageing). The latter effect is shown very clearly in the present results for mild steel at 200°C.

The changes which occur both in the mobile dislocation density and in the uniformity of the dislocation distribution during straining clearly imply that in general the flow stress depends on the previous strain-rate (and temperature) history. The general approach discussed in the Introduction, leading to equation (1), should in principle be capable of describing the present results; however, the usefulness of this approach is limited by the difficulty of identifying the large number of unknown functions and parameters involved. In particular, the number of terms in the summation and the laws relating the parameters s_i to the macroscopic variables cannot at present be determined. For practical purposes therefore it is necessary to adopt a more empirical approach, in which functional relationships are postulated without reference to the micro-mechanisms of flow. Such a relationship can be expected to be useful over limited ranges of the variables involved, and the appropriate ranges can only be established by experiment.

3.4.2 Macroscopic constitutive relations

The approach discussed by Klepaczko (1975) leads to a constitutive equation of the form

$$\tau = \tau_A (T, t, \gamma) \left[1 + f (T, \dot{\gamma}) \right] . \qquad (10)$$

It follows from this that if the strain rate is instantaneously changed, a finite increment in stress should occur. The present data for copper at low temperatures, and for titanium and mild steel at all temperatures, show such an increment. For copper at room temperature and below, however, the increment is very small or zero so that thermal activation appears to have little influence on the flow behaviour; thus the major reason for the variation in flow stress with strain rate is the strain-rate history.

The present results show that for copper at room temperature the stress difference between a jump-test curve and the low-rate curve depends on the incremental strain but is approximately independent of pre-strain (and hence time) for values of pre-strain from zero to 0.6. Thus it has been suggested (Campbell, Eleiche and Tsao 1975) that the flow stress may be represented by an hereditary integral or functional of the strain rate, with strain as the independent variable. The constant-rate data for copper may be expressed by the equation

$$\tau = f_1 (\gamma) + f_2 (\gamma, \dot{\gamma}), \qquad (11)$$

as suggested by Malvern (1951). For a strain-rate jump from $\dot{\gamma}_1$ to $\dot{\gamma}_2$ at a pre-strain α, (11) becomes

$$\tau = f_1 (\gamma) + f_2 (\gamma, \dot{\gamma}_1) + f_2 (\gamma - \alpha, \dot{\gamma}_2) - f_2 (\gamma - \alpha, \dot{\gamma}_1). \qquad (12)$$

Assuming linear superposition of the 'overstress' $f_2 (\gamma, \dot{\gamma})$, (12) can be generalized, for an arbitrary variation of strain rate given by $\dot{\gamma} = \eta(\gamma)$, as

$$\tau = f_1(\gamma) + f_2(\gamma, \eta_o) + \int_0^{\gamma} f_2'\left[\gamma - \alpha, \eta(\alpha)\right]\eta'(\alpha)\, d\alpha, \quad (13)$$

where

$$\eta' = d\eta/d\gamma, \quad f_2' = \partial f_2/\partial\dot{\gamma} \quad \text{and} \quad \eta_o = \eta(o).$$

Equations (11) and (12) have been shown (Campbell, Eleiche and Tsao 1975) to describe the present constant-rate and jump-test results for copper at room temperature, within experimental accuracy. Similar agreement is found for the results obtained for the same material at 200 and 400°C.

Further experiments using varying strain-rate histories are required to determine whether the more general equation (13) is valid.

For titanium, the data indicates that the effect of strain-rate history is relatively small, while the influence of the instantaneous strain rate is large. Thus the behaviour is nearer to that corresponding to a mechanical equation of state. However, significant deviations occur from such an equation; at low temperatures these deviations are of the same type as those observed in copper.

The behaviour of mild steel is more complex because of the yield drop at high rates and the occurrence of dynamic strain-ageing at elevated temperatures, with the consequent jerky flow. Both these effects are related to the pinning of dislocations by solute atoms, with a corresponding reduction in mobile dislocation density. One result of dynamic strain-ageing is that the total flow stress at high rate depends crucially on the degree of pre-straining; it may be very much higher than that obtained in a test at a high constant rate. This fact may be of considerable importance in processes such as machining, in which large increases in strain rate occur during plastic flow. A general constitutive relation for mild steel would be very complex, since temperature, time, strain rate and strain-rate history are all important in determining the flow stress.

SECTION 4

SUMMARY AND CONCLUSIONS

4.1 OFHC Copper

The flow stress is moderately rate and temperature sensitive at all strains up to 1.0 or more. At constant rates strain hardening is positive for shear strains up to 1.0, adiabatic heating at high strain rates having only a small effect.

A rapid change in strain rate by about 6 orders of magnitude causes a finite elastic stress increment at low temperatures. The magnitude of this increment increases with increasing pre-strain; at room temperature or above, the increment is very small; the subsequent flow stress rises slowly toward that required for the same strain imposed entirely at the high rate. Thus the observed rate sensitivity of the flow stress in constant-rate tests appears to be caused largely by strain-rate history effects, rather than by the instantaneous strain rate. Activation volumes, calculated either from the constant-rate data or from the elastic stress increments in the rate-jump tests, decrease with increasing strain and increase with increasing temperature.

The data are not consistent with the existence of a mechanical equation of state relating stress, strain, strain rate and temperature. It is concluded that in general the flow stress consists of a rate-independent component and components depending on the instantaneous strain rate and the strain-rate history. The second of these components is small, becoming measurable only at low temperatures; the third component can be described by means of an hereditary integral with strain as the independent variable.

4.2 Commercially-Pure Titanium

The material shows a well defined yield point, but no yield drop, at all temperatures. The strain-hardening rate is small, decreasing with increasing temperature but varying little with strain rate. Adiabatic heating causes significant reduction of flow stress at large strains, but

no flow instability occurs at strains up to 0.5.

In rate-jump tests, there is a large increment of stress at all temperatures. The value of the increment varies little with pre-strain but increases with temperature. At high temperatures the flow stress exceeds that obtained at a constant high rate. Strain-rate-history effects are much less marked than those in copper, while the instantaneous strain rate has a large influence. Thus the behaviour approximates more closely to that corresponding to a mechanical equation of state.

The activation volume for a strain of 0.1, calculated from the response to the strain-rate change, is essentially constant for temperatures up to 200°C; at 400°C a larger value is found, which is attributed to recovery processes occurring during pre-straining and causing a reduction in the dislocation density.

Micrographic examination confirms the importance of twinning as a deformation mechanism for static, dynamic and rate-jump tests. The distribution and size of twins varies with the amount of pre-strain in rate-jump tests.

4.3 Mild Steel

The low strain-rate results show a well-defined elastic limit but no yield drop; a small yield plateau is found at room temperature. The subsequent strain hardening shows a maximum at 200°C, when serrated flow occurs and the ductility is reduced (blue brittleness).

The high strain-rate results show a considerable drop of stress at yield. The post-yield flow stress decreases steadily with increasing temperature, apparently reaching a minimum at or above 400°. At room temperature and below, the strain-hardening rate becomes negative at large strains; this is attributed to the adiabatic temperature rise.

The initial response to a strain-rate jump is approximately elastic and has a magnitude which increases with decrease of testing temperature; it is little affected by the amount of pre-strain. At 200 and 400°C a yield drop occurs after the initial stress increment. The post-jump flow stress is always greater than that for the same strain in a constant-rate dynamic test; the strain-hardening rate becomes negative at large strains or low testing temperatures.

The activation volume, calculated from the initial stress increment in the jump tests, increases rapidly with increasing temperature. Micrographic examination shows that twinning occurs in specimens strained dynamically at temperatures below about -50°C. The amount of twinning is dependent on strain-rate history as well as on strain rate and temperature; it does not correlate in a simple manner with applied stress, since less twinning is observed in jump-test specimens than in specimens deformed entirely at the high rate, in spite of the larger stresses occurring in the former.

4.4 General

It has been shown that, in general, the rate dependence of the flow stress of a metal or alloy may be attributed to either or both of the following:

(a) the instantaneous strain and strain rate;

(b) the strain-rate history since the material was in the annealed state.

The relative importance of these two factors varies between materials. For the three tested, (a) appears to be dominant for titanium and (b) for copper, while for mild steel both factors are important.

Strain-rate-history effects are indicative of structure changes which take place during the deformation; such changes may be diffusion controlled or governed by micro-mechanisms (dislocation interactions, occurrence of twinning)

which depend on the deformation processes themselves.

In addition to the factors (a) and (b), the observed rate dependence may be affected by thermal softening caused by adiabatic heating. For copper, such softening is small, because of the relatively low temperature sensitivity of the flow stress; for titanium and mild steel, thermal softening may exceed strain hardening so that the flow stress falls with increasing strain. However, in the present experiments no catastrophic load drops occurred at strains less than 0.4, even at low temperatures; at room temperature and above, much larger strains were attained before fracture, the stress falling quite gradually during the latter part of the test. Thus no evidence was obtained, from the material response or from micrographic examination, of plastic instability causing highly localized flow at an early stage of deformation.

APPENDIX A

Theoretical wave analysis and actual observed wave structure as affected by the performance of the present clamp design

Fig. A1 shows the bar arrangement and dimensions, together with a characteristic x-t diagram of the elastic torsional wave fronts during a rate-change test and the corresponding torque equilibrium in the testing system. Only torsional waves are considered in this figure since the performance of the clamp is assumed to be ideal; possible generation of bending and axial waves when the clamp is released are therefore neglected.

Typical records obtained during the rate-change tests showed, however, certain characteristics in the output traces which are not predicted from Fig. A1. Thus, the trace level was not constant before the arrival of the main pulse to the output torque gauge station, and a marked dip was observed at about 800 μs after the start of the main pulse. These features were consistently obtained with copper, but were almost undetected with titanium or steel, as can be seen from the corresponding oscillograms. In I, it was suggested that when the clamp is released, axial waves are also initiated which travel at a higher speed down the two bars and are reflected partly as torsional waves at the motor end. Times of arrival of various ripples on the output trace agreed fairly well with this explanation.

Two other hypotheses have been examined in order to explain the source of axial waves in the system and the generation of the torsional precursor and reflected waves associated with it. The first hypothesis was based on the possible accumulation of specimen axial strain which may be associated with the large plastic twist during quasi-static

straining , as reported by Swift (1947) and Ronay (1965, 1967). To check this, the specimen gauge length was carefully measured before and after twisting to a shear strain of about 1.0; within experimental accuracy , no elongation was found. Furthermore, measurement was taken on the output bar of possible axial strains which may be produced by the slow rotary unit during quasi-static loading and none could be detected.

Next, the performance of the clamp was studied more carefully. Axial waves may be initiated when the clamp is released if the two opposite arms of the clamp are not exactly symmetrical with respect to the bar axis, or due to elastic lateral strains occurring at the input-bar section underneath the clamp. This can also result from the method of tightening the clamp to fracture the notched bolt holding its two arms together, since this is done usually by means of a lever or a torque wrench from only one side of the bar system. In order to investigate this experimentally, a dummy titanium specimen was attached to the input and output bars and the clamp subsequently tightened until fracture, without previously storing any torque in the input bar. Torsional and axial strains were both measured with strain gauges and an oscilloscope. Typical results of one such test are shown in Fig. A2 where the top and lower traces represent torsional and axial strains in the output bar respectively, both traces being delayed 100 μs after the clamp release. A tensile pulse followed by a torsional pulse of almost the same duration (~50 μs) can be seen to initiate at the clamp and to propagate and reflect at end obstacles along the system. This wave structure may explain therefore the peculiarities observed on the output torque trace in a rate-jump test. Thus, in this case, the axial pulse precedes the main torsional wave propagates down the

system and through the short plastically twisted specimen. This results in a combined axial and torsional wave, the degree of the interaction being mainly governed by the amplitude and duration of the axial pulse and the strain-rate sensitivity of the material tested (Clifton 1966, Lipkin and Clifton 1968, Hsu and Clifton 1974). This can also be observed in the oscillograms of Fig. A3, each showing as the top trace the signal from the output-bar torque gauges and as the lower trace the signal from the output-bar axial gauges; the latter gauges were centred 92mm further from the specimen than the former, i.e. 178mm from the end of the bar.

Fig. A3 (a) shows the results of an exclusively dynamic test. The same copper specimen was then used in a rate-change test; the result is shown in Fig. A3 (b). Finally, Fig. A3 (c) shows the results obtained in a clamp-release test with no torque stored in the input bar. As discussed before, Fig. A3 (b) is typical of the results obtained on copper in the course of the present research programme. Various features of the output trace, together with their arrival times at the measuring station can be fairly well predicted through an x-t diagram similar to that of Fig. A1 in which axial waves are also taken into account. That such features were almost unobservable in rate-change tests on titanium and steel can be explained by the difference in strain-rate sensitivity between these two materials and that of copper, as reported by Hsu and Clifton (1974).

APPENDIX B

Arrangement for testing at sub-ambient temperatures

Cooling below room temperature was carried out by controlling the flow of liquid nitrogen into a short horizontal container surrounding the specimen, which was directly attached to the input and output bars with Araldite epoxy cement. Two general views of the cryostat can be seen in Fig. B1, and these are self-explanatory.

Fig. B2 shows the container on its support, the specimen and parts of the input and output bars. Two glass-wool rings are used for insulation and strain-gauge protection. A copper-constantan thermocouple bead can be seen soldered to the brass gauze for temperature control, while specimen temperature was measured by a separated-junction copper-constantan thermocouple which is taped to one of the specimen shoulders.

A general view of the associated instrumentation used in low-temperature testing is shown in Fig. B3. This consists as usual of a millivolt potentiometer as a temperature read-out and a temperature controller energizing a valve in the flow path of the liquid nitrogen from its container to the specimen cryostat.

As mentioned above, all specimens were attached directly to the bars with Araldite epoxy cement which proved to be a reliable adhesive at all low temperatures down to -186°C. Temperature gradients along the bars within the cryostat were not serious enough to warrant the use of tapered extension pieces or to require modification of the method of data reduction. Proper strain-gauge factors were used, however; these were determined by direct calibration at each testing temperature. In addition, tests performed with dummy specimens indicated that the input wave propagated throughout the bar system without distortion.

APPENDIX C

Bonding of the test specimen to the torsion bars in split-Hopkinson-bar experiments for testing at various temperatures

The torsional version of the split Hopkinson-bar method of testing materials at dynamic strain rates has proved its superiority over the axial version for determining the flow stress of materials, especially at large strains. The major, and perhaps the only serious difficulty facing the experimenter in using this apparatus is the devising of a reliable method for bonding the specimen to the input and output bars. Under testing conditions, such bonds should be rigid enough to withstand the input torque so that the observed partition of the travelling waves into reflected and transmitted portions can be considered as truly representative of the specimen deformation.

For testing at room and lower temperatures down to liquid nitrogen temperature (-186°C), the difficulty can be overcome by using suitable industrial epoxy cements, such as Araldite, which combine strength with fast setting at room temperature.

For elevated-temperature testing, industrial adhesives can no longer be used with complete reliability since most common epoxies lose their strength drastically at high temperatures (Cotter and Mockney 1974). Even for those bonding systems specially designed for high-temperature applications, such as Polyimide adhesives, a maximum temperature of 250°C is usually recommended for bonds of moderate strength. Furthermore, the curing of these adhesives is generally elaborate and complicated and appears to be more of an art than systematic procedure. Although such adhesives have been used successfully in previous work for bonding aluminium specimens to stainless steel bars for testing at temperatures up to 250°C

(Eleiche and Duffy 1975), it was felt worthwhile to develop other methods for bonding various dissimilar materials for reliable use at higher temperatures.

Various possibilities have been reported in the literature (Zimmer 1963, Oberle et al. 1965, Thackery and Dugdale 1972). These and other methods include: brazing, inertia welding, electron-beam welding, powder-metallurgy techniques, mechanical bonding, or a combination of these, according to the materials to be bonded, their thermal coefficients of expansion and the maximum application temperature.

In terms of cost, reliability, availability and bonding time, only brazing and mechanical joining were considered attractive. The aim was to bond copper, mild steel and titanium specimens directly or indirectly to the titanium torsion bars. In I, a solution was adopted for bonding copper at temperatures up to 400°C indirectly to the bars by use of silver brazing, intermediate stainless-steel extension tubes and room-temperature epoxy adhesive. The same procedure worked successfully with the mild-steel specimens. With titanium, however, it was impossible to braze the specimens to stainless steel with the silver solder, and although special brazing alloys containing 80% palladium are apparently available (NASA 1965), their cost and application requirements were found difficult enough to make further trials of this method discouraging.

Various mechanical assemblies were subsequently tried. These ranged from axial threaded joints to the use of lateral screws to grip the specimen flanges, and shrink-fitting. None of these proved reliable, since wave distortion always occurred to different degrees when dummy specimens were tested. A final mechanical assembly was designed, which proved successful. As shown in Figs. C1 and C2, it consists of two stainless steel grips resting flat on the specimen flanges and attached to each by means of four axial Allen screws. The whole assembly is subsequently brazed to stainless-steel extension tubes which are in turn cemented to the

titanium bars with Araldite. Tests with dummy specimens were not found completely ideal, as can be seen from results obtained at 200 and 400°C, shown in Fig. C3. Nevertheless, they were considered acceptable, especially since in testing a standard specimen only a small portion of the input torque is usually transmitted through the specimen because of its yielding and further plastic deformation. Results shown in the main text (see Figs. 5 (h), (i), (j) and (k)) also indicated the reliability of this method of assembly since all traces were found to be fairly smooth with no indication of reflections occurring at any of the joints.

REFERENCES

Alden, T.H. 1972 Phil. Mag. 25, 785. 1973 Met. Trans. 4, 1047. 1975 Met. Trans. 6A, 1597.

Baird, J.D. 1971 Metall. Rev. No. 149, Metals and Mater. 5, 1. 1973 'The Inhomogeneity of Plastic Deformation', p.191, A.S.M., Metals Park, Ohio.

Barraclough, D.R. and Sellars, C.M. 1974 'Mechanical Properties at High Rates of Strain' (Ed. J. Harding), p.11, Conf. series No. 21, Inst. Physics, London.

Bocek, M. 1975 Mat. Sci. Eng. 17, 31.

Campbell, J.D. and Duby, J. 1956 Proc. Roy. Soc. (London) A236, 24.

Campbell, J.D., Eleiche, A.M. and Tsao, M.C.C. 1975 Battelle Colloquium on Fundamental Aspects of Structural Alloy Design (to be published).

Campbell, J.D. and Briggs, T.L. 1974 J. Less Common Met. 40, 235.

Chou, S-C. and Ting, T.C.T. 1974 Proc. Symp. Mech. Behaviour of Materials, Kyoto, Japan, 63.

Clifton, R.J. 1966 Proc. 5th U.S. Nat. Cong. Appl. Mech. Univ. of Minnesota, 465.

Clough, W.R., Jackman, L.A. and Andrew, Y.G. 1968 J. Basic Engineering, Trans. ASME 90D, 13.

Conrad, H., Doner, M. and de Meester, B. 1973 'Titanium Science and Technology' (Ed. R.I. Jaffee and H.M. Burte), p.969, Plenum Press, New York.

Cotter, J.L. and Hockney, M.G.D. 1974 Int. Metall. Reviews 19, Review 183, 103.

Conrad, H., 1966 Acta Met. 14, 1631.

Cottrell, A.H. and Bilby, B.A. 1949 Proc. Phys. Soc. 62A, 49.

Cottrell, A.H. and Stokes, R.J. 1955 Proc. Roy. Soc. (London) A223, 17.

Doner, M. and Conrad, H. 1973 Met. Trans. 4, 2809.

Dowling, A.R., Harding, J. and Campbell, J.D. 1970 J. Inst. Metals 98, 215.

Eleiche, A.M. and Campbell, J.D. 1974 Rep. No. 1106/74, Dept. Engng. Sci., Univ. of Oxford.

Eleiche, A.M. and Duffy, J. 1975 Int. J. Mech. Sci. 17, 85.

Frantz, R.A., Jr. and Duffy, J. 1972 J. Appl. Mech., Trans. ASME 39E, 939.

Garde, A.M., Santhanam, A.T. and Reed-Hill, R.E. 1972 Acta Met. 20, 215.

Garde, A.M., Aigeltinger, E. and Reed-Hill, R.E. 1973 Metall. Trans. 4, 2461.

Greenman, W.F., Vreeland, T., Jr., and Wood, D.S. 1967 J. Appl. Phys. 38, No. 9, 3595.

Güleç, A.S. and Baldwin, D.H. 1973 Metall. Trans. 4, 1315.

Haasen, P. and Kelly, A. 1957 Acta Met. 5, 192.

Hahn, G.T. 1962 Acta Met. 10, 727.

Hammad, F.H. and Nix, W.D. 1966 Trans. ASM. 59, 94.

Hammad, F.H., Ahlquist, C.N. and Nix, W.D. 1970 Met. Trans. 1, 2179.

Harding, J. 1971 Acta Met. 19, 1177.

1974 Tech. Rep. No. 1108/74, Dept. Engng. Sci., Univ. of Oxford.

Hart, E.W. 1970 Acta Met. 18, 599.

Holloman, J.H. 1947 Trans. AIME 171, 535.

Hsu, J.C.C. and Clifton, R.J. 1974 J. Mech Phys. Solids 22, 233.

Jonas, J.J., Sellars, C.M. and Tegart, W.J. McG. 1969 Metall. Rev. 14 (No. 130) 1.

Johnston, W.G. and Gilman, J.J. 1959 J. Appl. Phys. 30, 129.

Kelly, A. 1956 Phil. Mag. 1,835.

Kissel, W.R. and Sinnott, M.J. 1953 Trans. AIME 197, 331.

Klepaczko, J. 1968 J. Mech. Phys. Solids 16, 255.

1975 Mat. Sci. Engng. 18, 121.

Kocks, U.F. and Westlake, D.G. 1967 Trans. AIME 239, 1107.

Kocks, U.F., Argon, A.S. and Ashby, M.F. 1975 'Thermodynamics and Kinetics of Slip'. Progress in Materials Science 19, Pergamon Press, Oxford.

Langenecker, B. 1961 Acta Met. 9, 937.

Li, J.C.M. 1967 'Dislocation Dynamics' (ed. A.R. Rosenfield et al.) p.87, McGraw-Hill, New York.

Lipkin, J. and Clifton, R.J. 1968 Proc. 12th Int. Cong. Appl. Mech., Stanford Univ., 292.

Longo, W.P. and Reed-Hill, R.E. 1970 Scripta Met. 4, 765.

1974, Metallography 7, 181.

Ludwik, P. 1909 Elemente der technologischen Mechanik, Springer, Berlin.

Luster, D.R., Went, W.W. and Kaufmann, D.W. 1953 Mater. and Methods 37, 100.

Macgregor, C.W. and Fisher, J.C. 1946 Trans. ASME 68, A-11.

Madhav, N.M. and Armstrong, R.W. 1974 Metall. Trans. 5, 1517.

Monteiro, S.N., Santhanam, A.T. and Reed-Hill, R.E. 1970 in The Science, Technology and Application of Titanium, p.503, Pergamon Press, New York.

Nakamura, T., Sakui, S. and Ohtakara, Y. 1968 Trans. JIM 9, Supplement, 905.

NASA 1965 Tech. Brief 65-10060, (March 1965).

Oberle, T.L., Loyd, C.D. and Carlton, M.R. 1965 Metal Progress 87, 104.

Reed-Hill, R.E. 1973 'The Inhomogeneity of Plastic Deformation'. p.285, A.S.M., Metals Park, Ohio.

1974 Reviews on High Temperature Materials 2, 217.

Ronay, M. 1965 British J. Appl. Phys. 16, 727.

1967 Int. J Solids Structures 3, 167.

Sakui, S., Sato, K., Abe, K., Kakuma, T. and Mori, T. 1968 Trans. JIM, 9, Supplement, 899.

Santhanam, A.T., Ramachandran, V. and Reed-Hill, R.E. 1970 Met. Trans. 1, 2593.

Santhanam, A.T. and Reed-Hill, R.E. 1971 Met. Trans. 2, 2619.

Smith, R.C. 1961 Exp. Mech. 1, 153.

Stevenson, M.G. and Campbell, J.D. 1974 Rep. No. 1098/74, Dept. Engng. Sci., Univ. of Oxford.

Swift, H.W. 1947 Engineering 163, 253.

Tanaka, K., Nofima, T. and Ishikawa, H. 1972 Proc. 15th Congress Materials Research, 99.

Thackery, P.A. and Dugdale, R.A. 1972 Atom, No. 187.

Turner, N.G. and Roberts, W.T. 1968 J. Less-Common Met. 16, 37.

Zener, C. and Hollomon, J.H. 1944 J. Appl. Mech. 15, 22.

1946 J. Appl. Mech 17, 69.

Zeyfang, R. Buck, O. and Seeger, A. 1974 Phys. Stat. Sol. (b) 61, 551.

Zimmer, F. 1963 Metal Progress 8 , 101.

TABLE 1

Composition of materials tested

a) Copper (OFHC)

Analysis of polycrystalline copper specimen material (ppm)

Ca	Fe	Pb	Mg	Ag	Na
<1	<1	1	<1	70	<1

Gas analysis of polycrystalline copper specimen material (ppm)

O	H	N
31.5	2.4	1.0

b) Titanium (IMI 130)

Typical maximum metallic impurity levels (ppm)

Al	500	Cu	200	Si	200
As	5	Fe	300	Sn	500
Cd	5	Mg	20	Ta	15
Co	5	Mn	500	V	500
Cr	10	Ni	15	U	10

Typical maximum interstitial impurity levels (ppm)

C	H	N	O	$O_{eq.}$ (at. %)*
200	30	90	2000	0.7

*N = 20, C = $\frac{3}{4}$ O, H = 0 (Conrad, 1966)

c) Mild steel (EN1B)

Typical composition as supplied (%)

C	Si	Mn	S	P
0.125	0.02	1.15	0.37	0.021

TABLE 2

Material condition as supplied and as tested

Material	As supplied	Heat treatment of specimens	Grain density (mm^{-2})
Copper (OFHC)	Hot-rolled annealed rod	400°C x 2 hrs@ 10^{-4} - 10^{-5} torr	360
Titanium (IMI 130)	Hot-rolled annealed rod	700°C x 1½ hrs@ 10^{-4} - 10^{-5} torr	75
Mild Steel (EN1B)	Hot-rolled	None	690

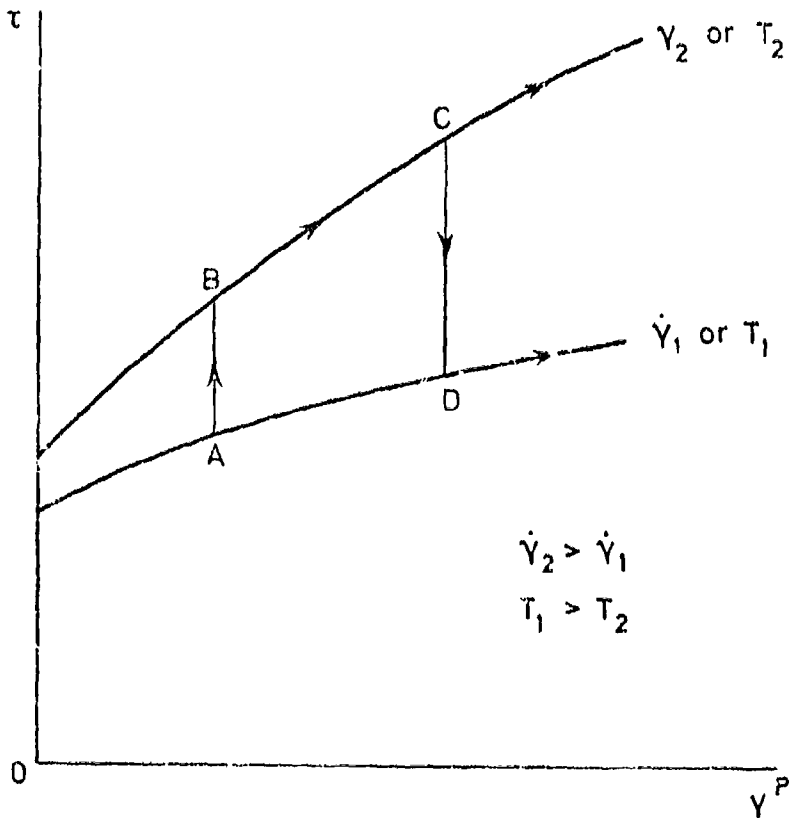

Fig. 1. Illustrating implications of mechanical equation of state

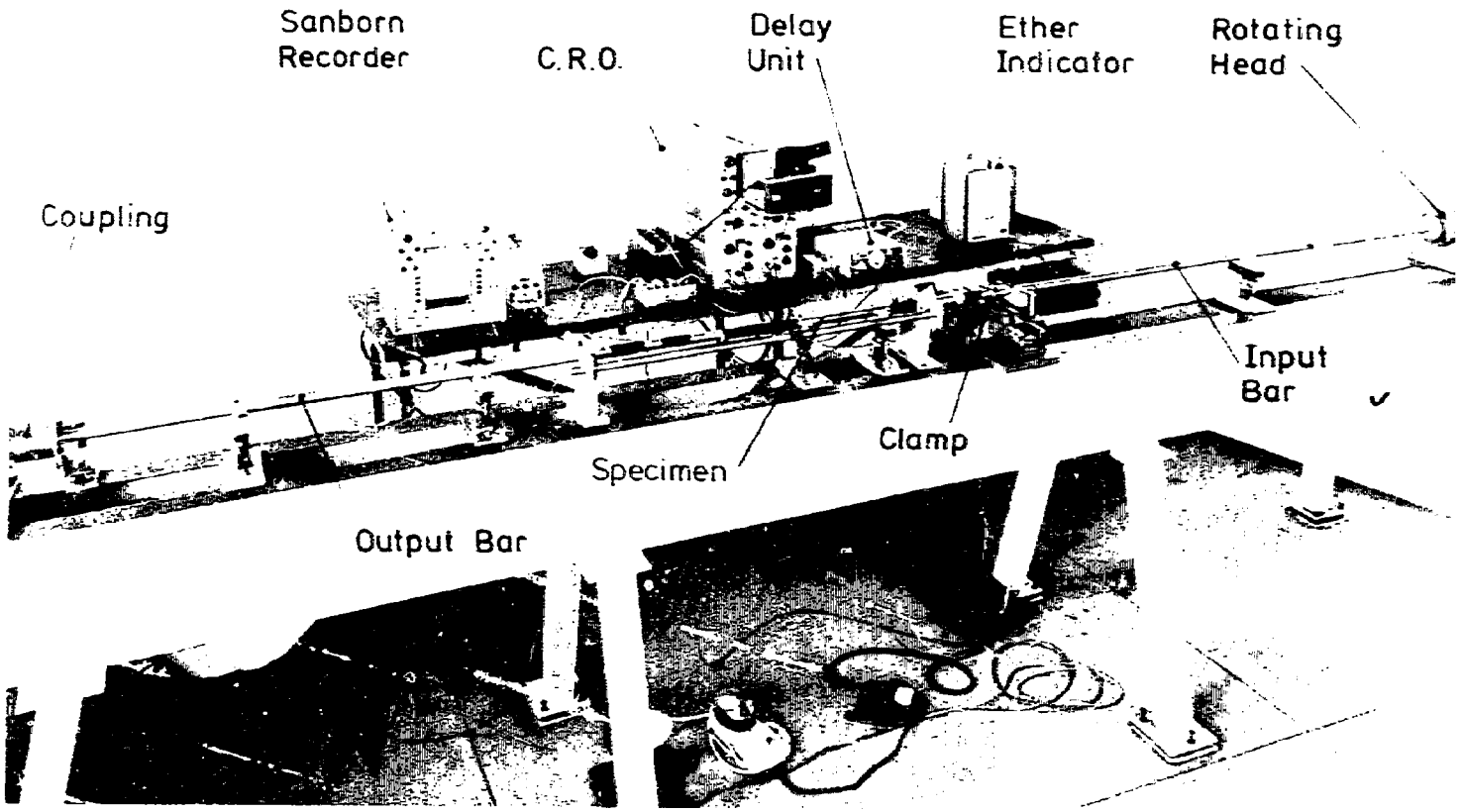

Fig. 2 General view of apparatus.

	l	D
Copper	2·54	23·93
Titanium	1·27	25·4
Mild Steel	1·27	22·71

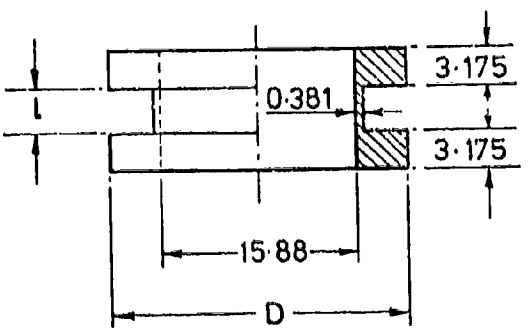

Dimensions in mm.

Fig. 3. Specimen configurations

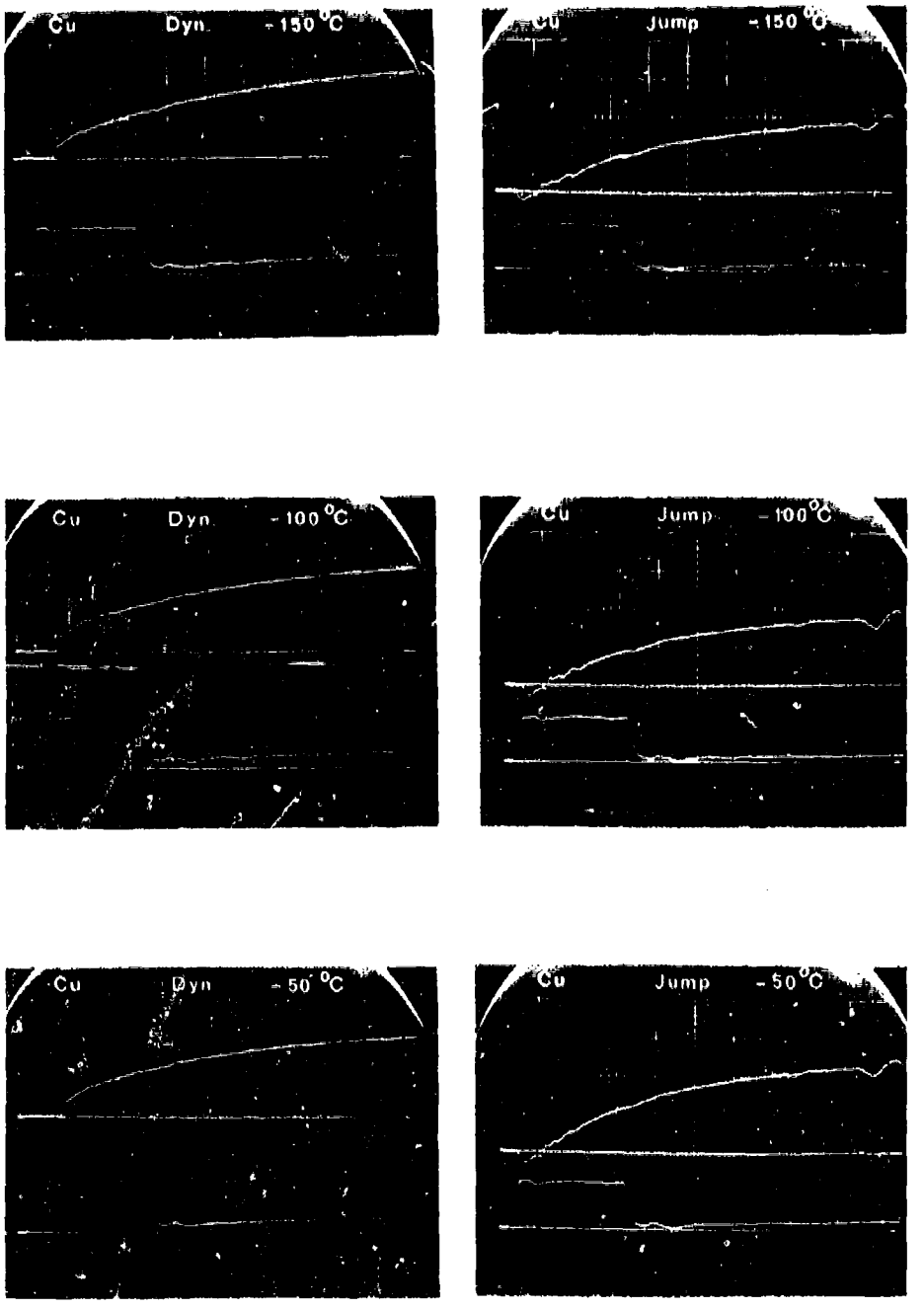

Fig. 4. Oscilloscope records for tests on copper.
(See list of illustrations for calibrations)

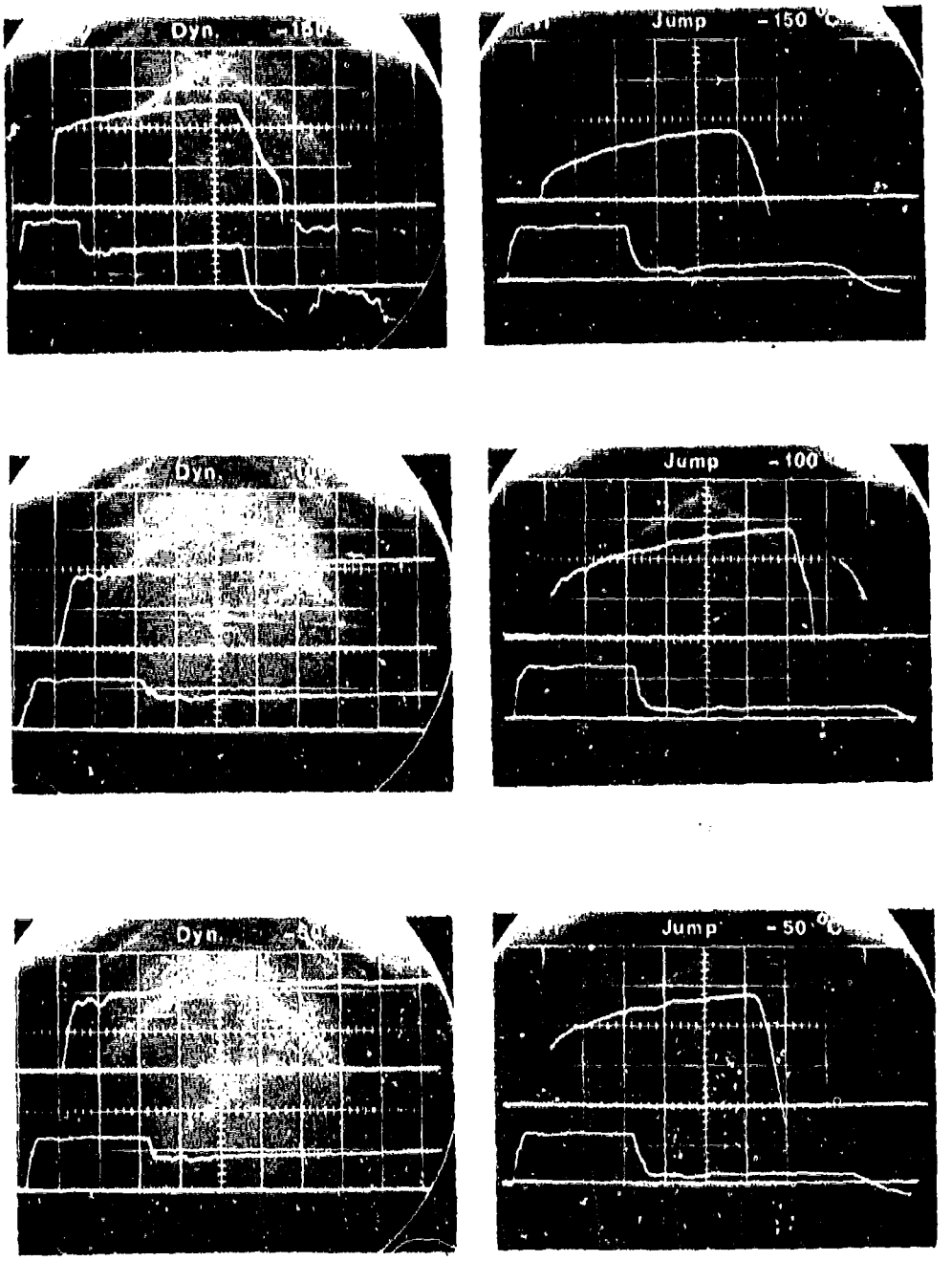

Fig. 5. Oscilloscope records for [illegible]
(See text of [illegible])

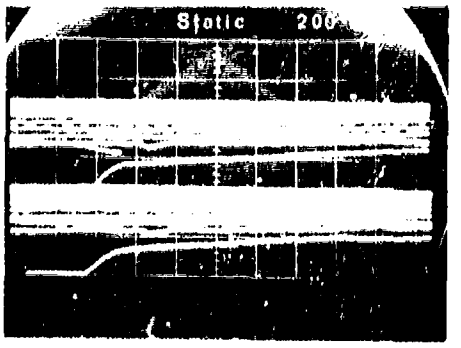

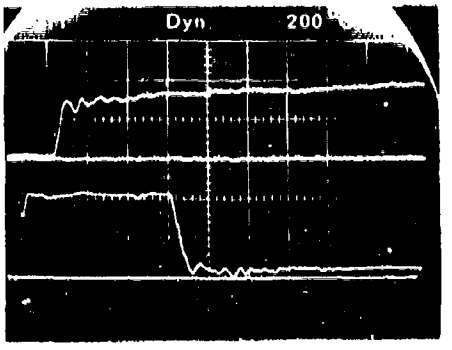

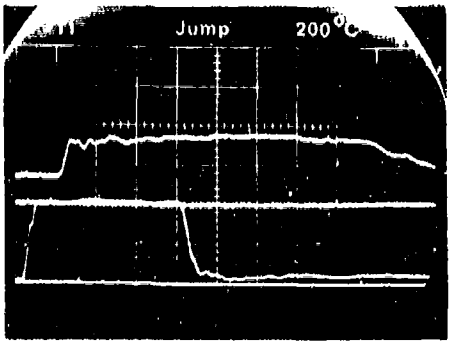

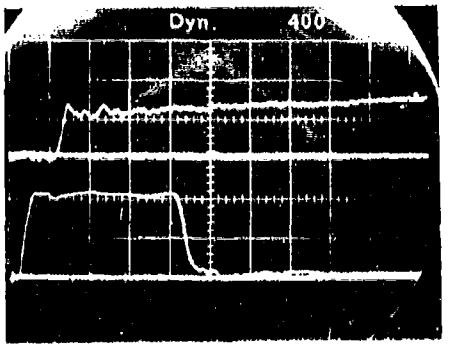

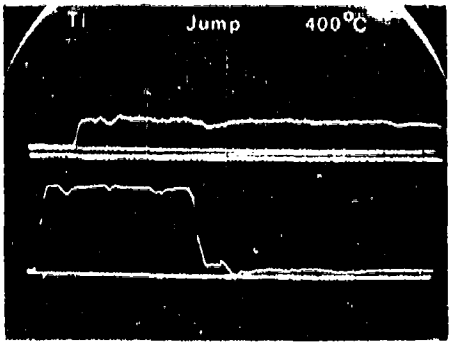

Fig. 5. (continued) Oscilloscope records for tests on titanium.

(See list of illustrations for explanations)

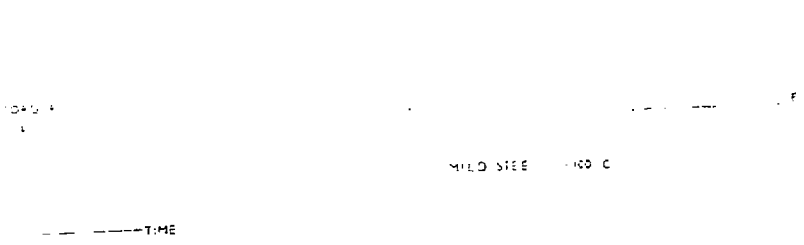

(a)

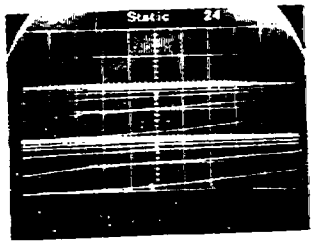

(b)

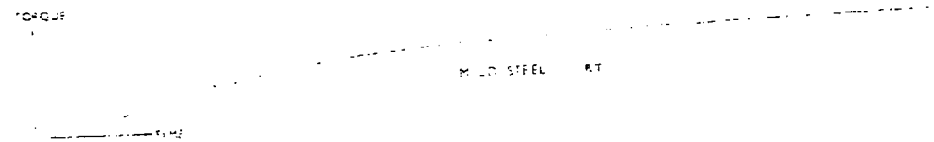

(c)

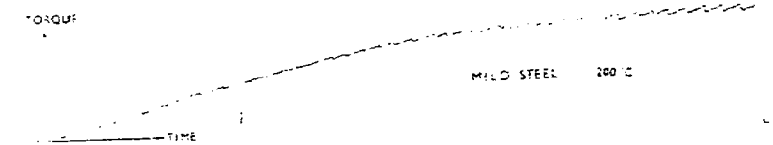

(d)

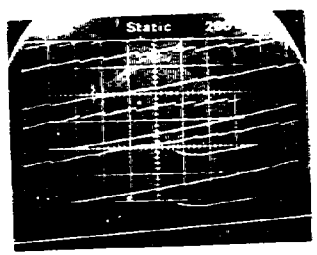

(e)

Fig. 6. Records for static tests on mild steel.

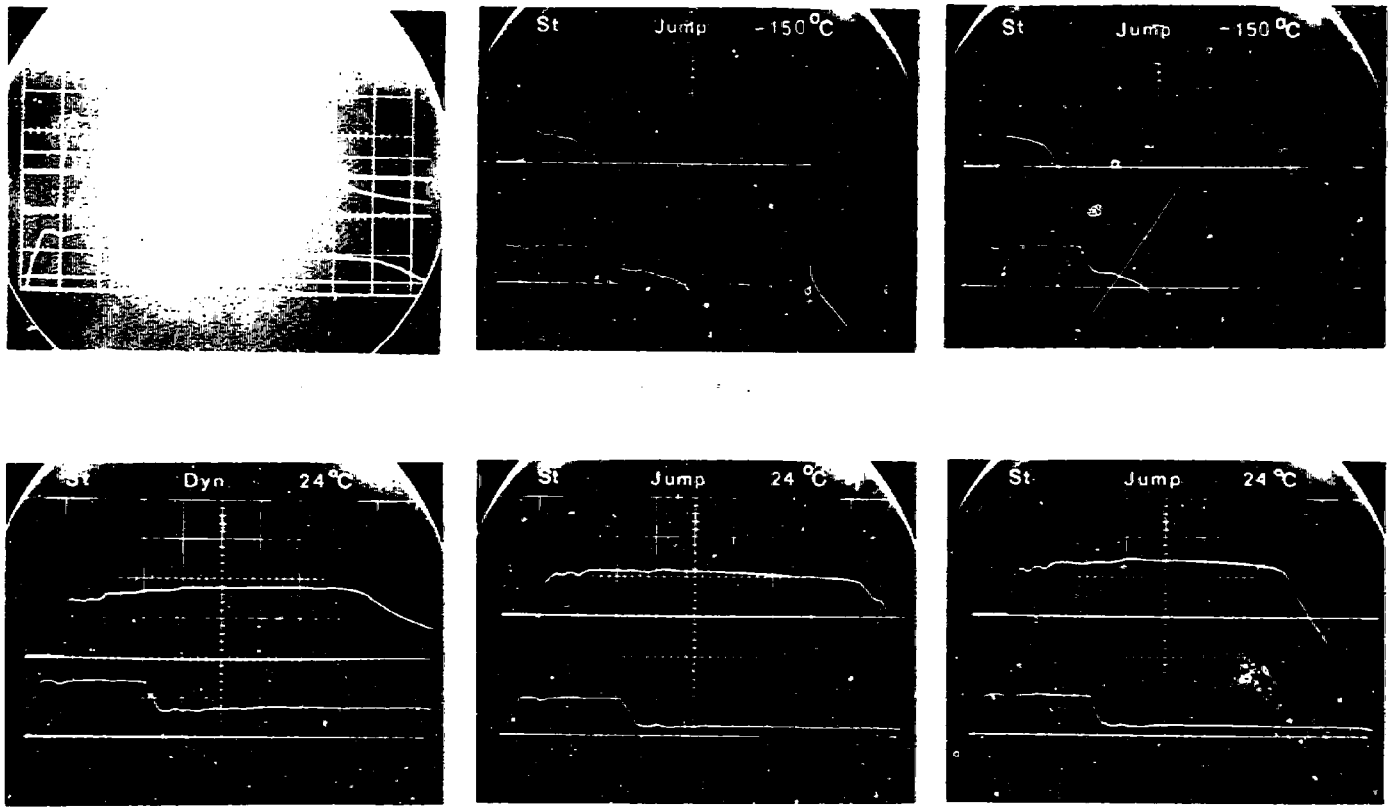

Fig. 6. (continued) Oscilloscope records for tests on mild steel.
(See list of Illustrations for calibrations)

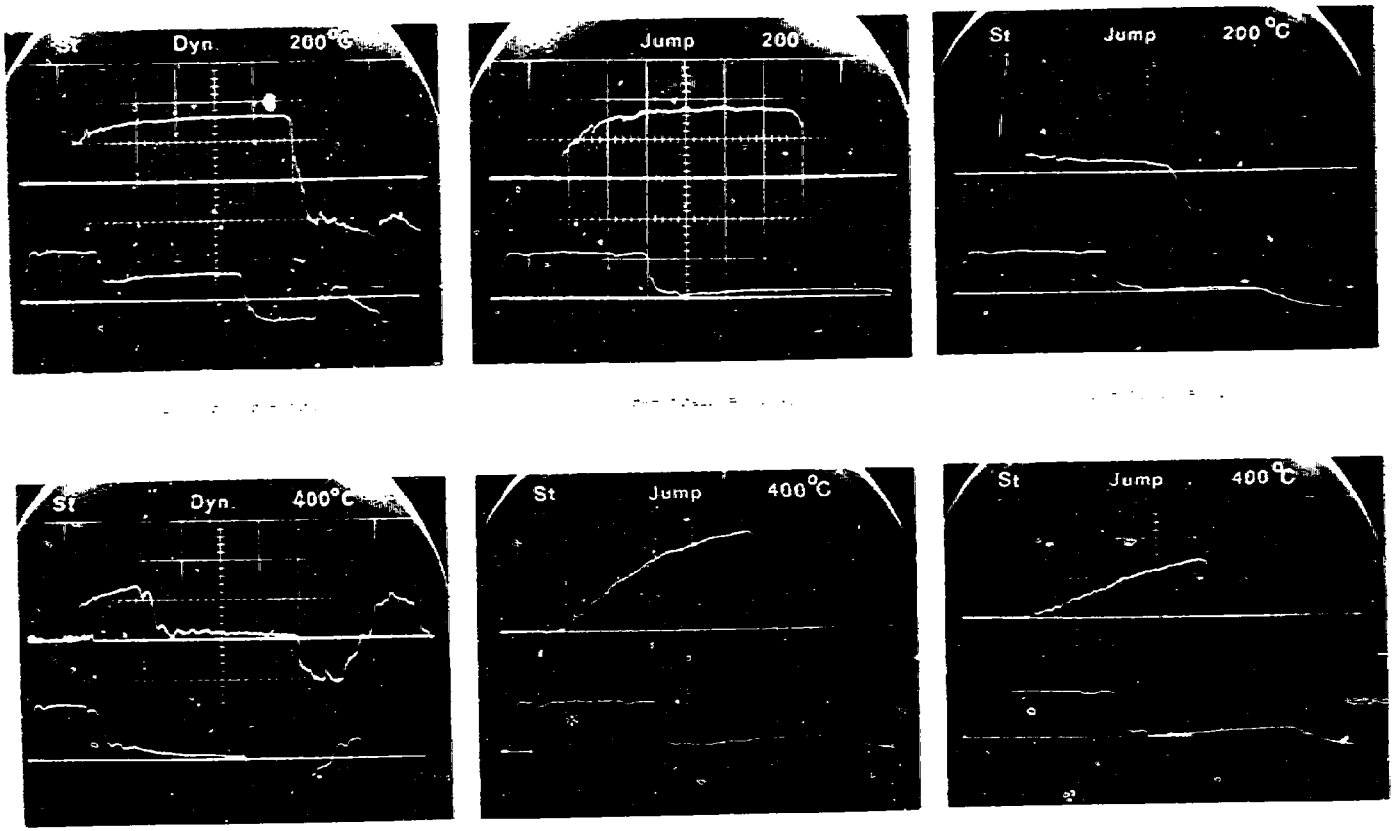

Fig. 6 (continued) Oscilloscope records for tests on mild steel
(See list of Illustrations for calibrations)

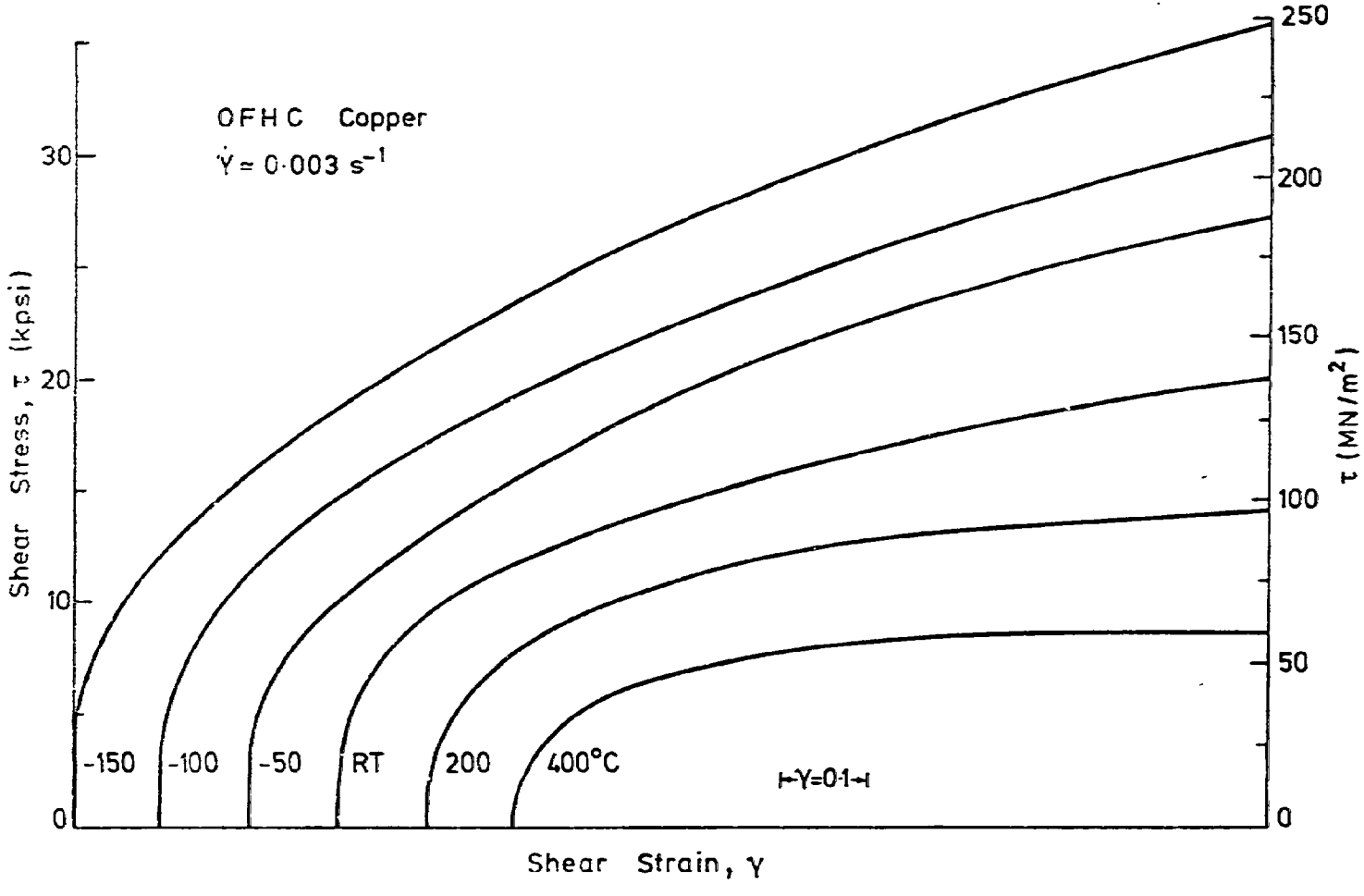

Fig. 7. Quasi-static stress-strain curves for copper at various temperatures

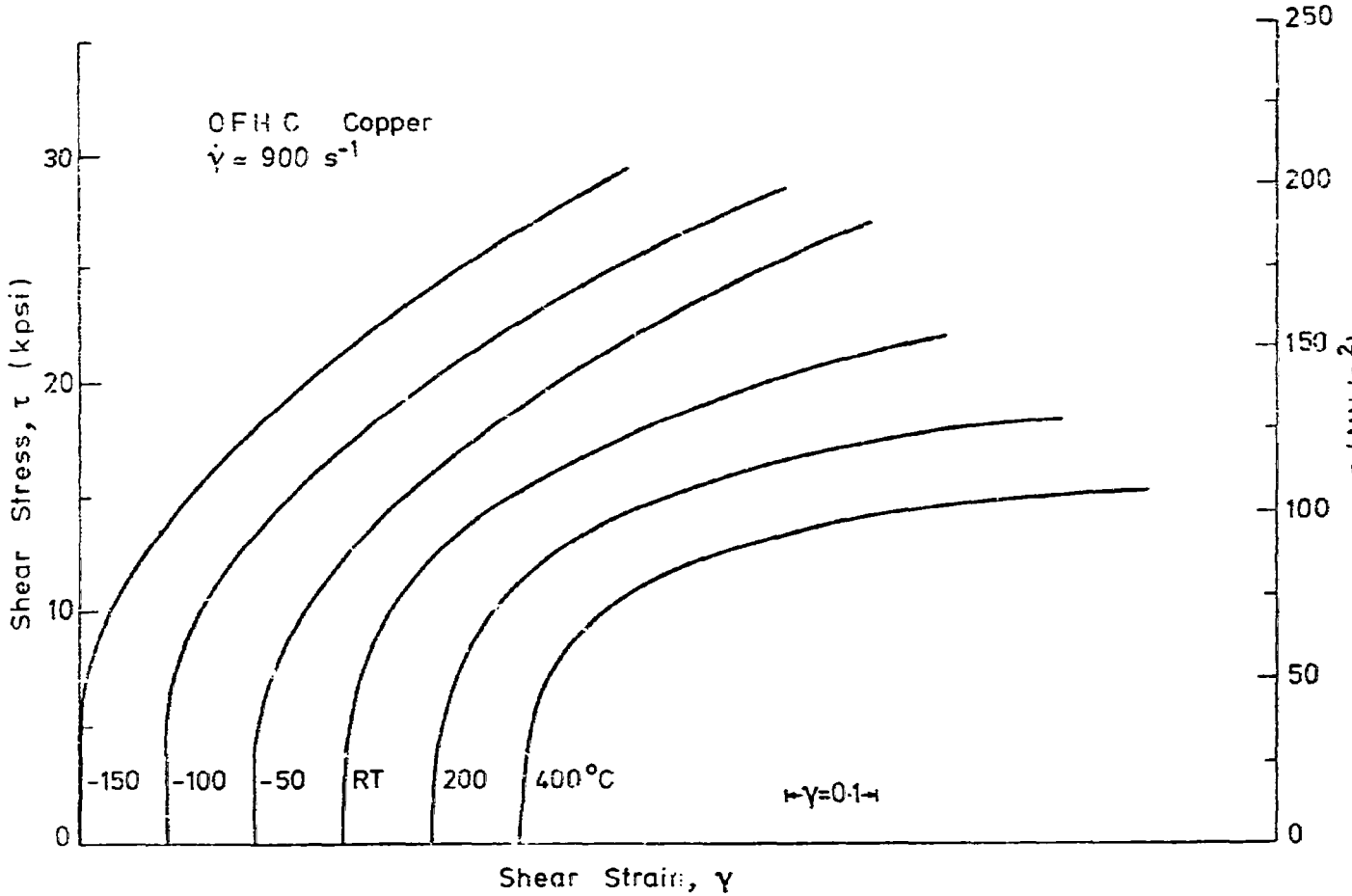

Fig. 8. Dynamic stress-strain curves for copper at various temperatures

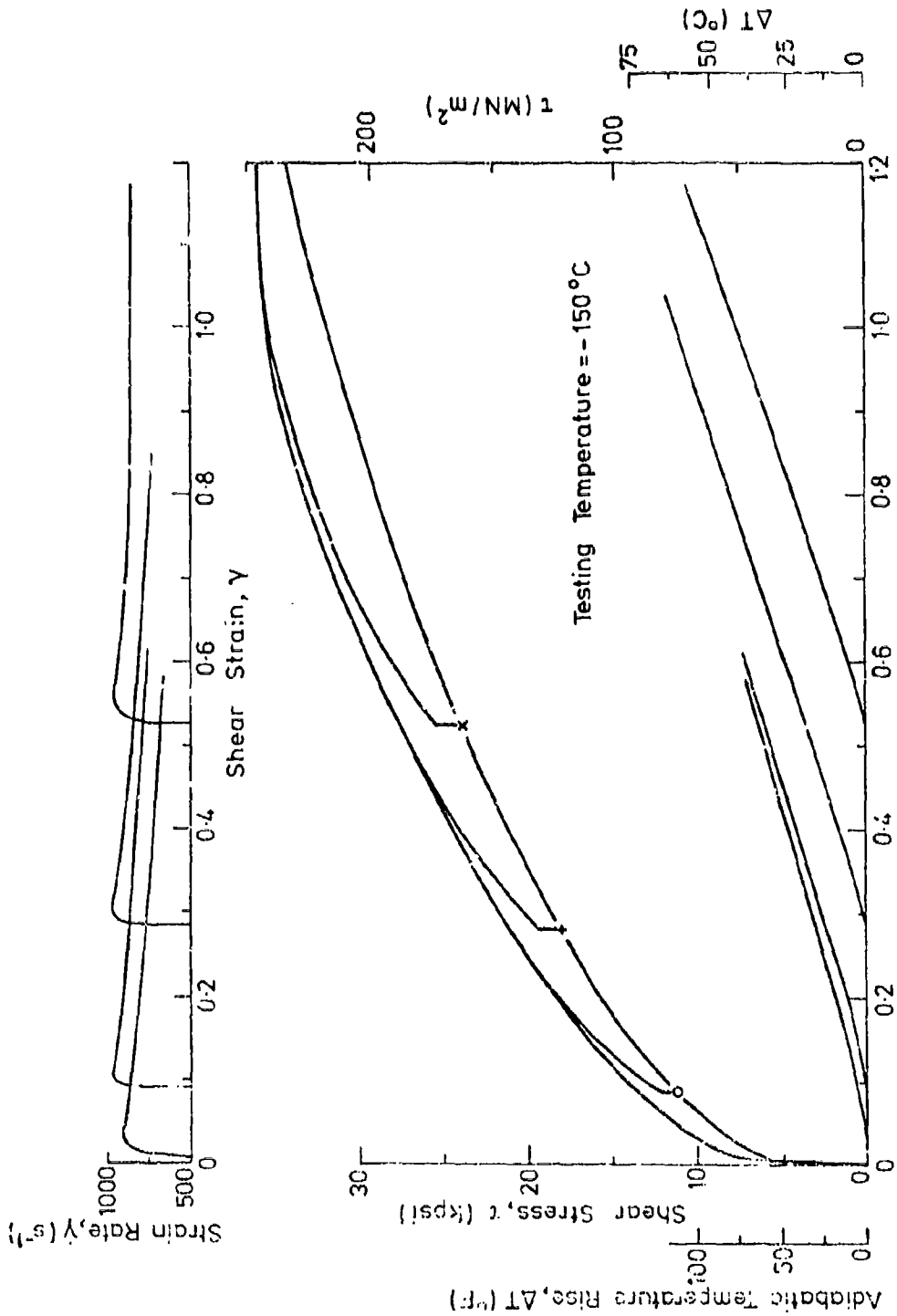

Fig. 9(a) Test results for copper at -150°C; pre-strains 0.086, 0.280, 0.523

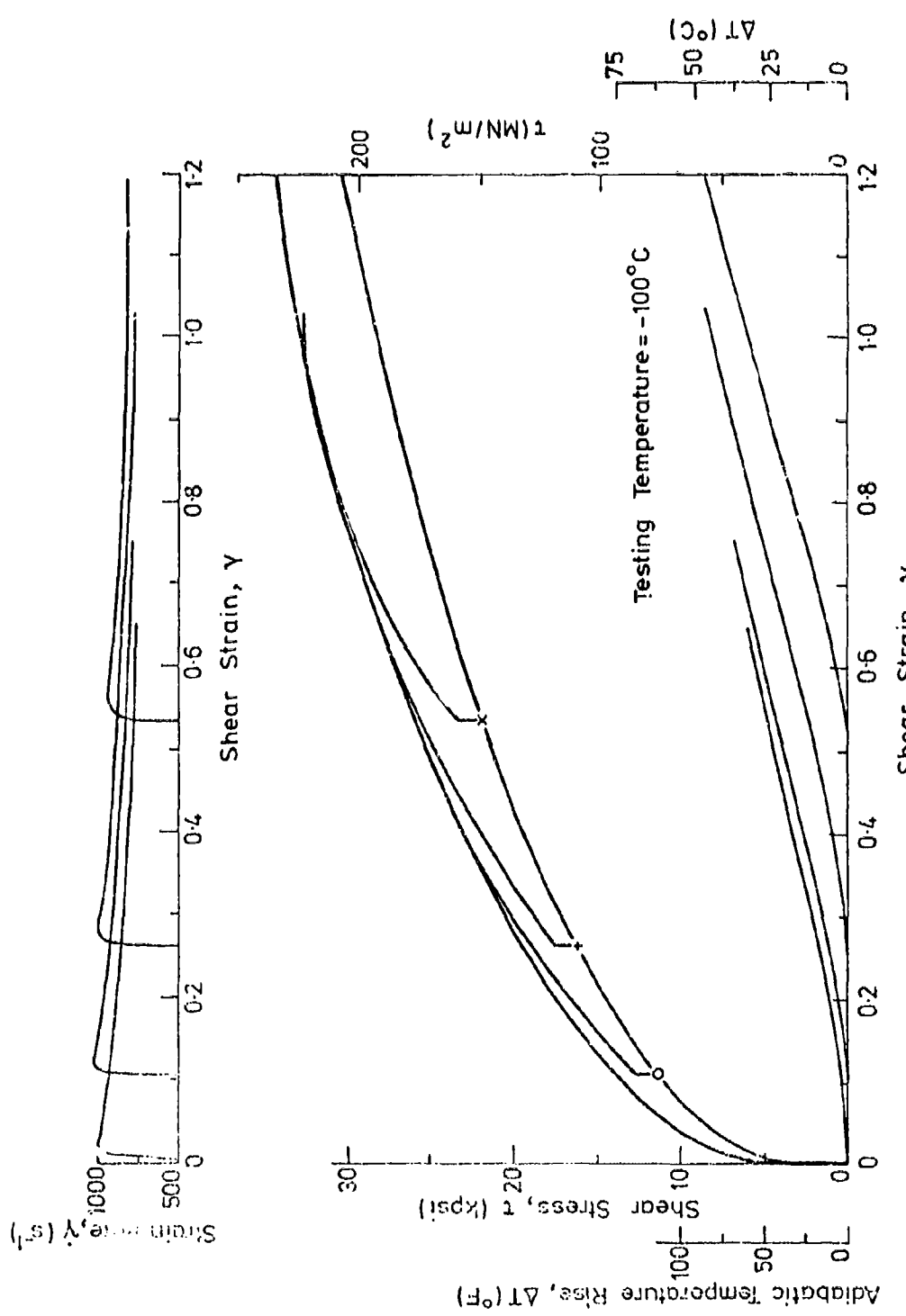

Fig. 9(b) Test results for copper at -100°C; pre-strains 0.108, 0.265, 0.538

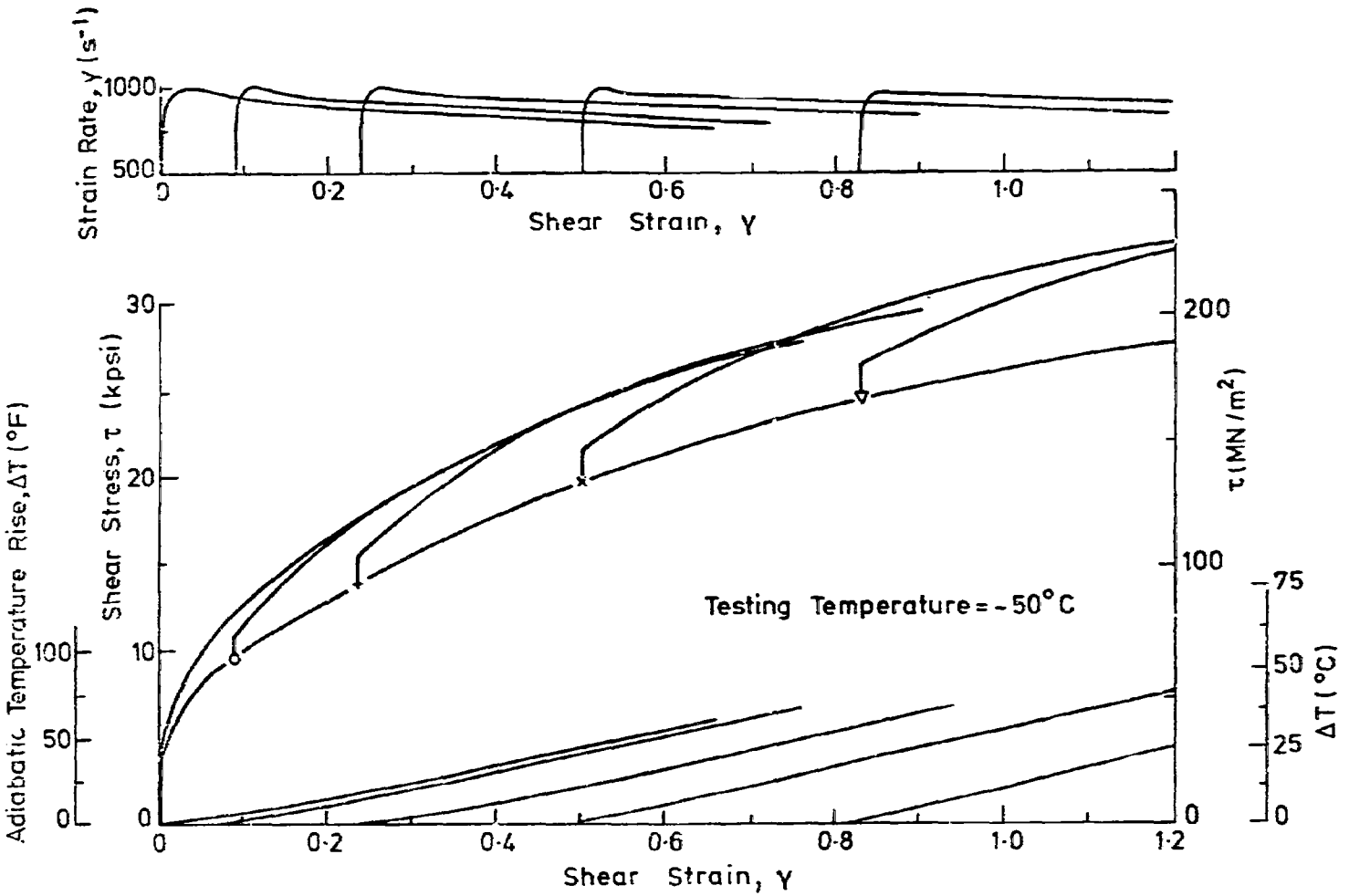

Fig. 9(c) Test results for copper at -50°C; pre-strains 0.087, 0.235, 0.500, 0.828

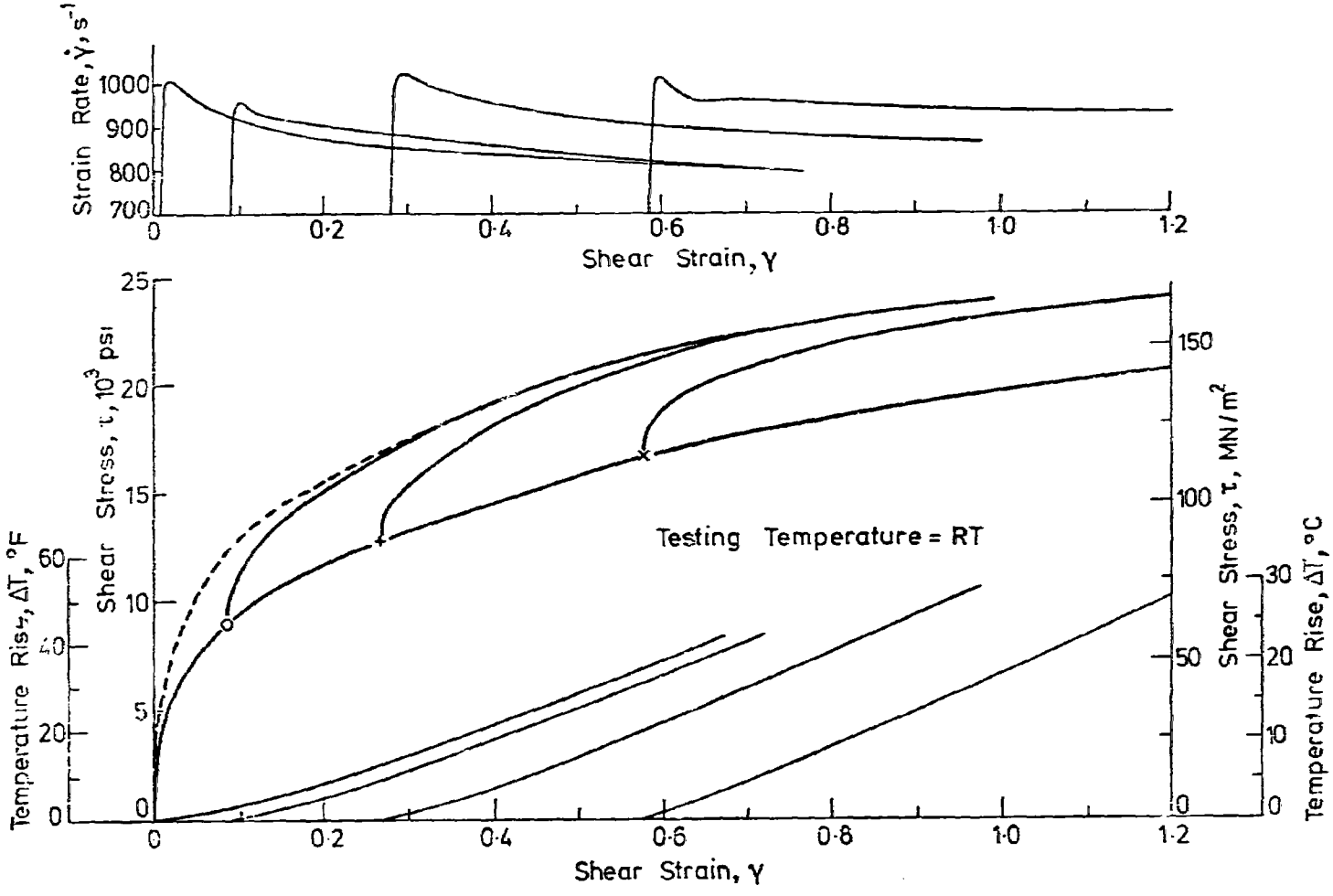

Fig. 9(d) Test results for copper at RT; pre-strains 0.085, 0.268, 0.580

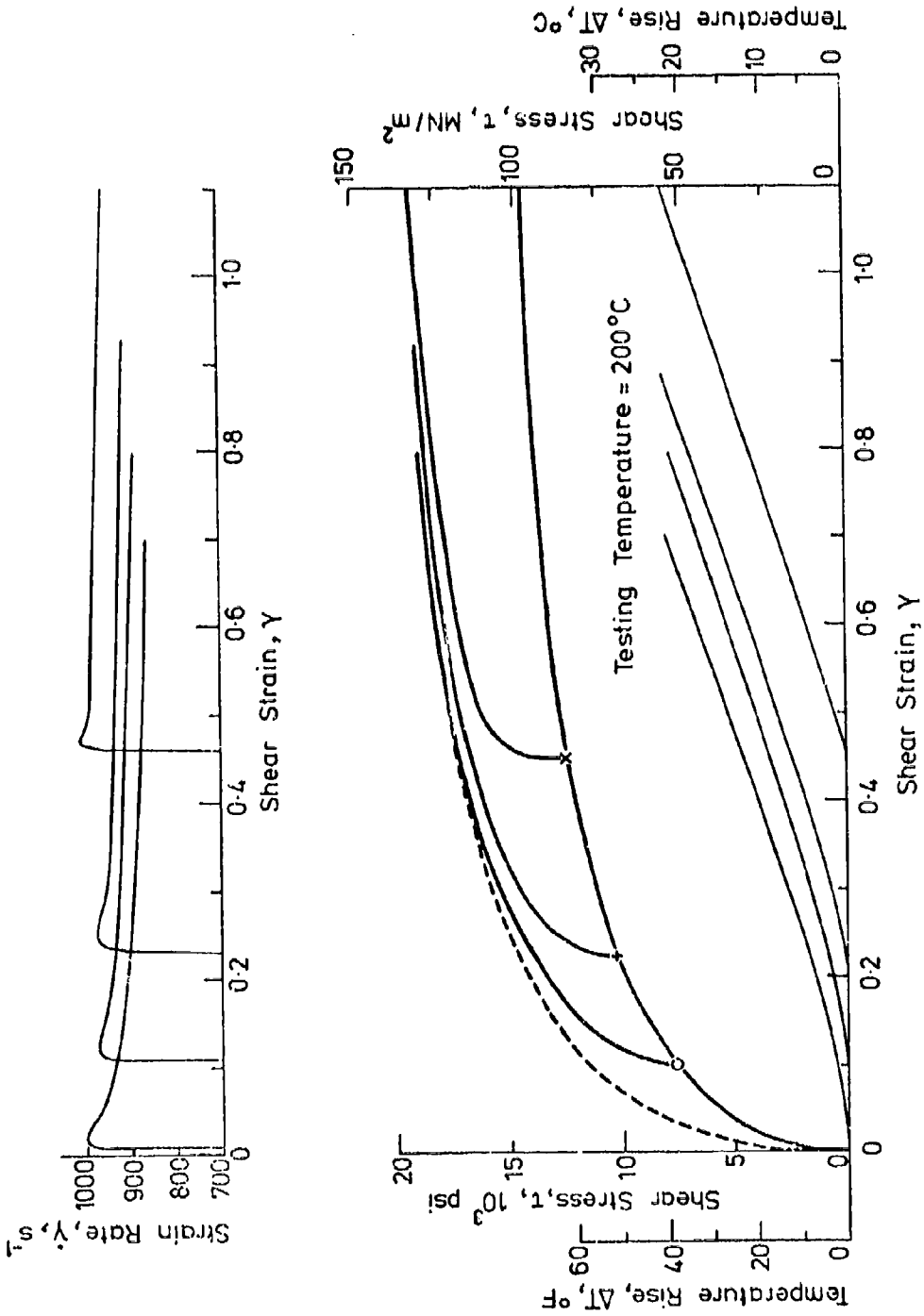

Fig. 9(e) Test results for copper at 200°C; pre-strains 0.100, 0.225, 0.450

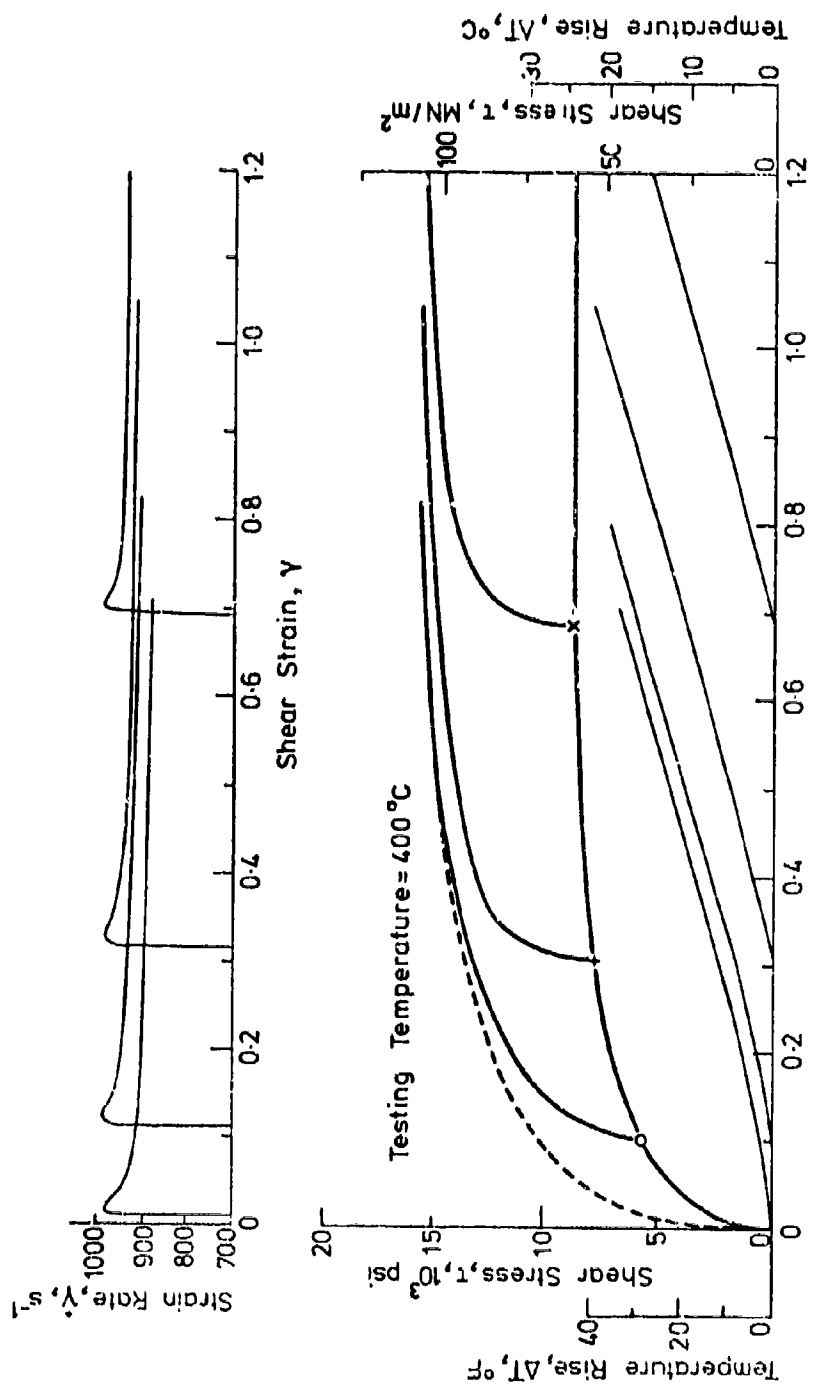

Fig. 9(f) Test results for copper at 400°C; pre-strains 0.103, 0.338, 0.688

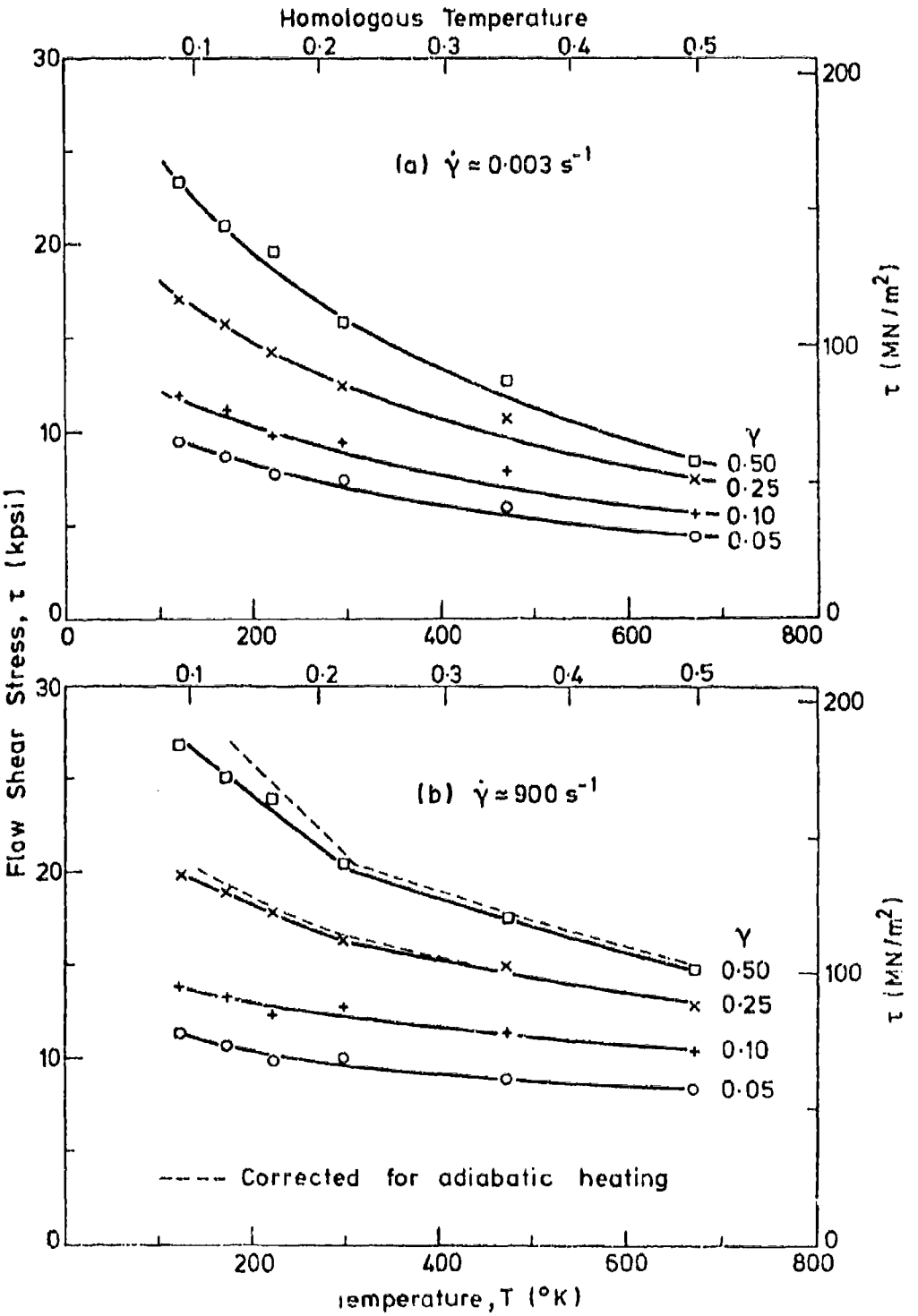

Fig. 10. Temperature dependence of flow stress of copper, at (a) low and (b) high strain rates

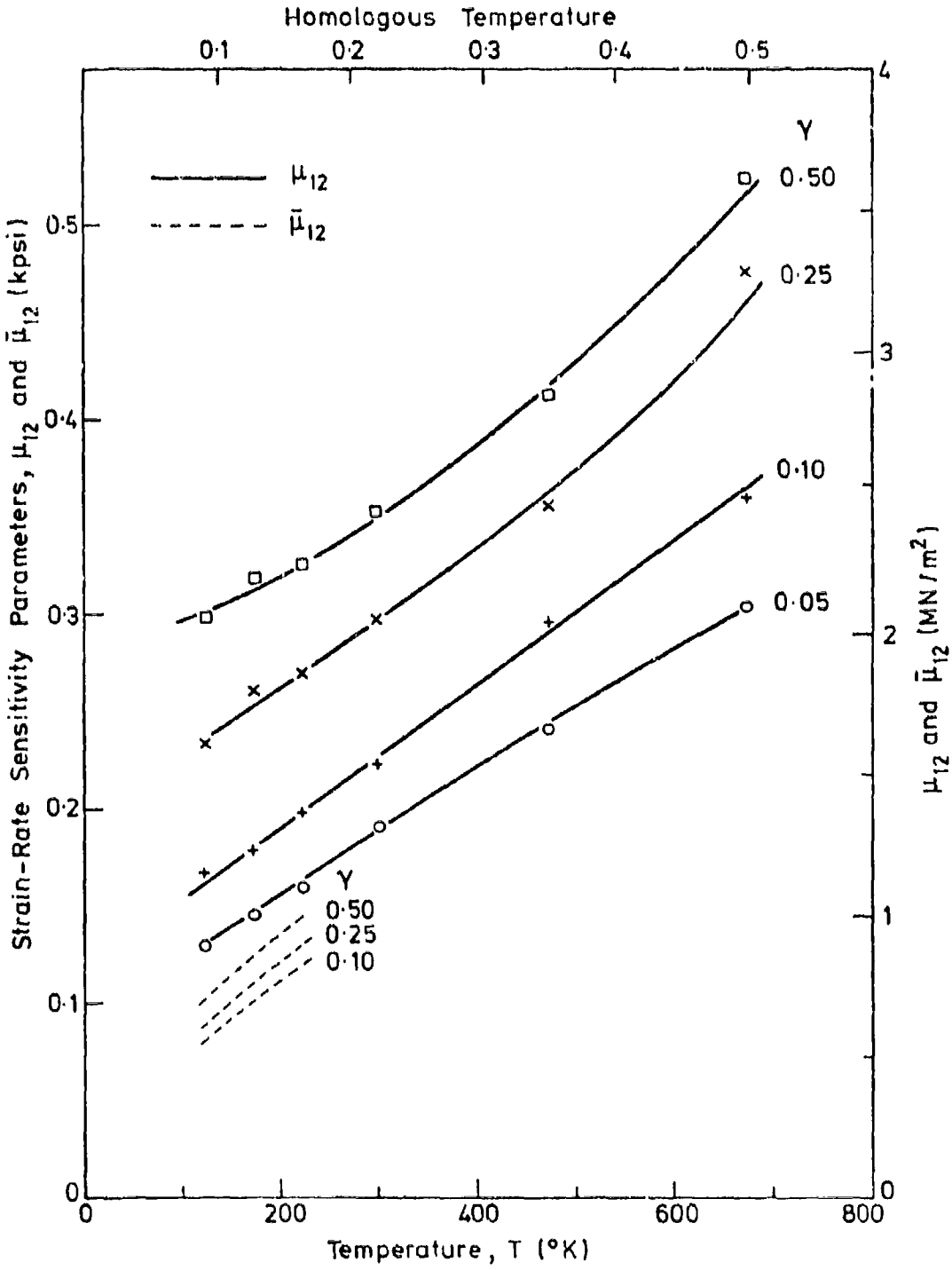

Fig. 11. Temperature dependence of apparent and intrinsic strain-rate sensitivities of copper, at constant strains.

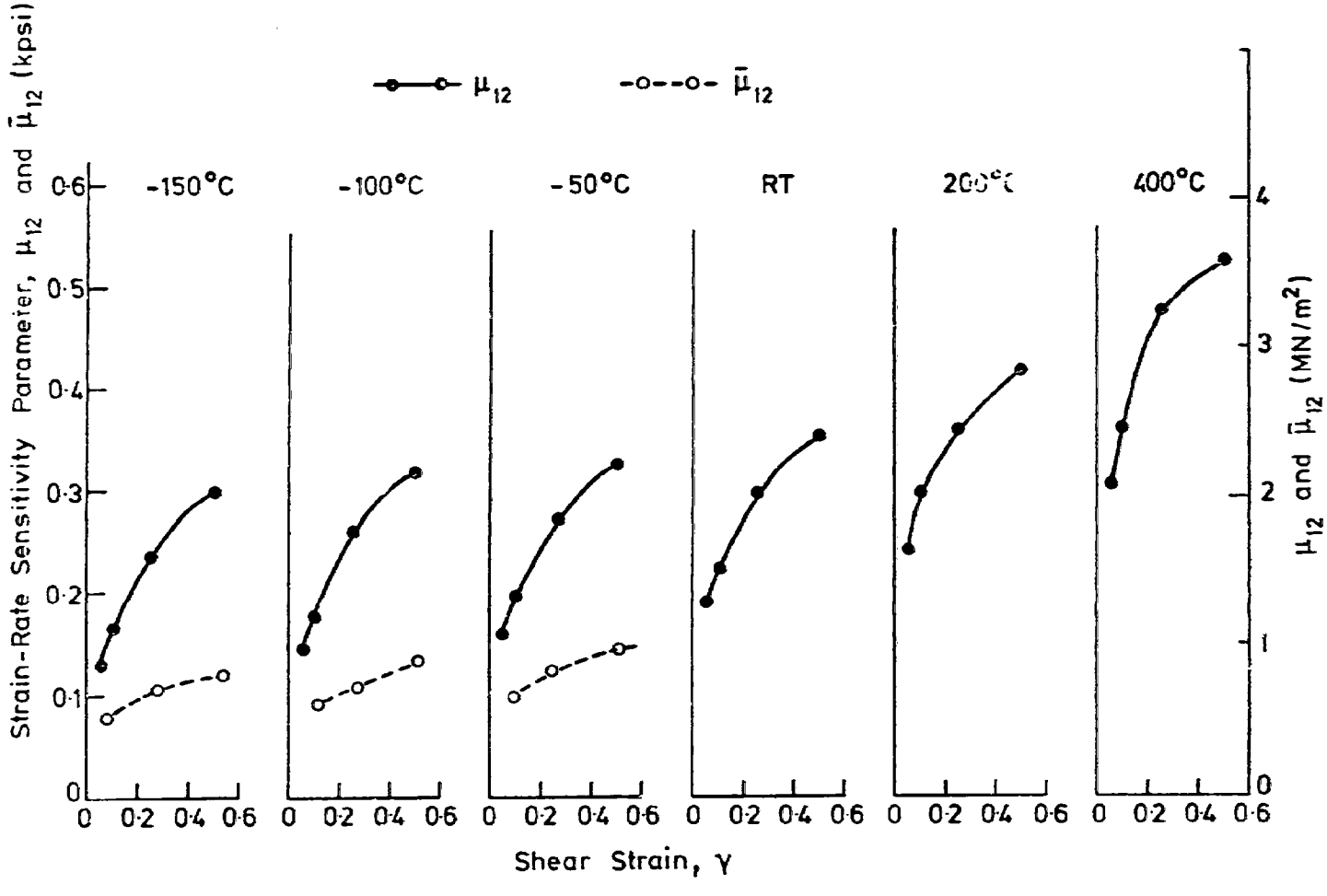

Fig. 12. Strain dependence of apparent and intrinsic strain-rate sensitivites of copper, at constant temperatures

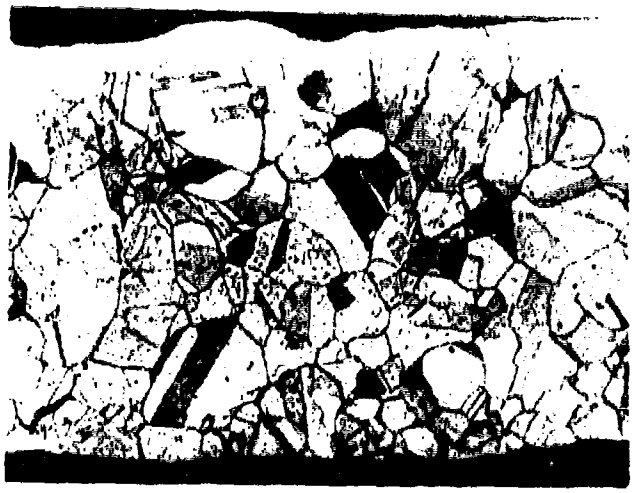

(a)

Room temperature

Zero pre-strain

(b)

400°C

Pre-strain = 0.308

0.1 mm

Fig. 13 Dynamically strained copper specimens (longitudinal section)

(c)

-50°C

Pre-strain = 0.234

(d)

-100°C

Zero pre-strain

0.1 mm

Fig. 13 (continued) Dynamically strained copper specimens (longitudinal section)

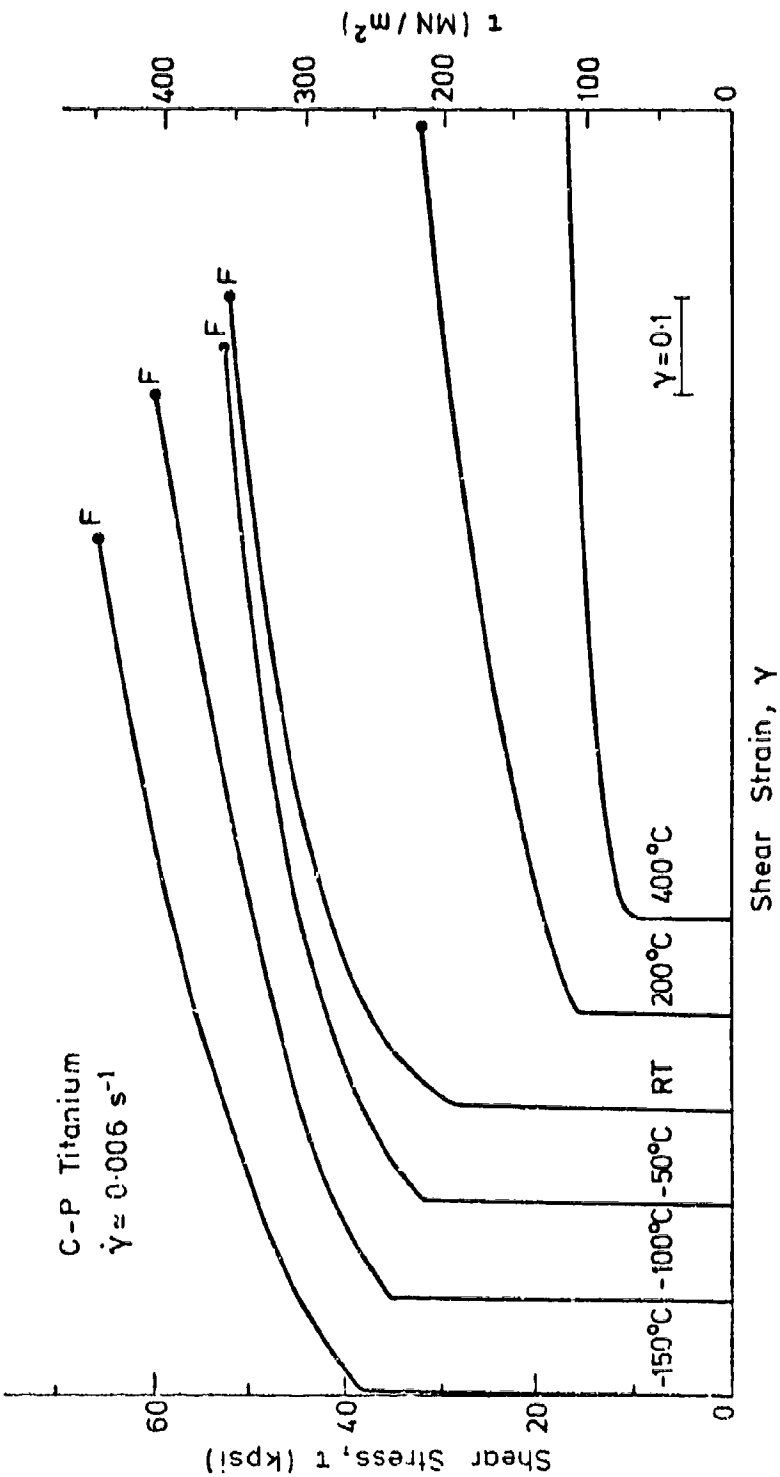

Fig. 14. Quasi-static stress-strain curves for titanium at various temperatures

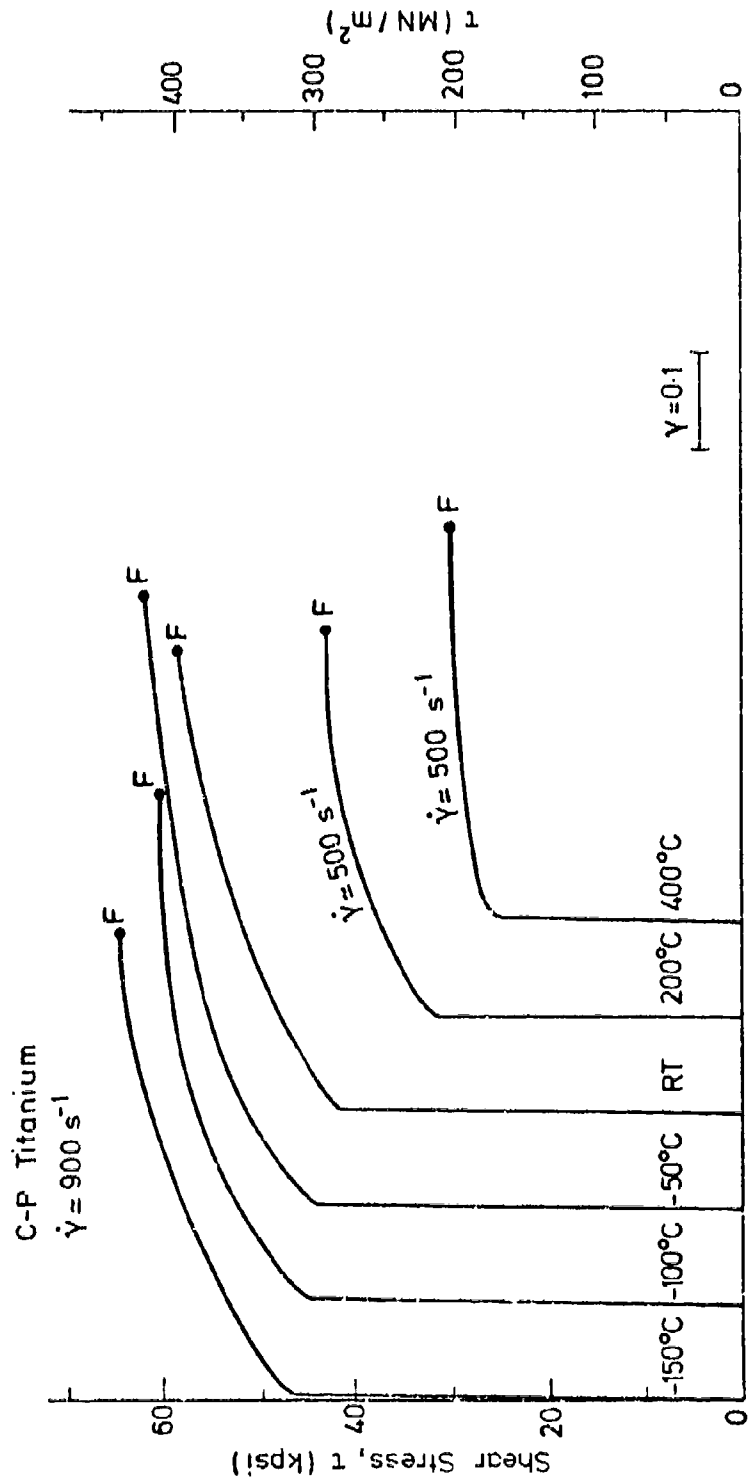

Fig. 15. Dynamic stress-strain curves for titanium at various temperatures

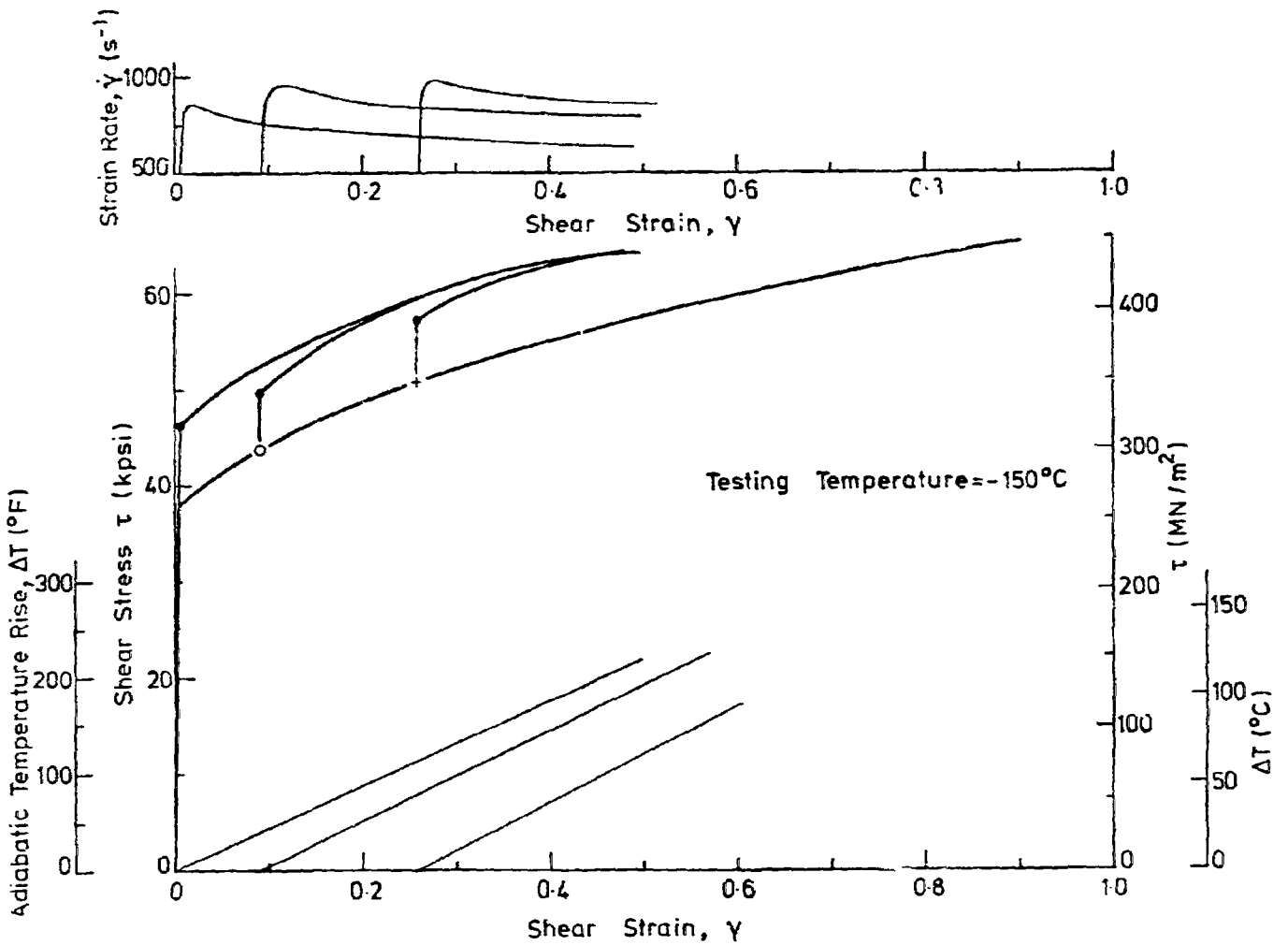

Fig. 16(a) Test results for titanium at -150°C; pre-strains 0.090, 0.258

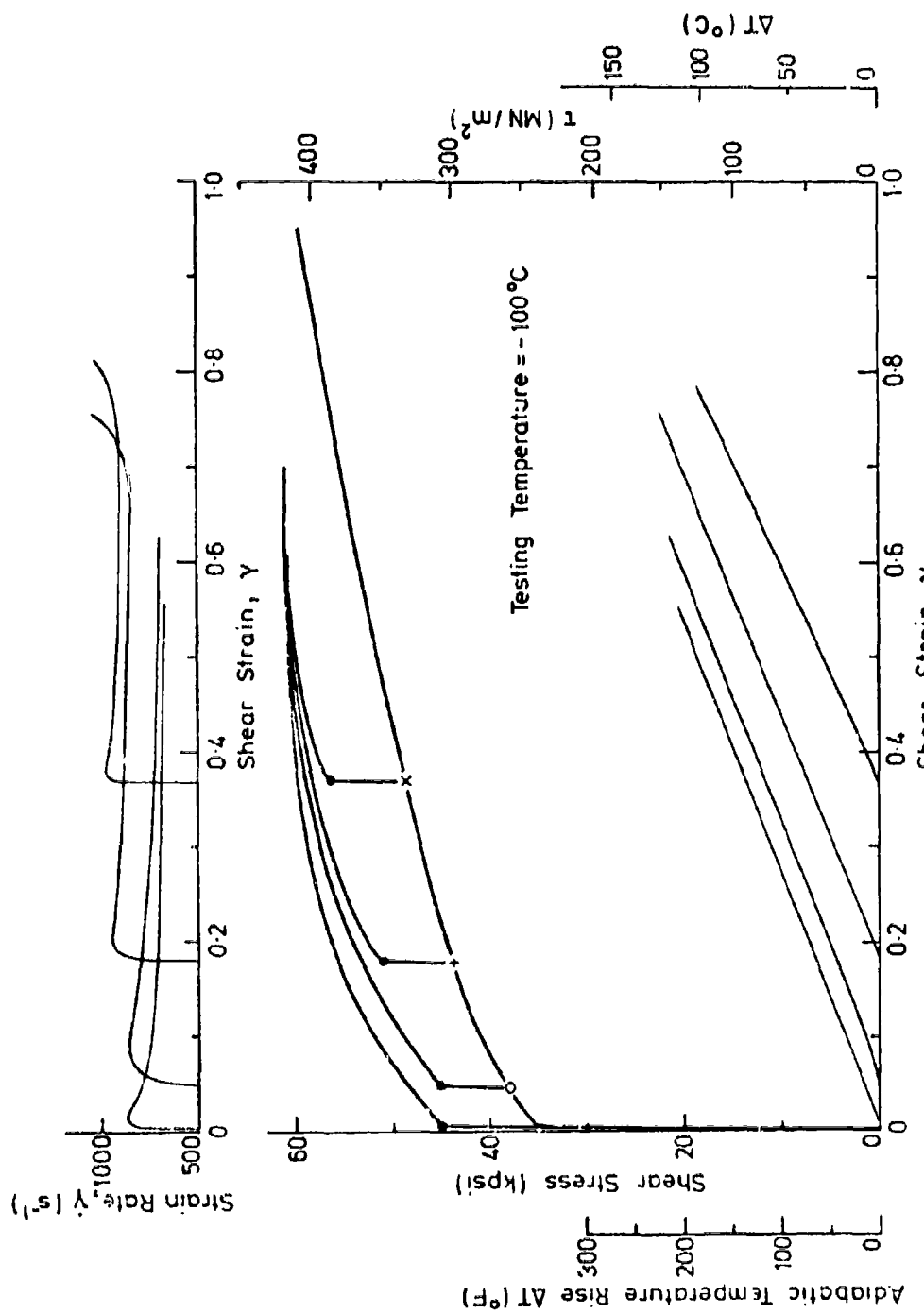

Fig. 16(b) Test results for titanium at -100°C; pre-strains 0.045, 0.178, 0.368

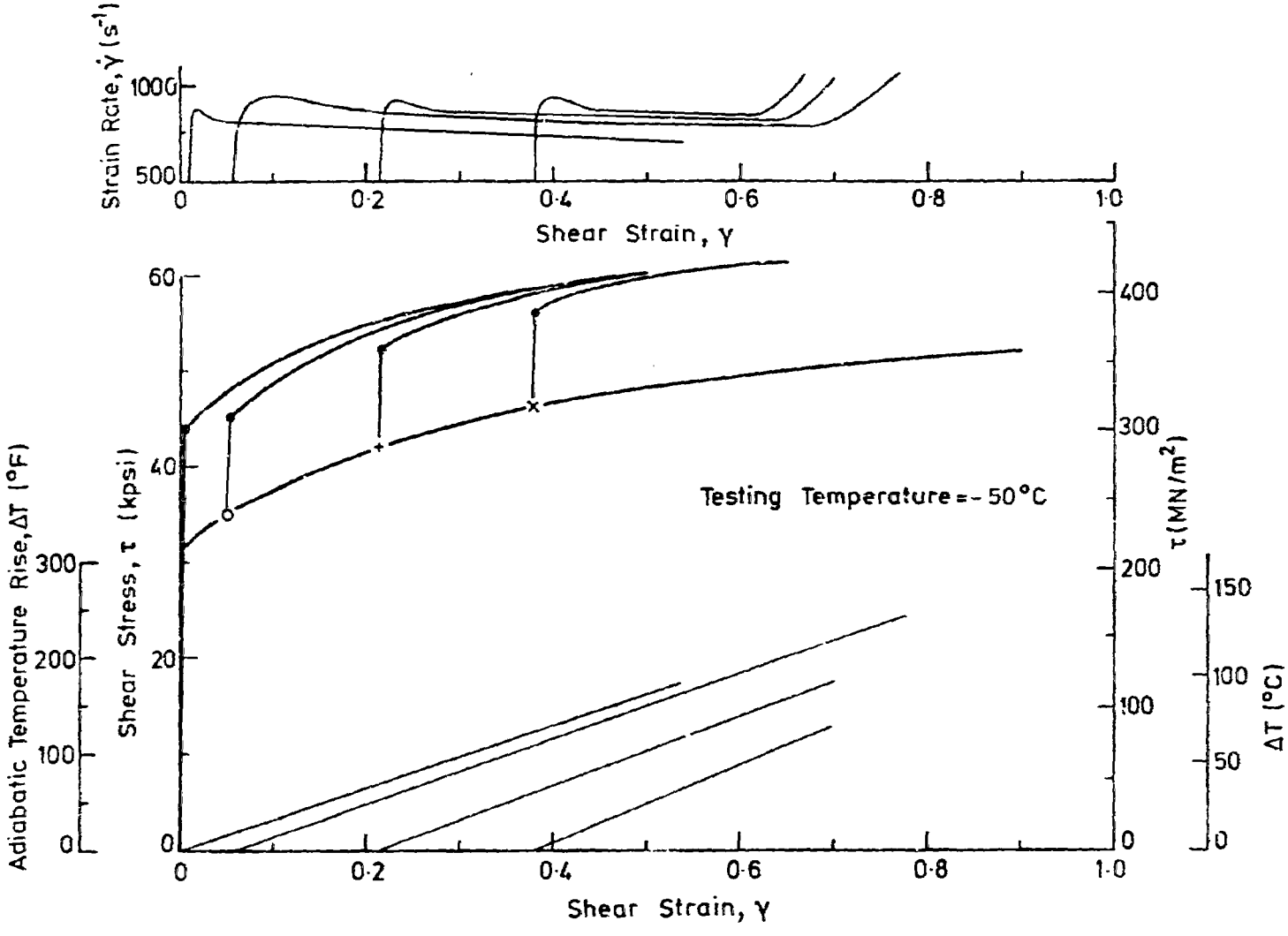

Fig. 16(c) Test results for titanium at -50°C; pre-strains 0.050, 0.213, 0.578

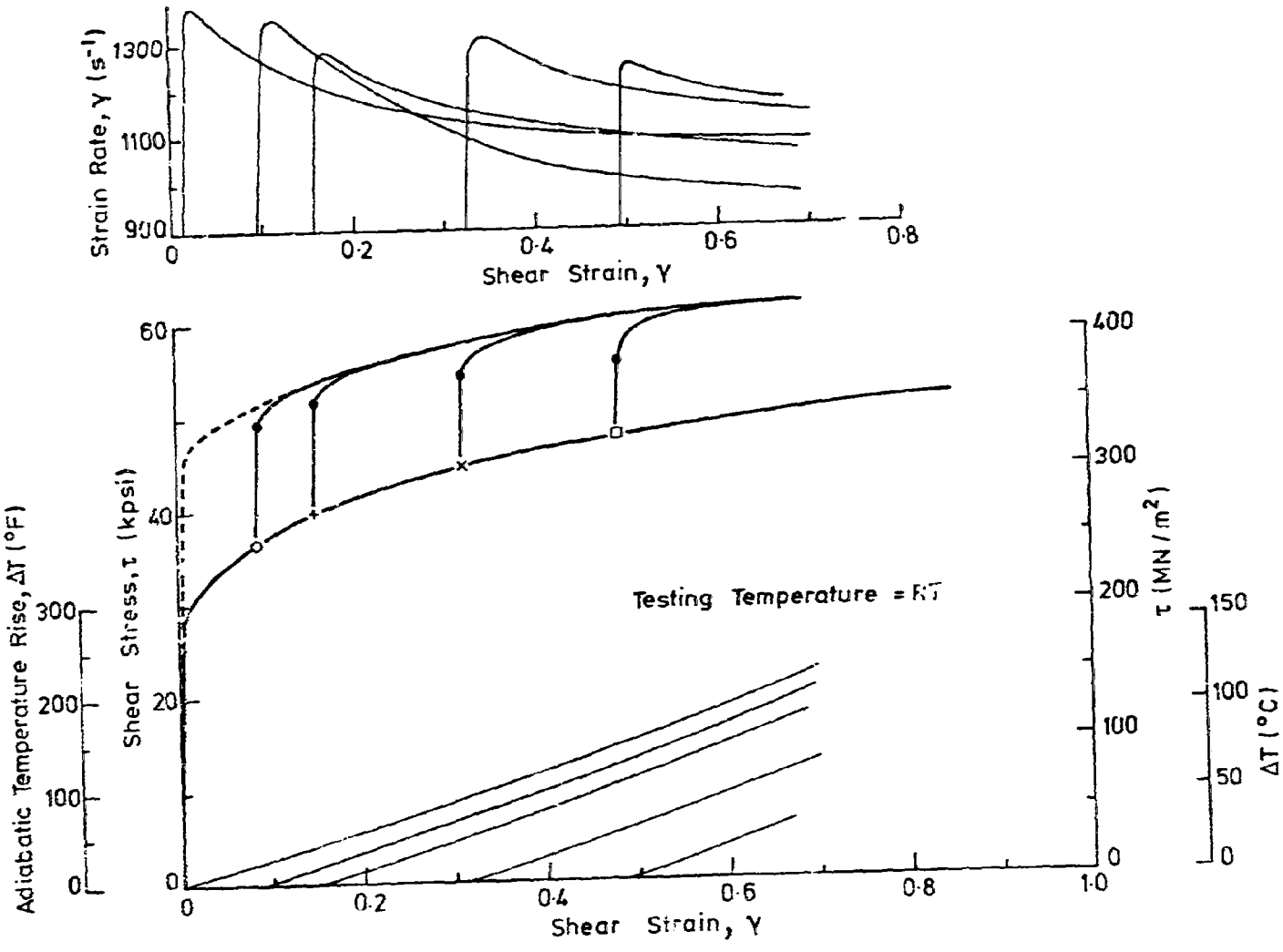

Fig. 16(d) Test results for titanium at RT; pre-strains 0.088, 0.150, 0.314, 0.482

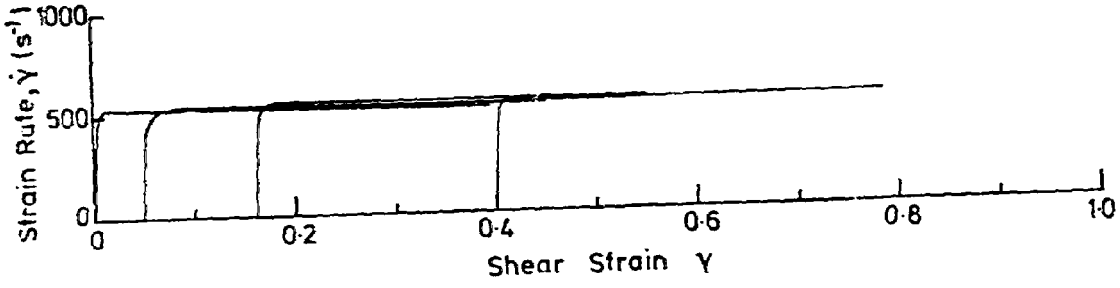

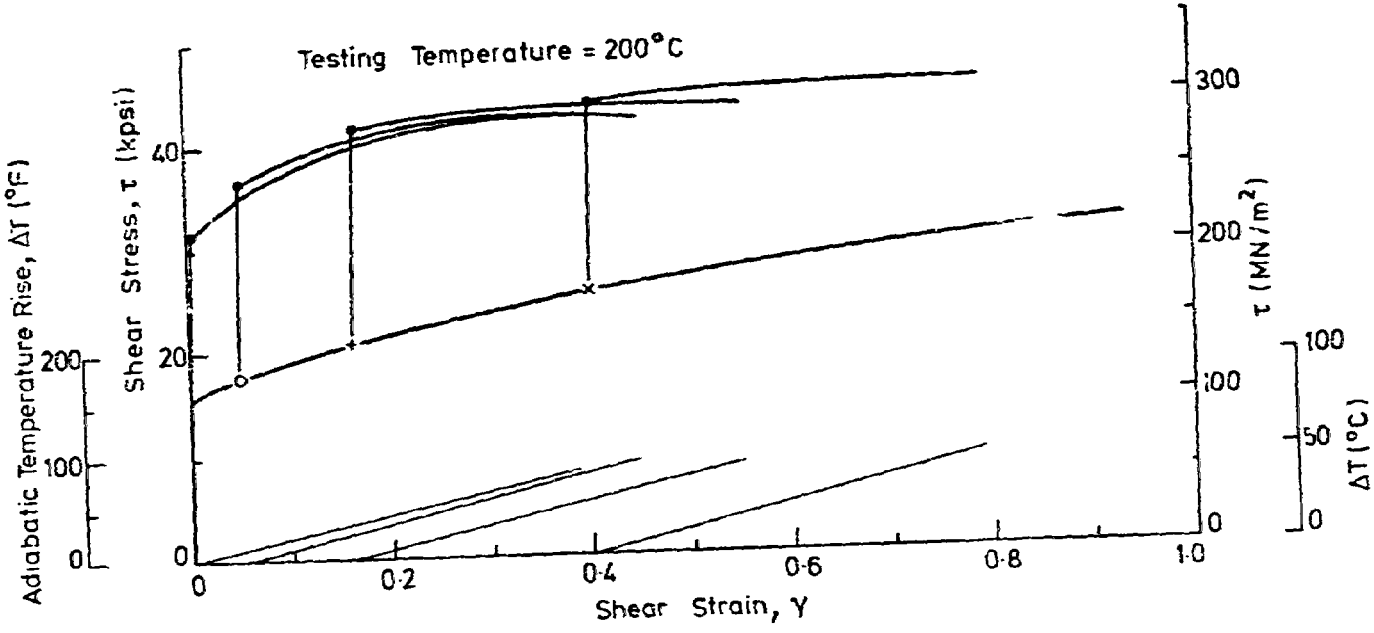

Fig. 16(e) Test results for titanium at 200°C; pre-strains 0.050, 0.163, 0.400

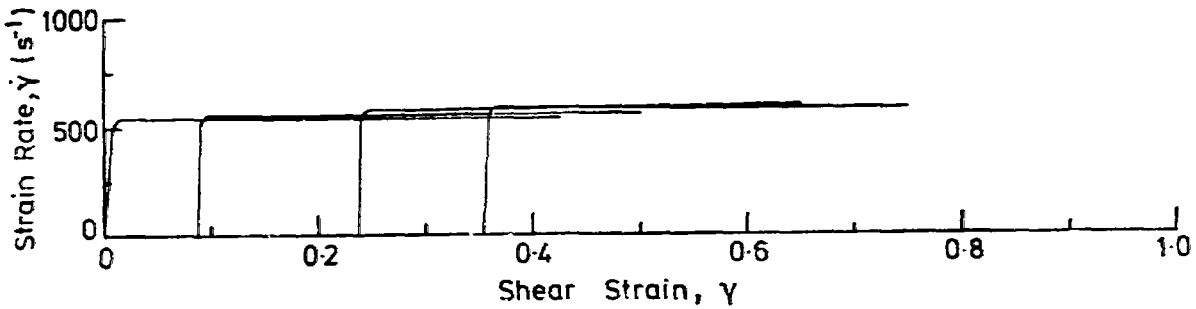

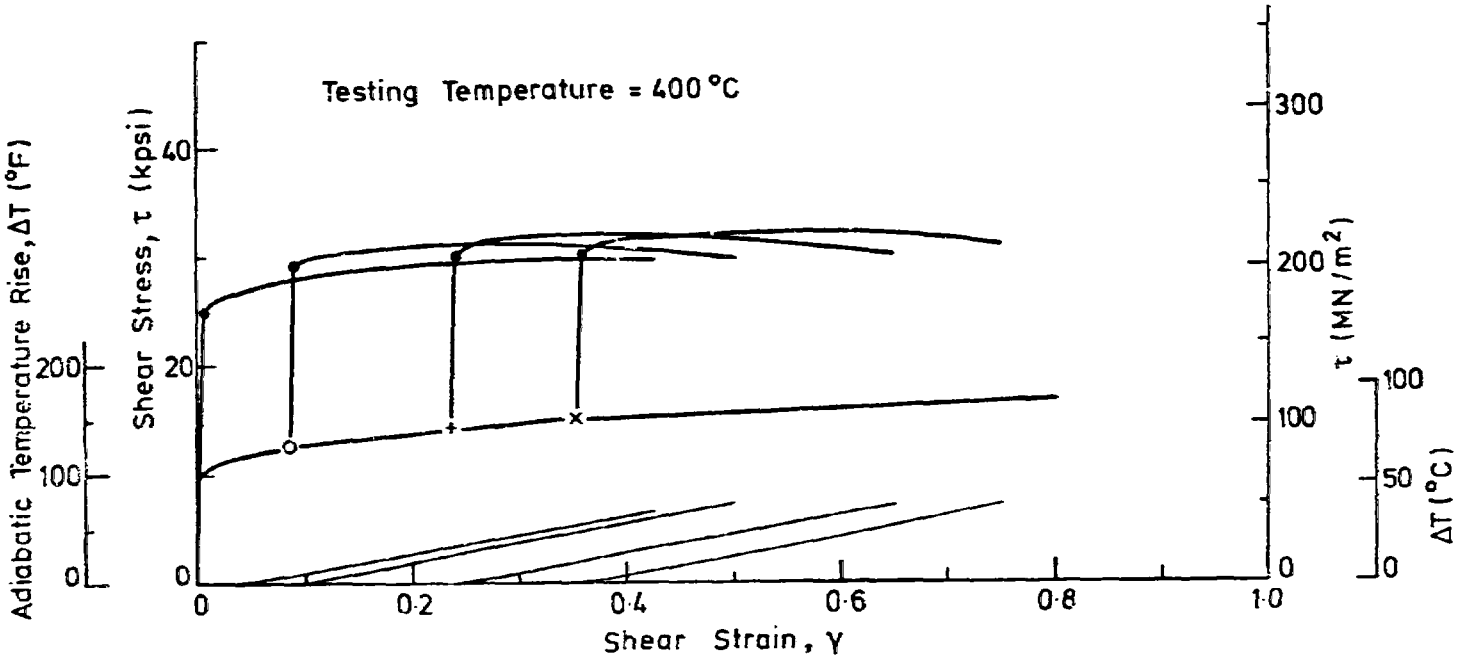

Fig. 16 (f) Test results for titanium at 400°C; pre-strains 0.088, 0.238, 0.355

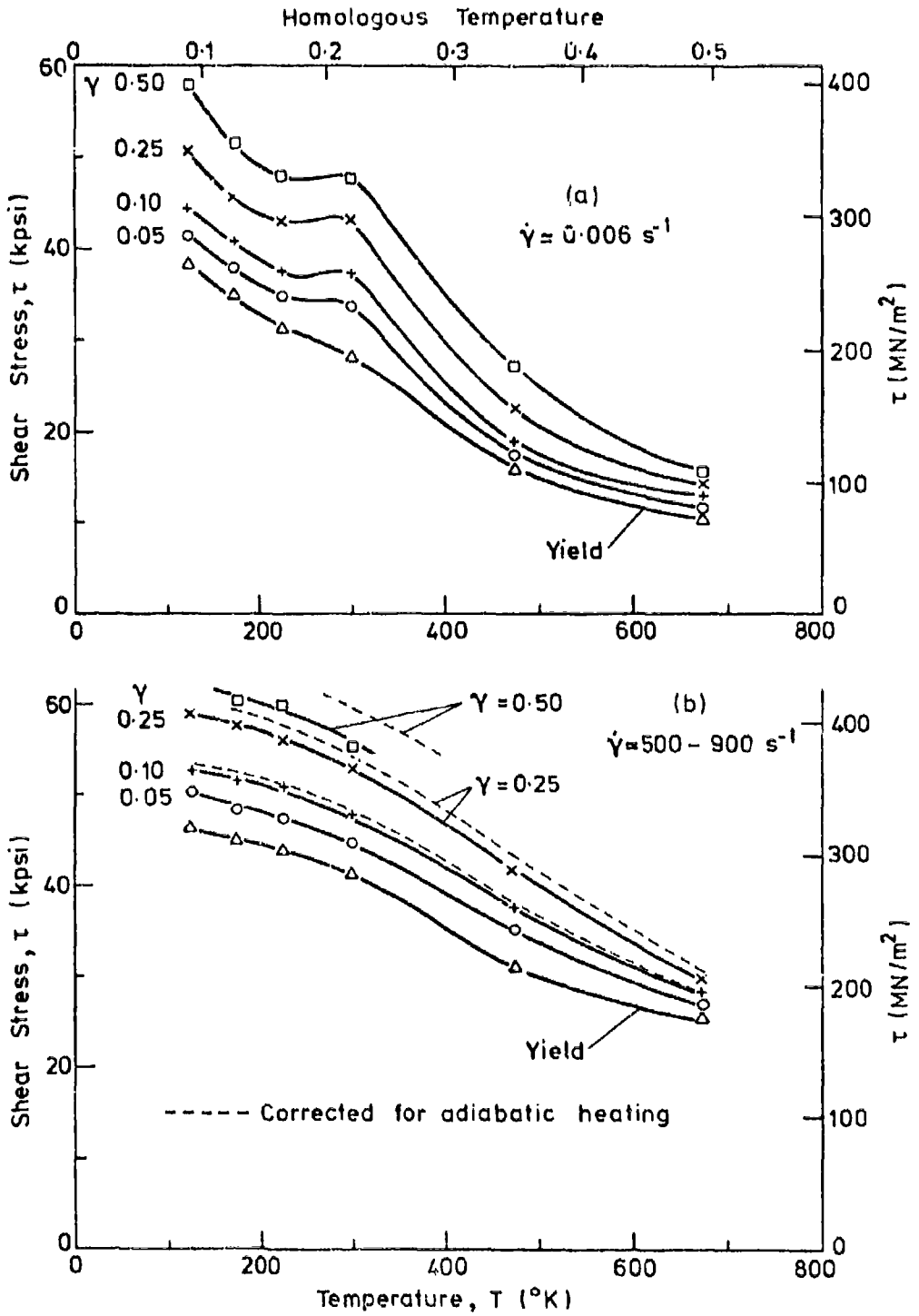

Fig. 17. Temperature dependence of flow stress of titanium, at (a) low and (b) high strain rat

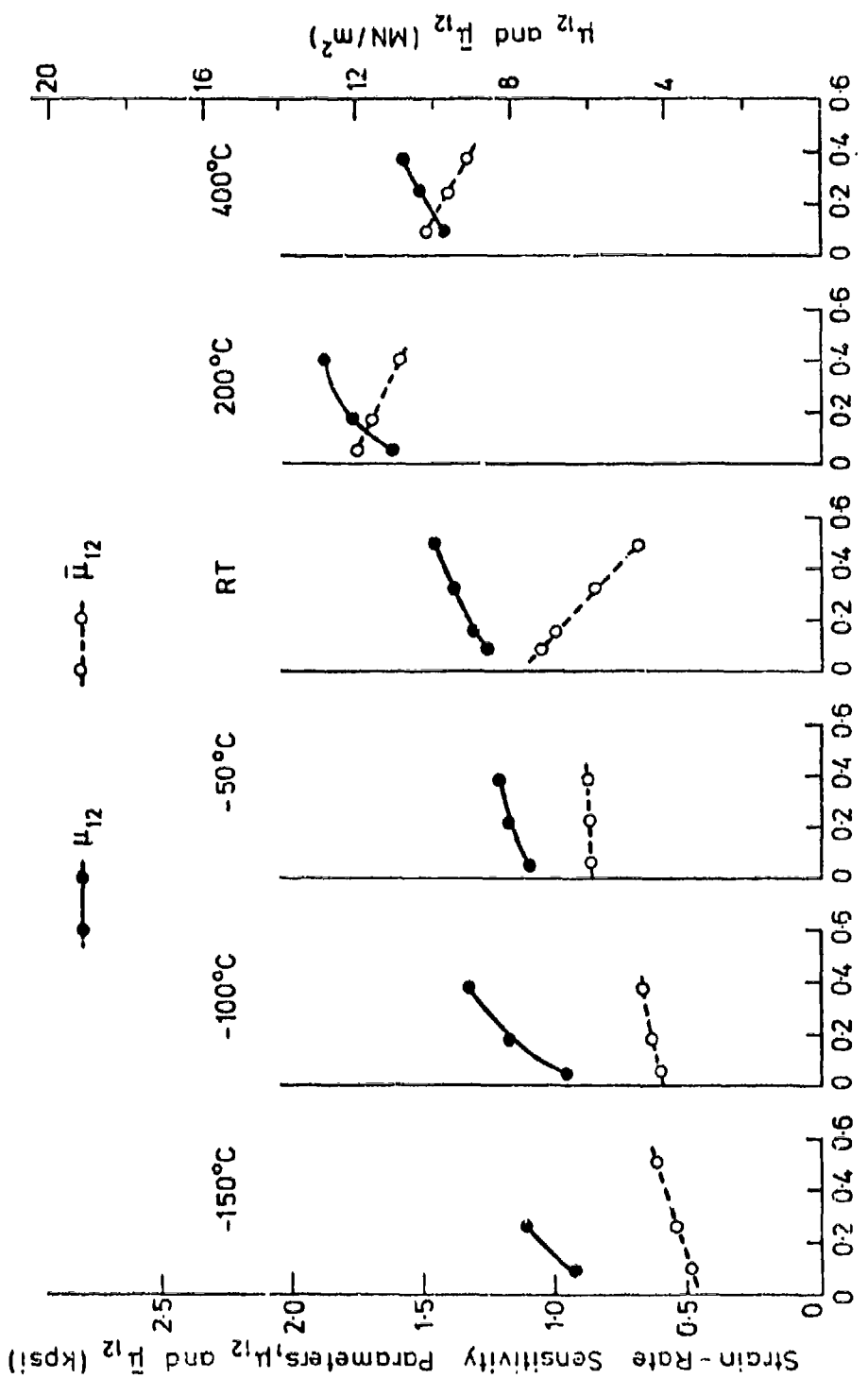

Fig. 18. Strain dependence of apparent and intrinsic strain-rate sensitivities of titanium, at constant temperatures

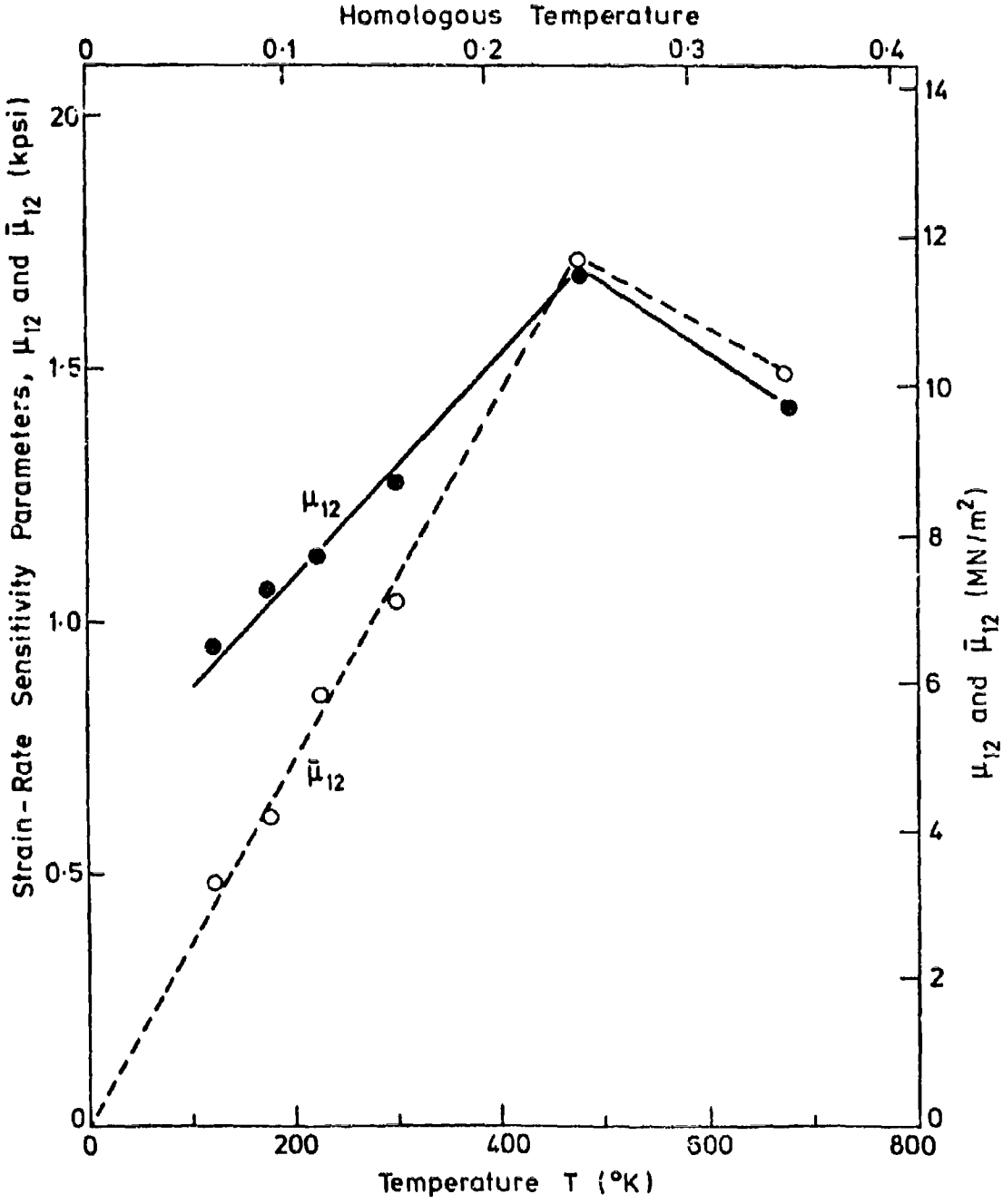

Fig. 19. Temperature dependence of apparent and intrinsic strain-rate sensitivities of titanium, at $\gamma = 0.1$

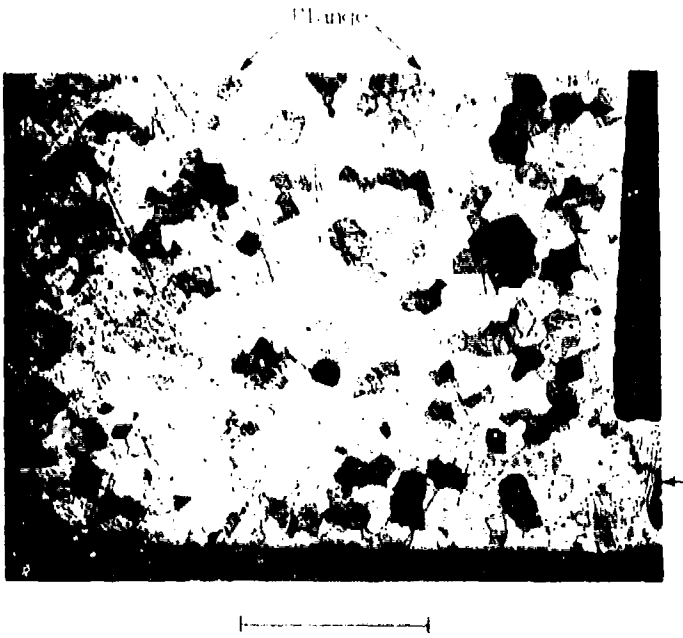

1 mm

(a)

General view;

-50°C

Zero pre-strain

0.2 mm

(b)

Detail of

test section

conditions

as for (a).

Fig. 20 Dynamically strained titanium specimen (longitudinal section)

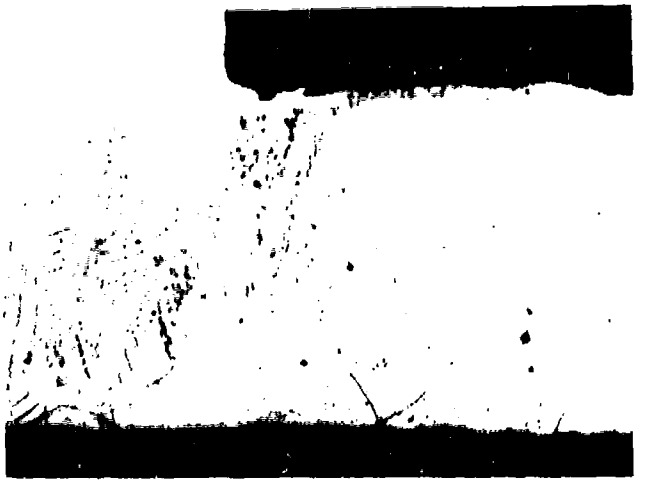

(c)

-50°C

Pre-strain = 0.213

(d)

-50°C

Pre-strain = 0.378

0.1 mm

Fig. 20 (continued) Dynamically strained titanium specimens (longitudinal section)

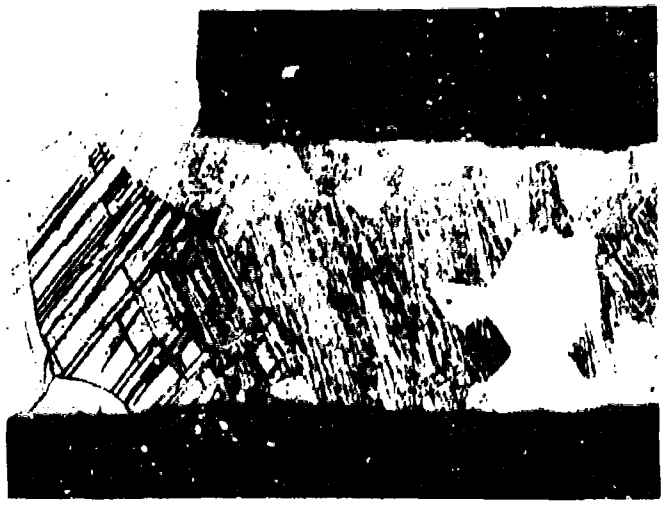

(e)

-150°C

Zero pre-strain

(f)

-150°C

Pre-strain = 0.258

0.1 mm

Fig. 20 (continued) Dynamically strained titanium specimens (longitudinal section)

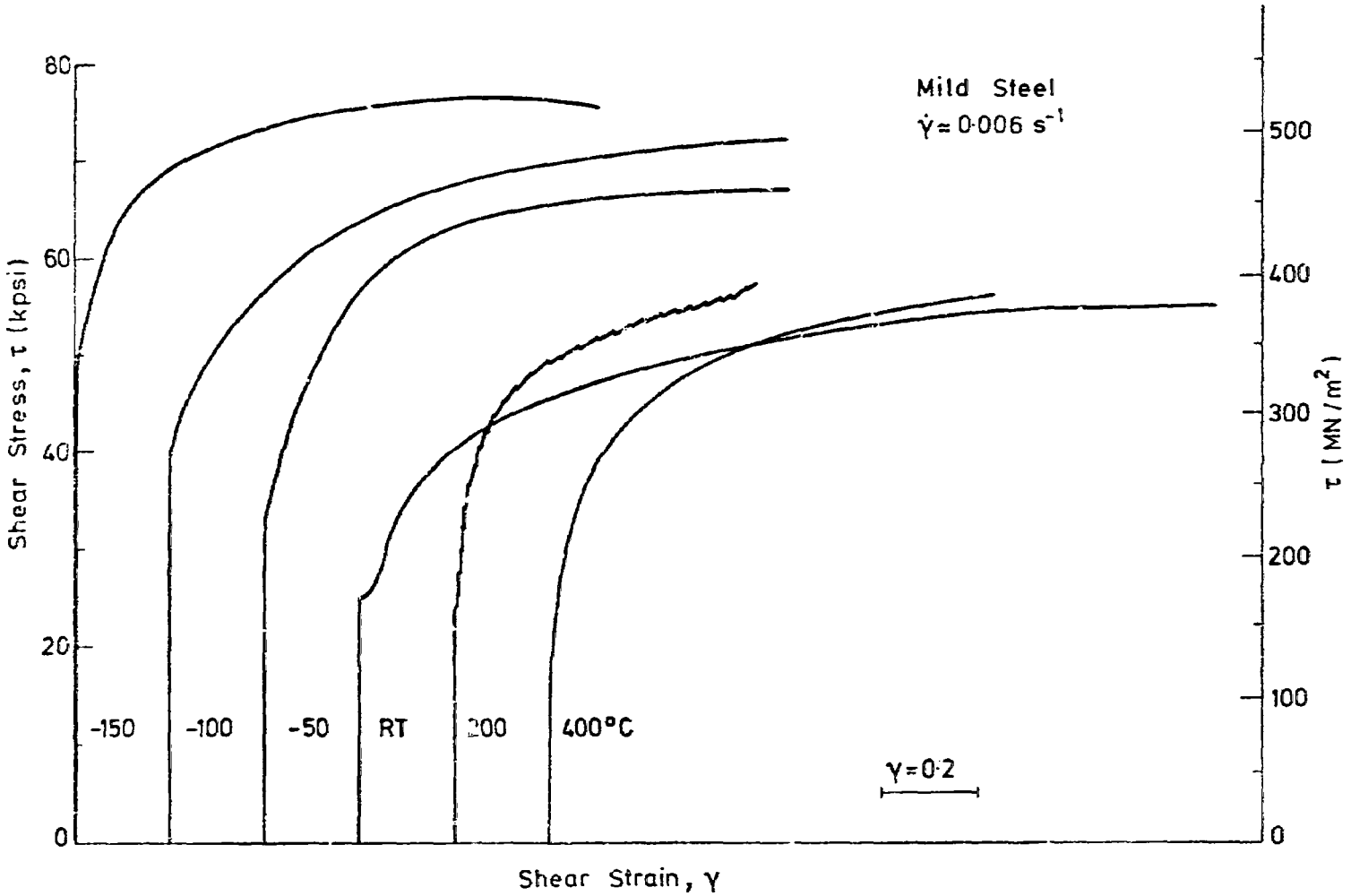

Fig. 21. Quasi-static stress-strain curves for mild steel at various temperatures

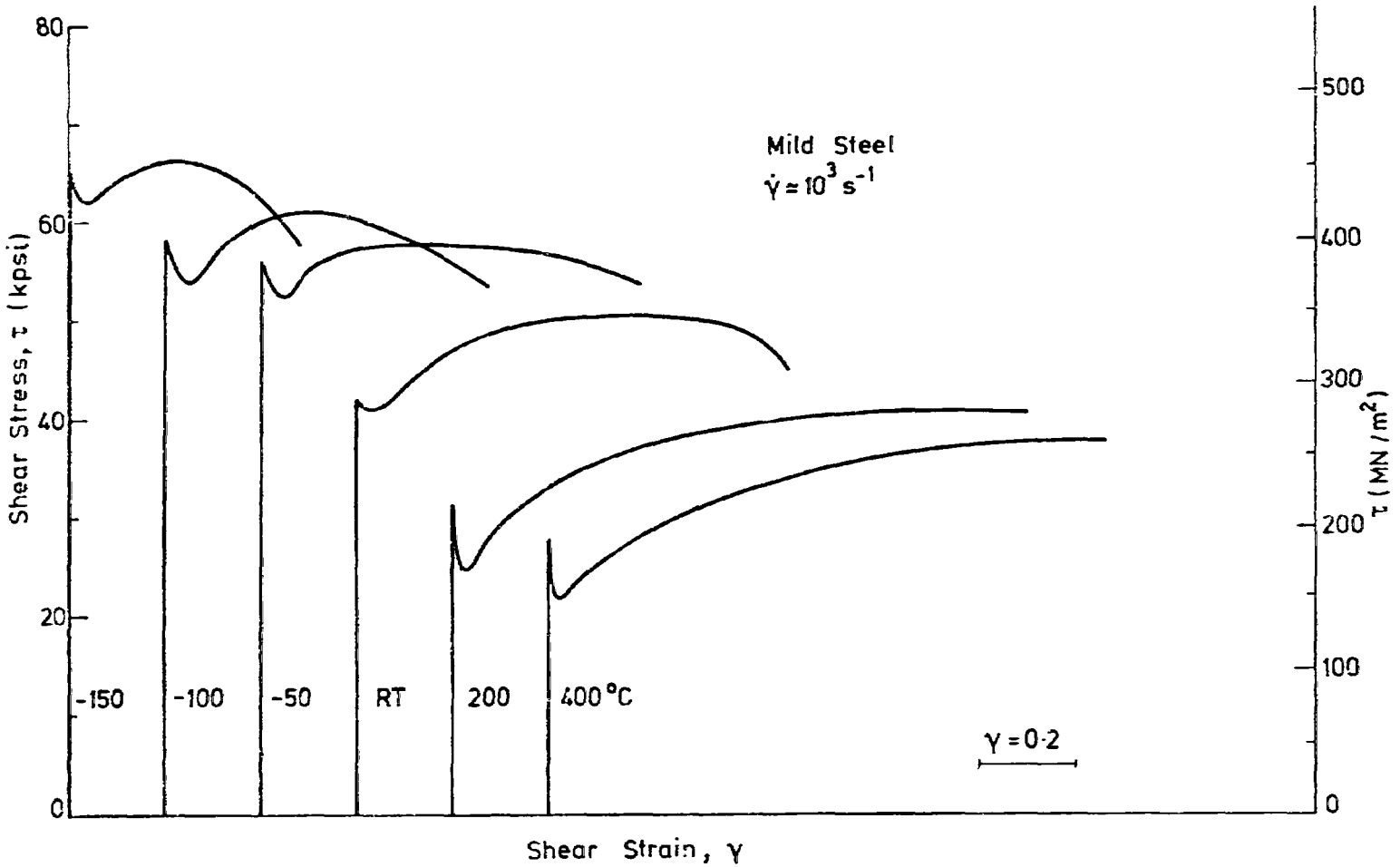

Fig. 22. Dynamic stress-strain curves for mild steel at various temperatures

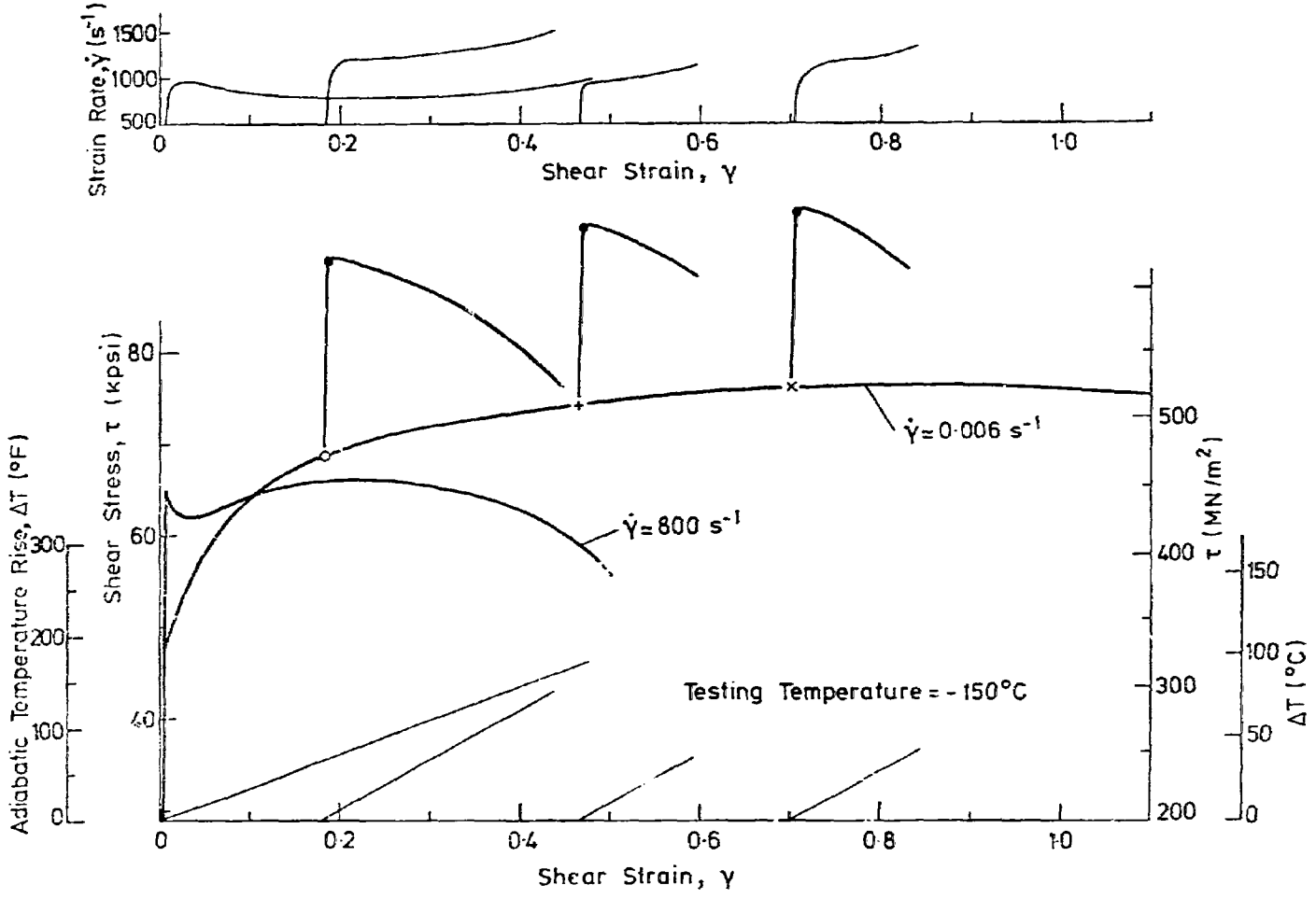

Fig. 23(a) Test results for mild steel at -150°C; pre-strains 0.183, 0.465, 0.700

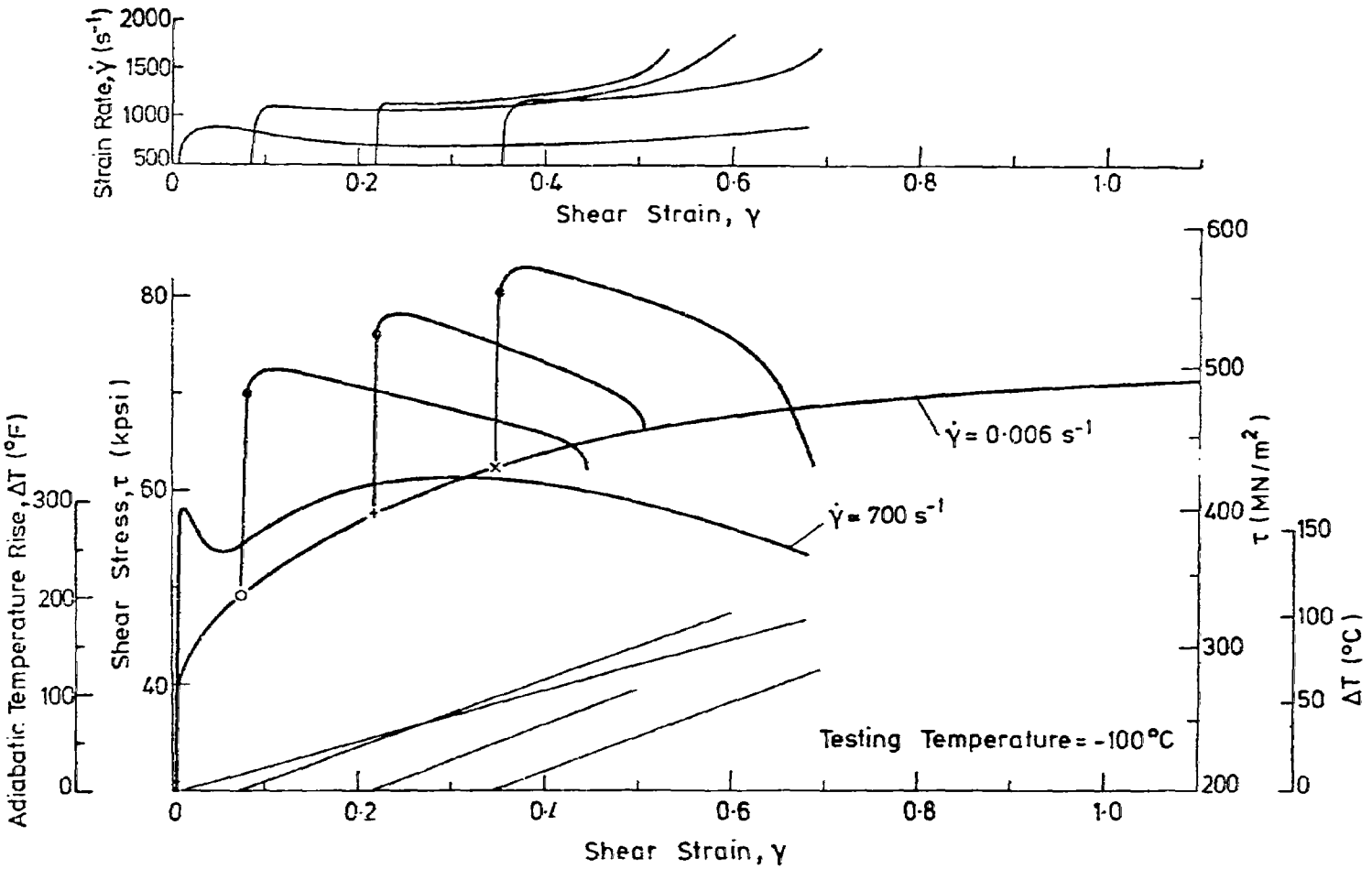

Fig. 23(b) Test results for mild steel at -100°C; pre-strains 0.075, 0.218, 0.348

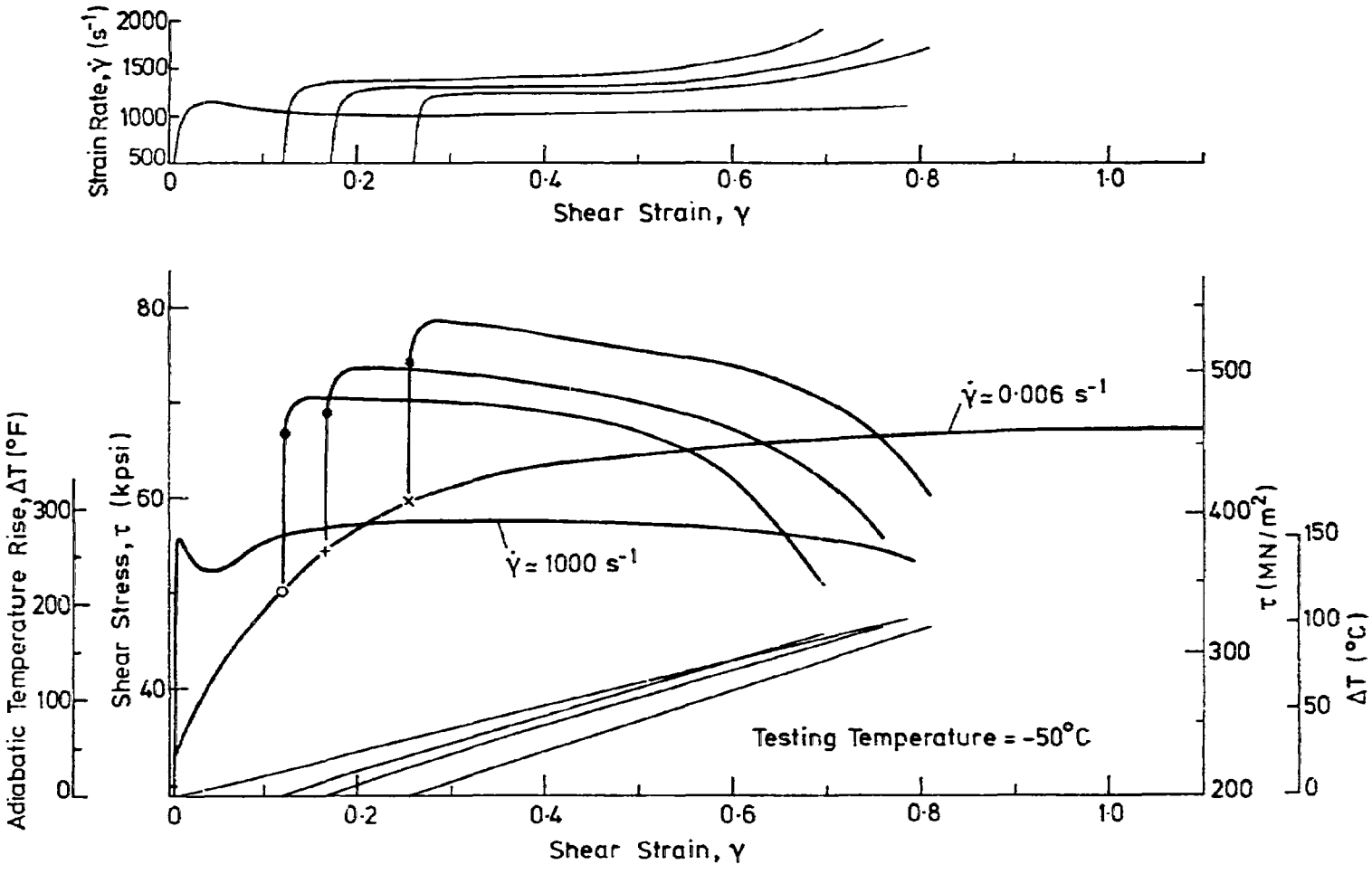

Fig. 23(c) Test results for mild steel at -50°C; pre-strains 0.120, 0.165, 0.255

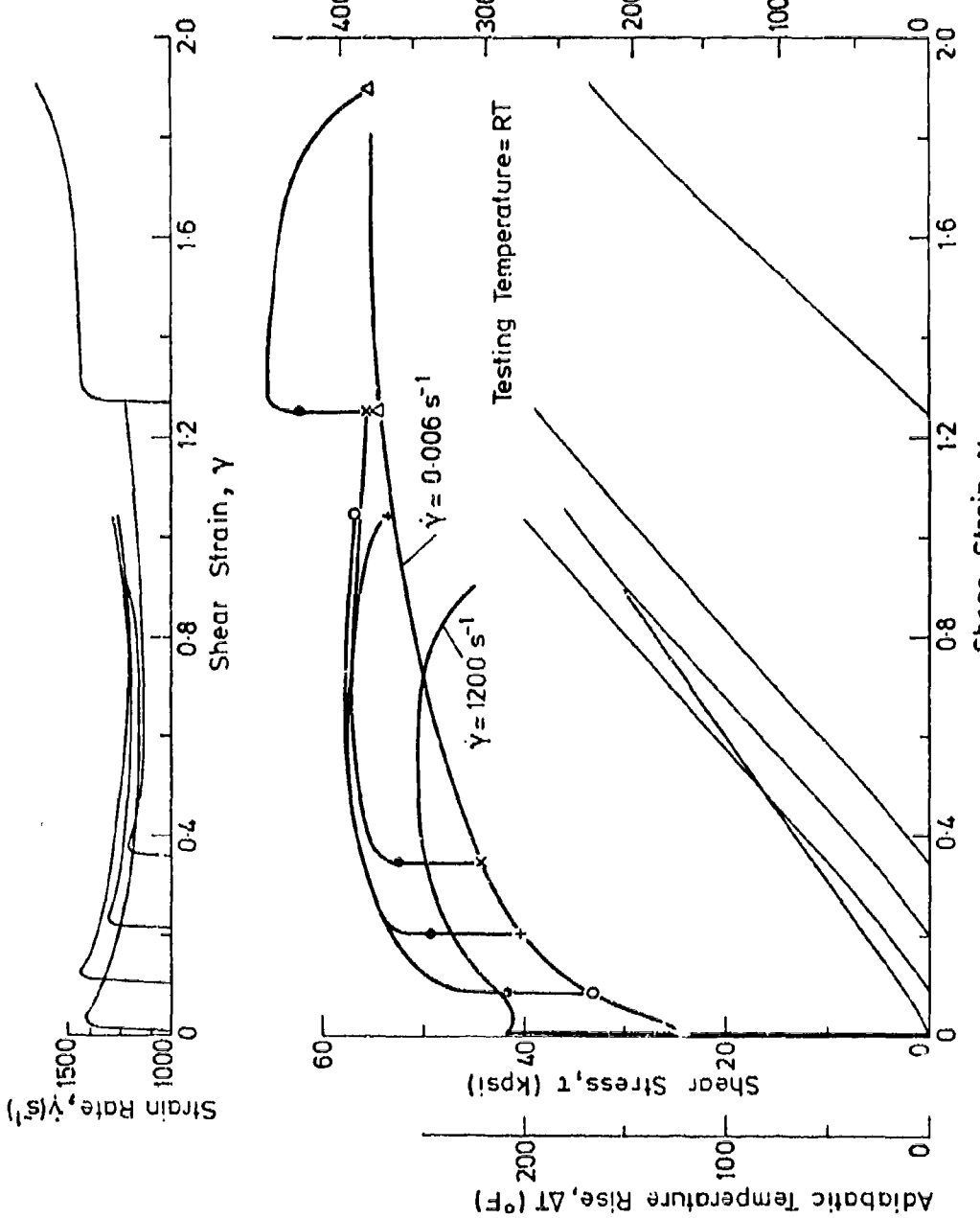

Fig. 23(d) Test results for mild steel at RT; pre-strains 0.085, 0.200, 0.345, 1.25

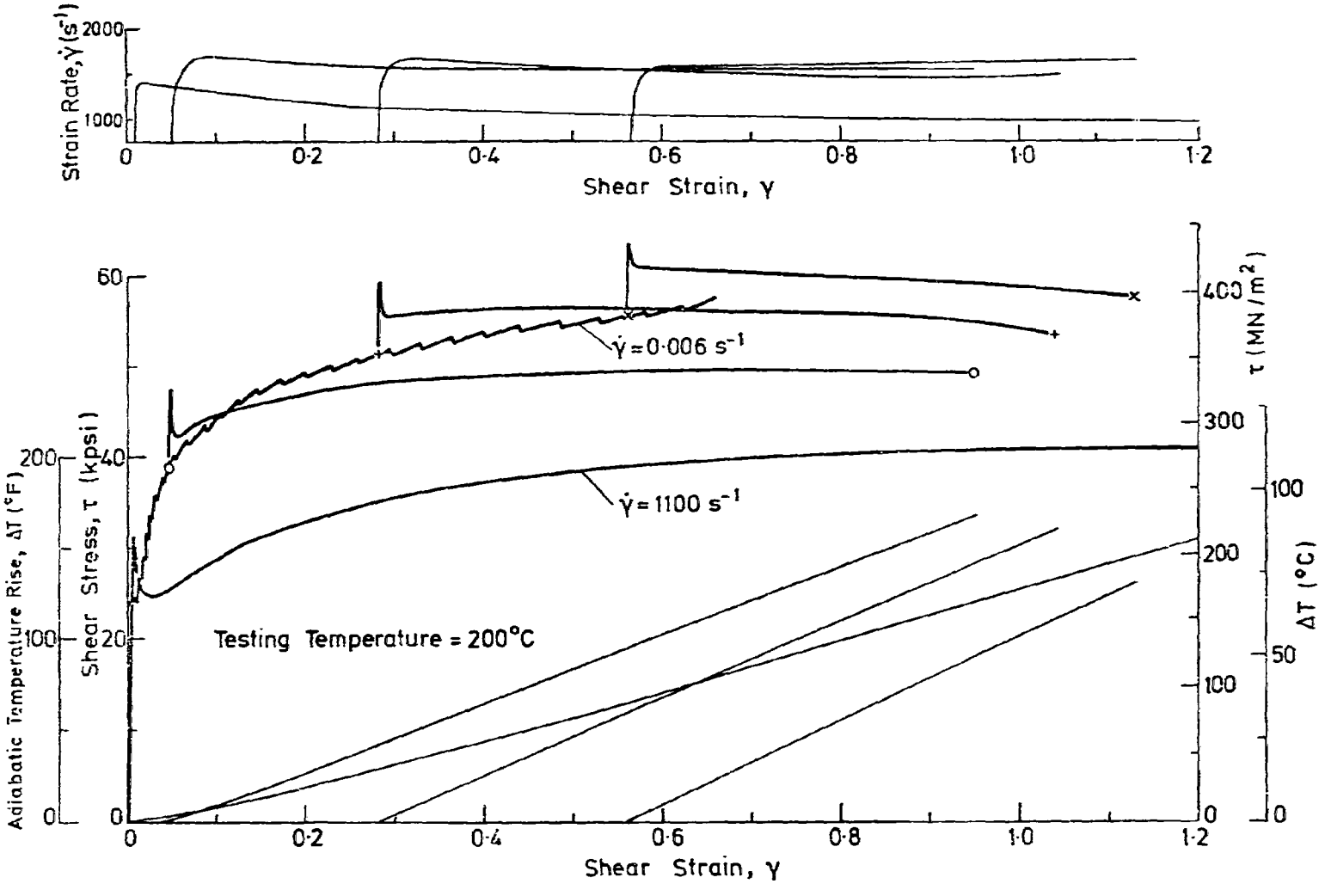

Fig. 23(e) Test results for mild steel at 200°C; pre-strains 0.045, 0.280, 0.560

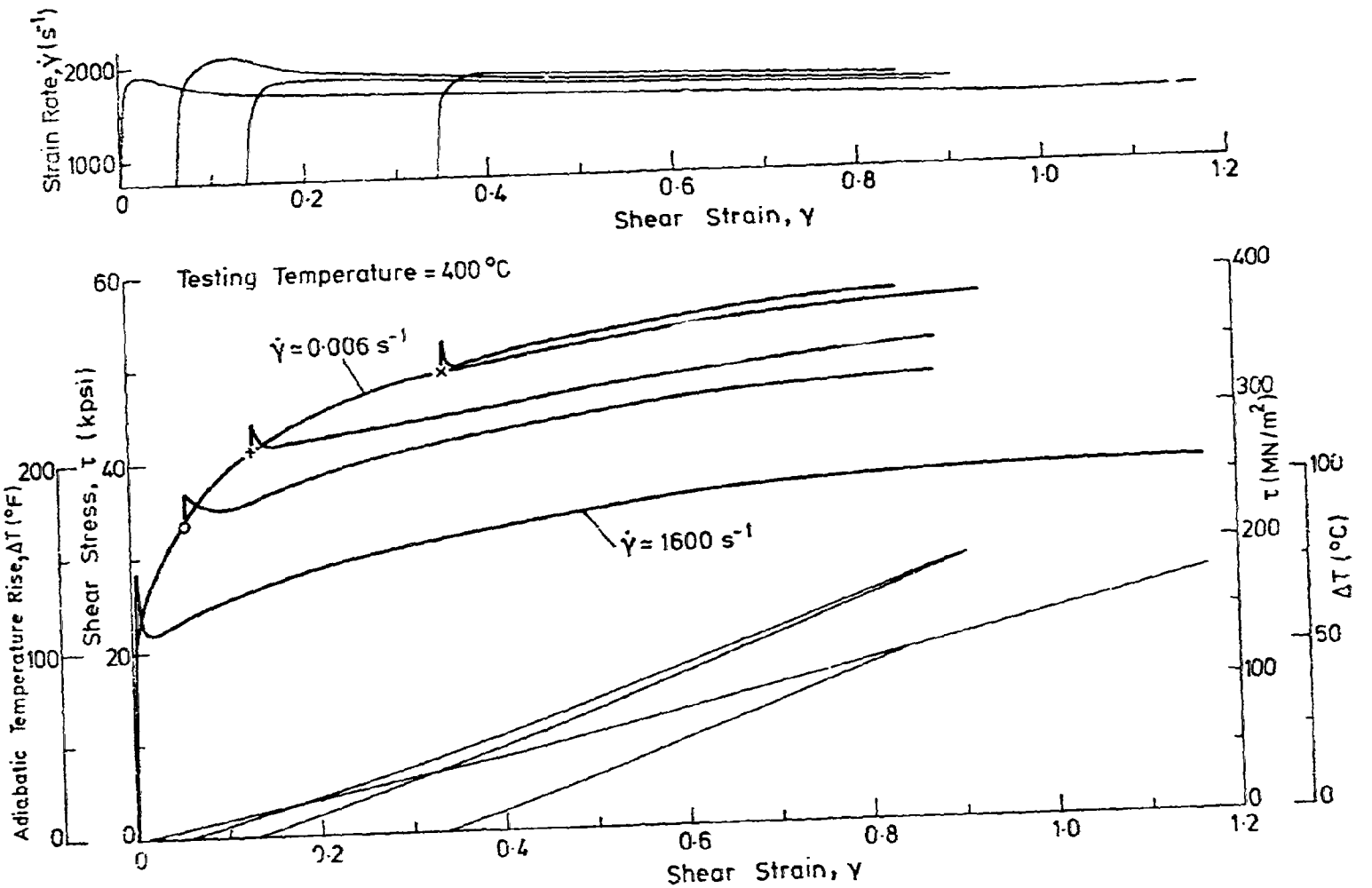

Fig. 23(f) Test results for mild steel at 400°C; pre-strains 0.058, 0.133, 0.342

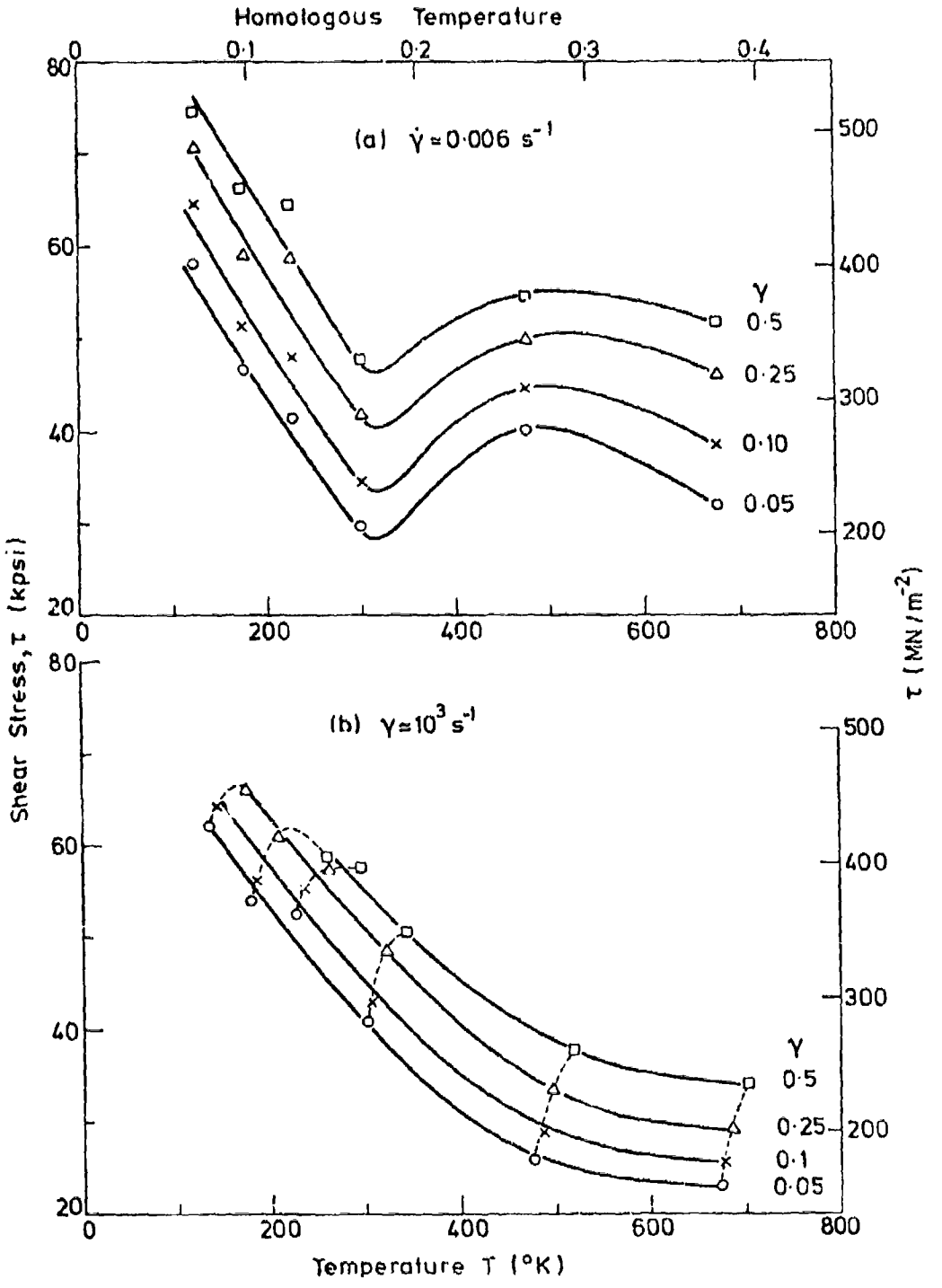

Fig. 24. Temperature dependence of flow stress of mild steel, at (a) low and (b) high strain rate

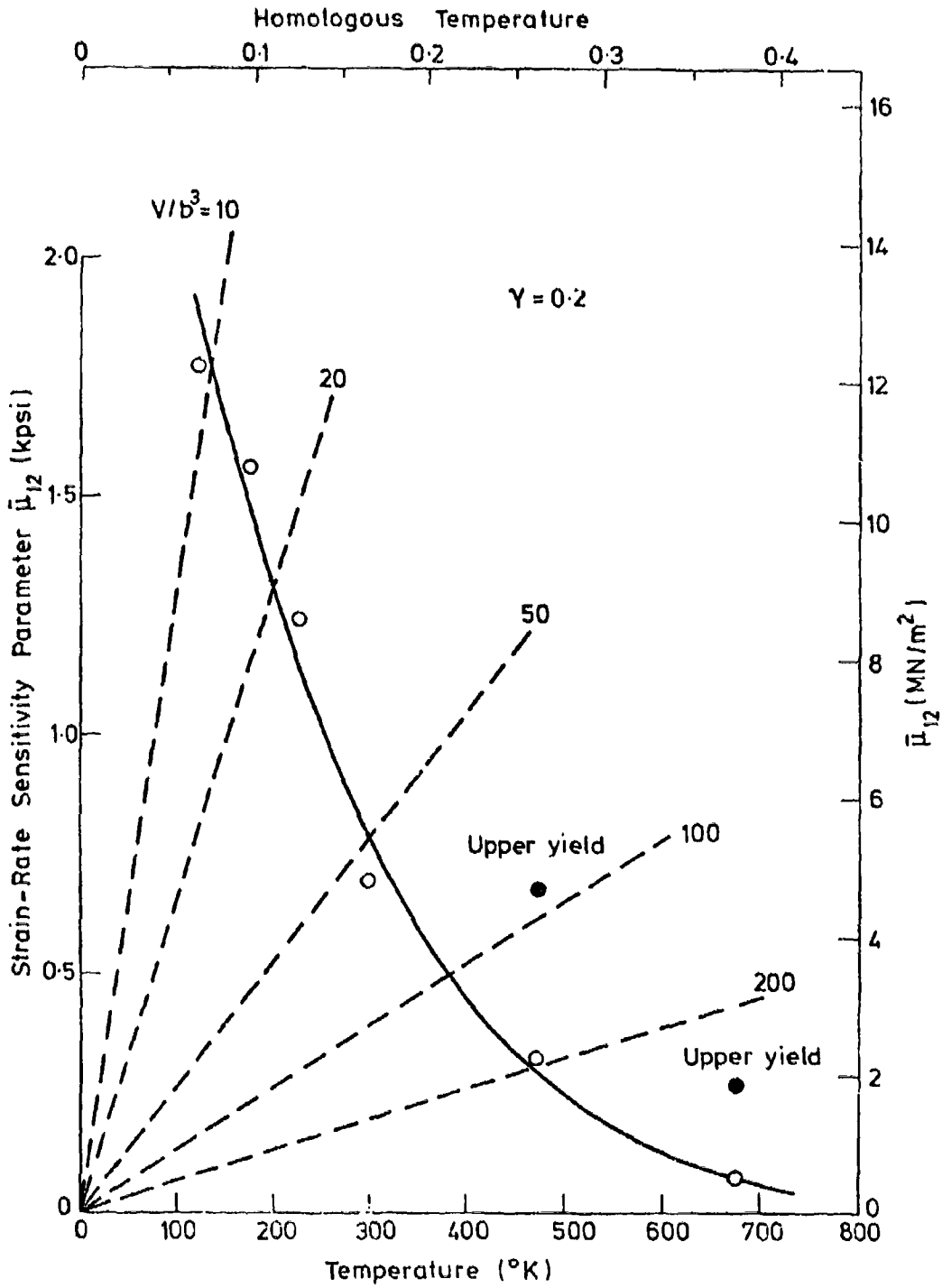

Fig. 25. Temperature dependance of intrinsic strain-rate sensitivity of mild steel

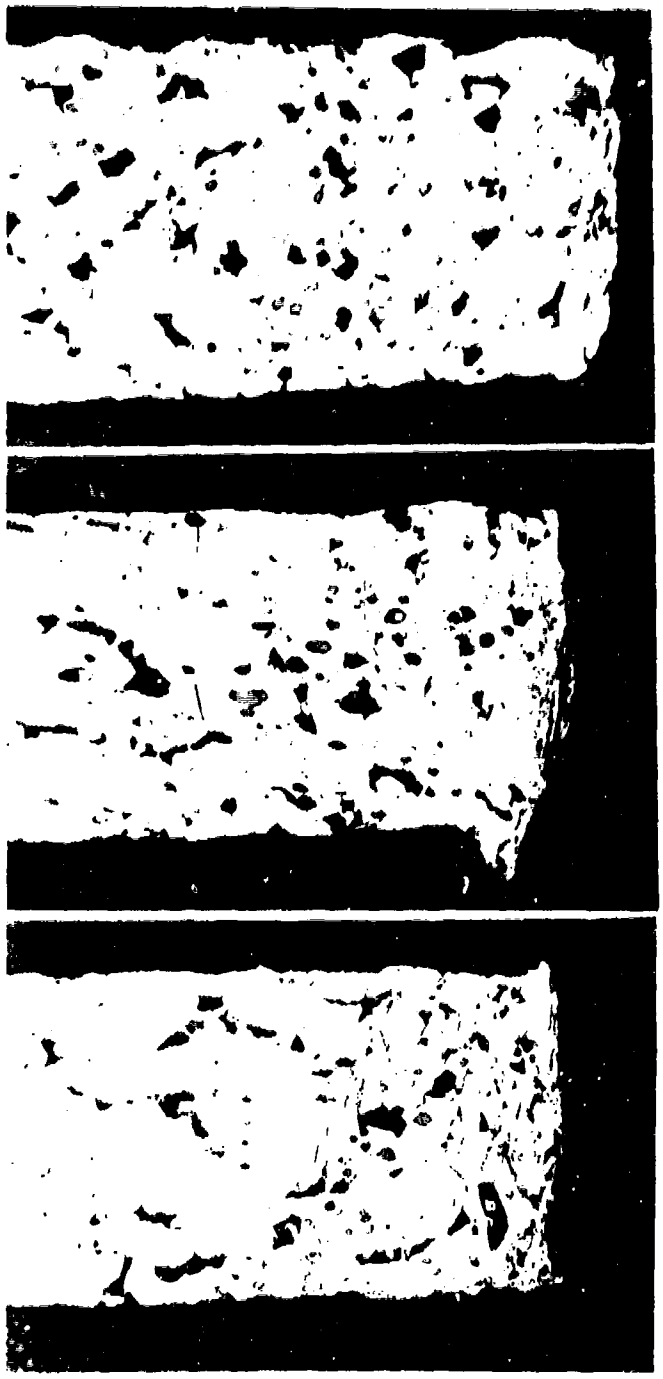

(a)

24°C

Zero pre-strain

(b)

-100°C

Zero pre-strain

(c)

-150°C

Zero pre-strain

Fig. 26. Dynamically strained steel specimens (longitudinal section)

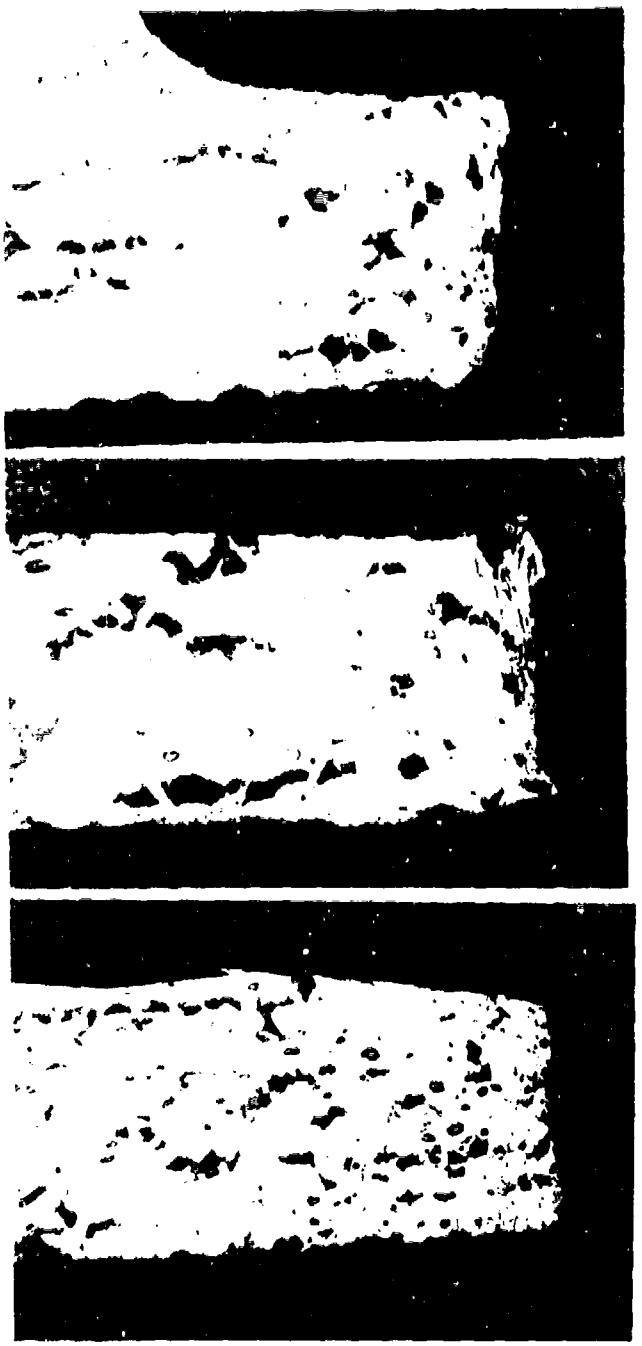

(d)

-100°C

Pre-strain = 0.075

(e)

-150°C

Pre-strain = 0.180

(f)

-150°C

Pre-strain = 0.465

Fig. 26 (continued) Dynamically strained steel specimens (longitudinal section)

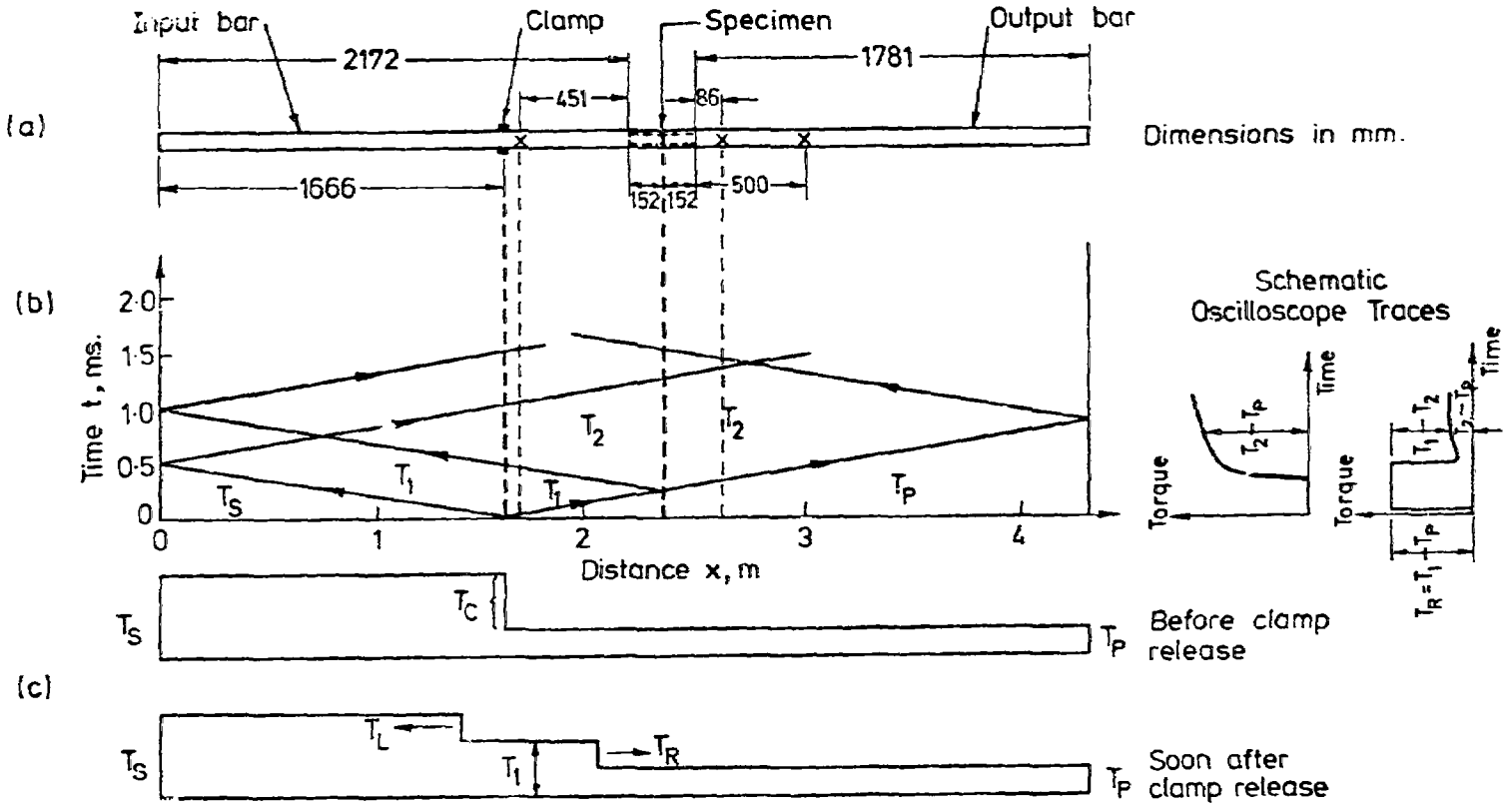

T_S = Stored torque

T_P = Pre-load torque

T_C = Clamp torque

T_2 = Total specimen torque

$T_L = T_R = \frac{1}{2}(T_S - T_P)$

$T_1 = \frac{1}{2}(T_S + T_P)$

Fig. A1. Torsional bar apparatus

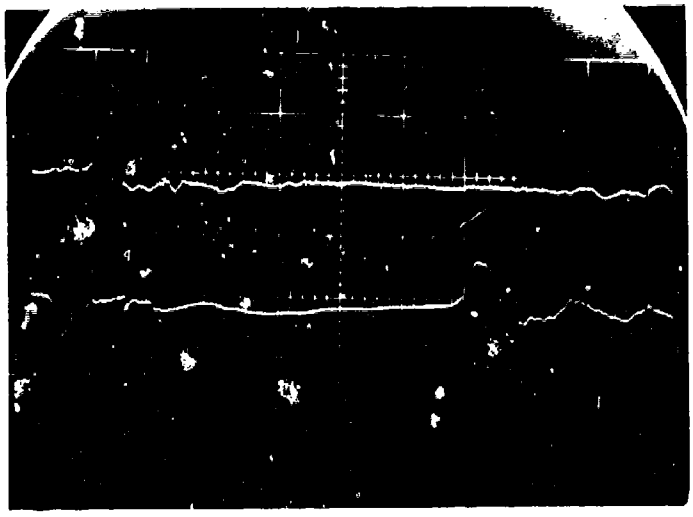

Fig. A2. Waves generated by release of the clamp (dummy specimen, no stored torque).

Timebase: 100 μs/div; upper trace delay: 100μs

Upper trace: torque, 5.4 Nm/div.

Lower trace: axial force, 1.88 kN/div. (compression upward).

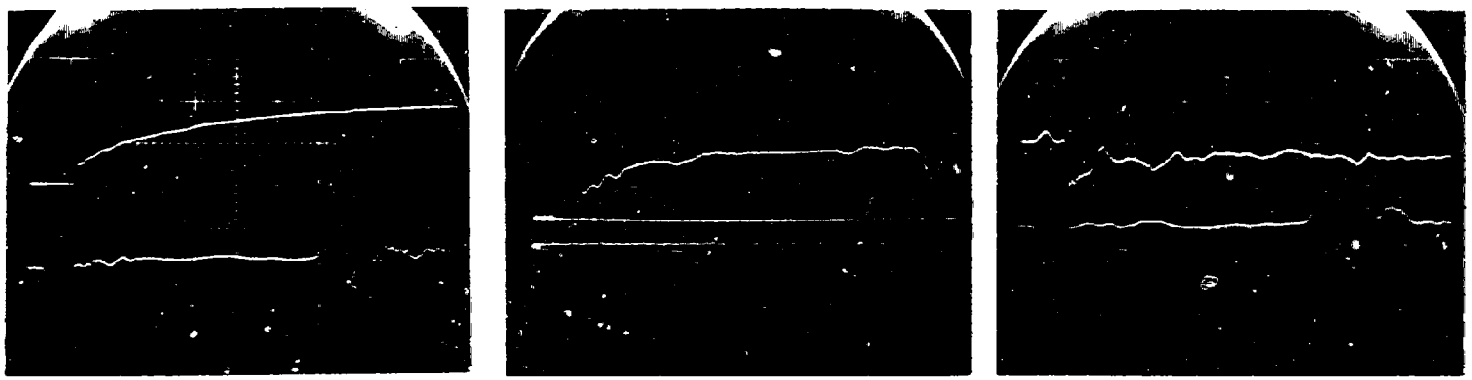

Fig. A3 Comparison of torsional wave (upper trace) with axial wave (lower trace) for tests on copper. Timebase 100μs/div.

(a) dynamic test; torque 21.6 Nm/div., axial force 0.378 kN/div.

(b) jump test; torque 5.4 Nm/div., axial force 0.378 kN/div.

(c) Clamp-release test; torque 2.2 Nm/div, axial force 0.943 kN/div.

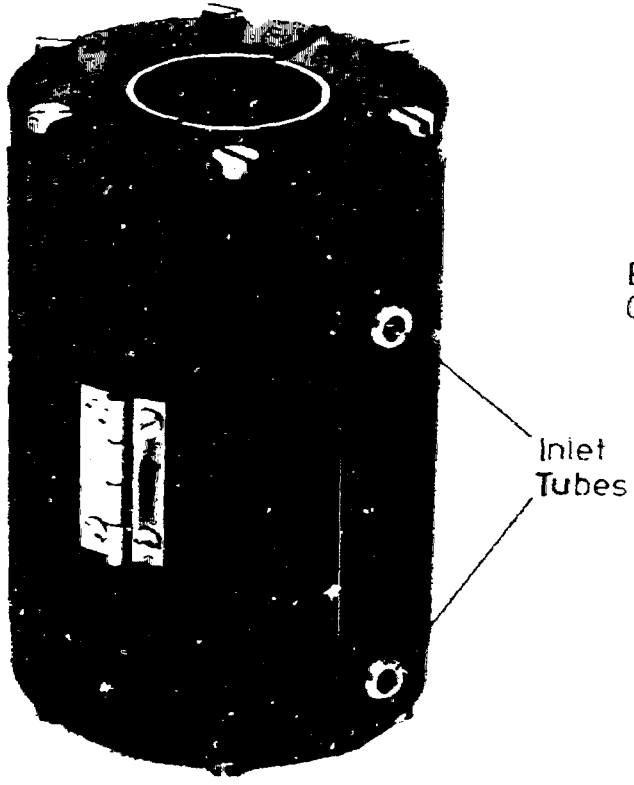

(a)

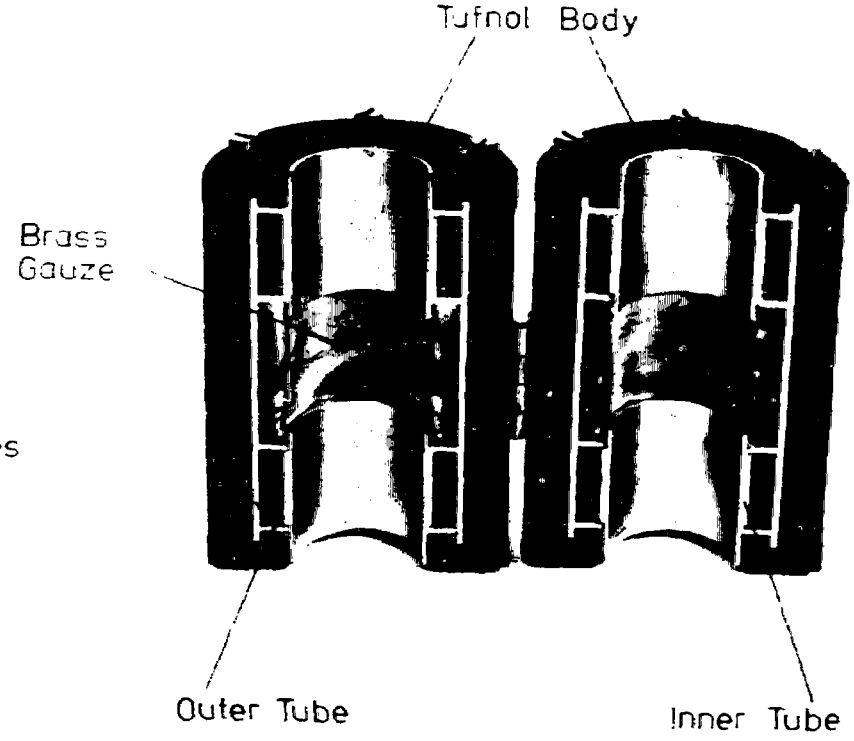

(b)

Cryostat.

Fig. B 1

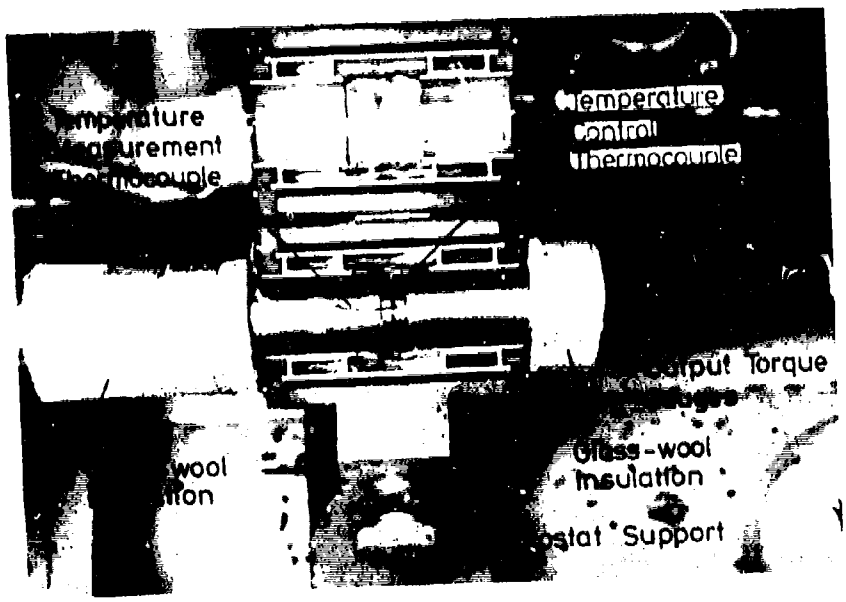
Temperature control thermocouple
Output Torque
Glass-wool insulation
Support

Fig. B 2

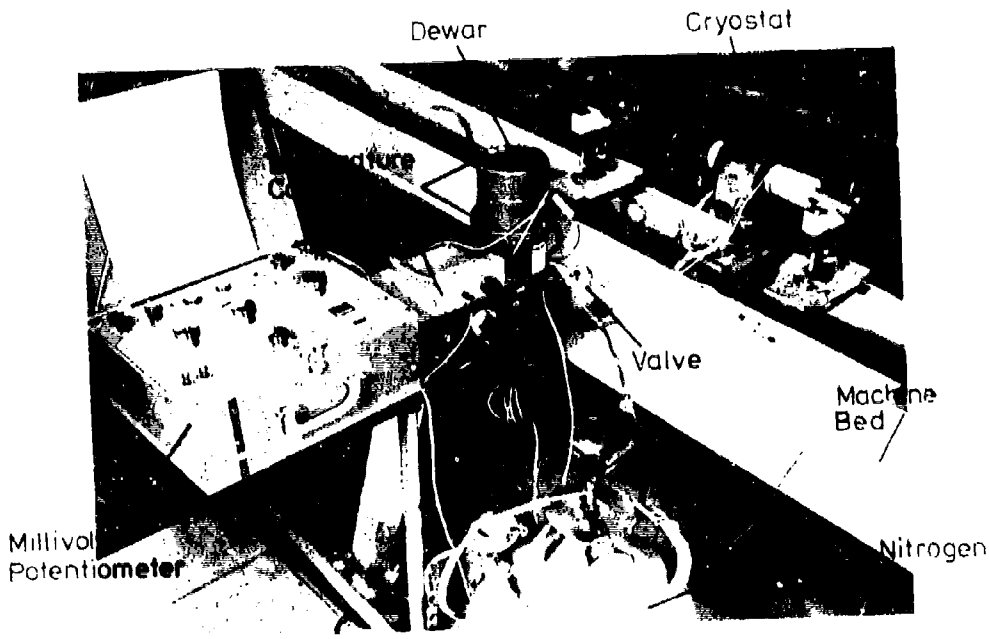
Dewar
Cryostat
Valve
Machine Bed
Nitrogen

Fig. B 3

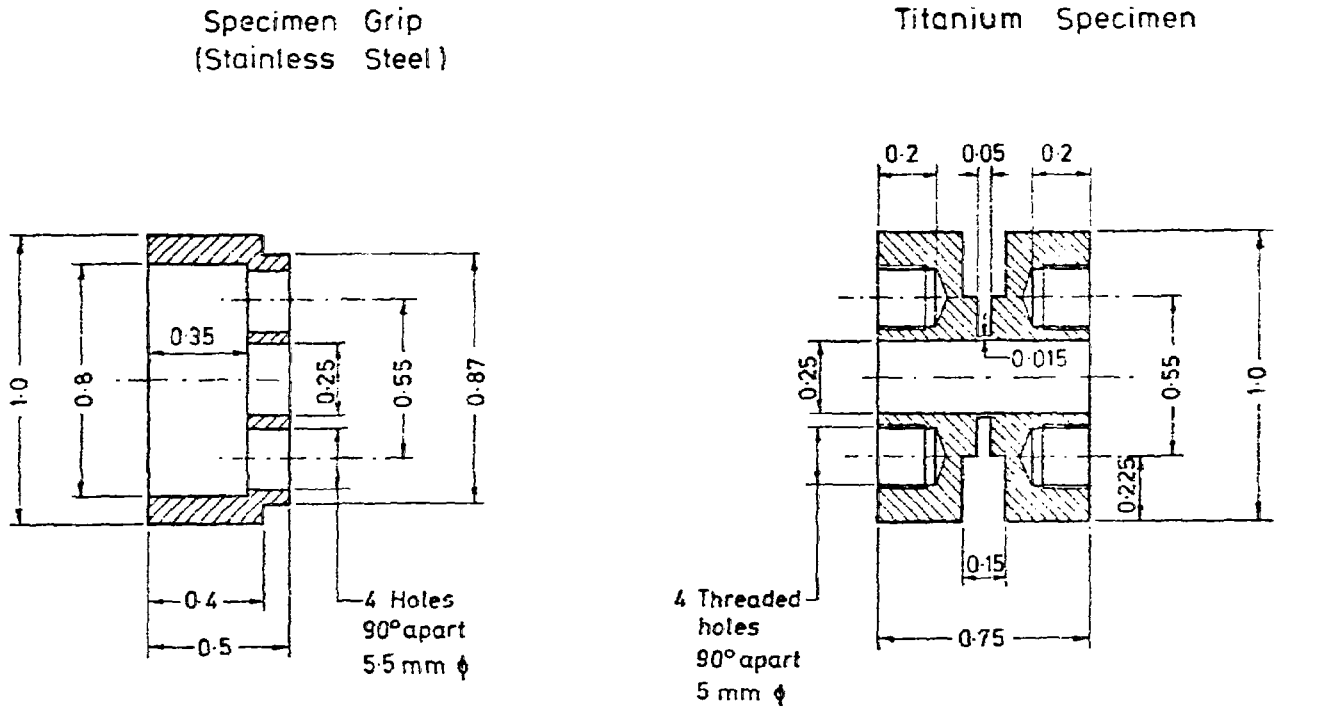

Fig. C1. Design of high-temperature titanium specimen and grip

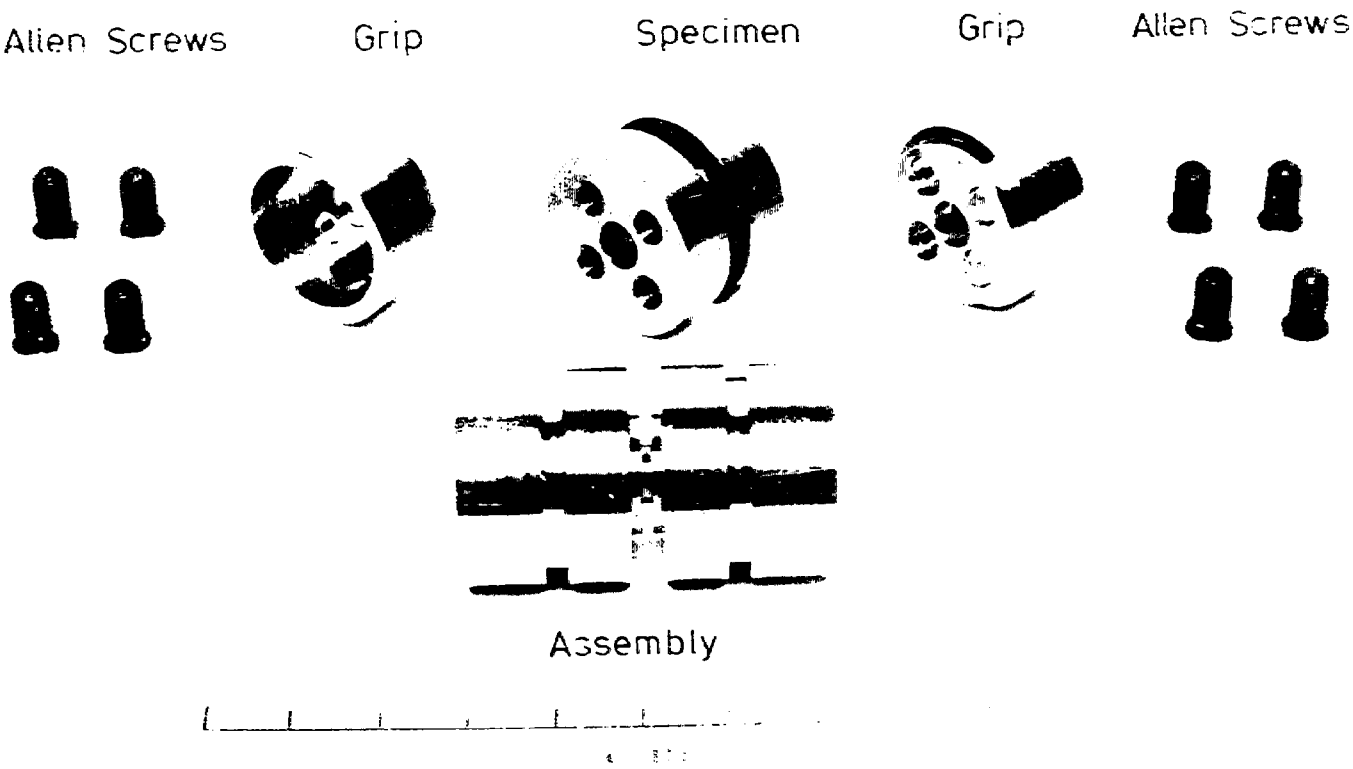

High Temperature Titanium Specimen and Stainless Steel Grips.

Fig. C2

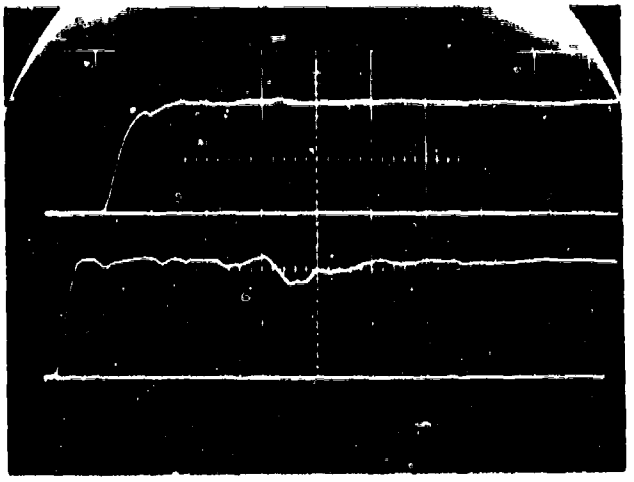

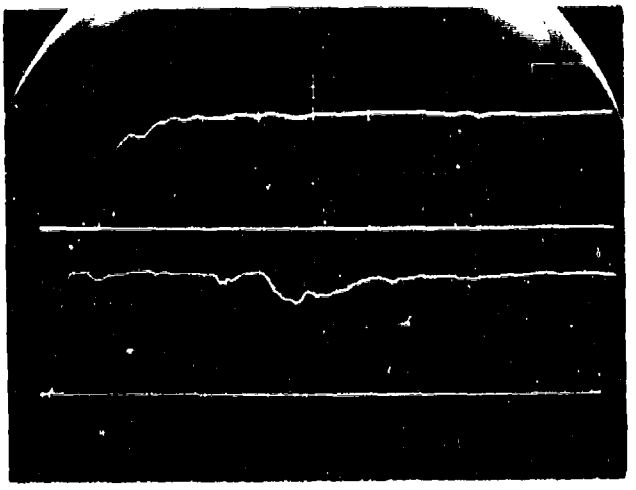

Fig. C3. Transmission of torsional wave through mechanical connectors.
Timebase, 100μs/div. Upper trace delay, 200 μs.
Upper trace, 37.0 Nm/div; lower trace, 38.0 Nm/div.